CHARACTERIZATION AND MATURATION OF SELECTED OIL AND CONDENSATE SAMPLES AND CORRELATION WITH SOURCE BEDS, SCOTIAN SHELF

P. K. Mukhopadhyay
Global Geoenergy Research Ltd.
P.O.Box 9469, Station A
Halifax, Nova Scotia
B3K 5S3

For

Scientific Authority, John A. Wade
Basin Analysis Subdivision
Atlantic Geoscience Centre (GSC)
Bedford Institute of Oceanography
Dartmouth, Nova Scotia
B2Y 4A2

SSC File No. OSC90-00245-(014)
Contract No. 23420-0-C070/01-OSC
Financial Codes: 260-120-00000-720104-04W1
260-120-00000-810034-04W1

December 31, 1990

ABSTRACT

Selected light oil and condensate samples from various reservoirs (Wyandot, Logan Canyon, and Missisauga Formations) and five selected source rock extracts were examined by liquid chromatography, gas chromatography, stable carbon isotope, and GC-MS of the aromatic fraction.

A complete source rock characterization was made based on earlier data, which suggests presence of multiple oil, condensate, and gas-bearing source rocks and possible presence of thin and local oil-prone source rock associated with the carbonates and sandstones in the Missisauga Formation and Misaine Member. Based on the combination of earlier and present data, it is observed that vitrinite reflectance and fluorescence of organic matter is related to overpressuring in the sediments. These data suggest the possible presence of more deeper condensate in the Basin and indicate the possible timing of onset of overpressuring.

The data acquired by the GC-MS of the aromatic fraction of the petroleum when compared with stable carbon isotope, light hydrocarbon GC and liquid chromatography data revealed the following: (a) Cohasset-Panuke-Sable Island oils belong to a non-thiophenic (low-sulfur) group and the S. Venture/ Glenelg condensates belong to a moderately thiophenic group (relatively high sulfur). Based on Methylphenanthrene Index and the ratio between chrysene to benzo(α)anthracene, Cohasset-Panuke oils are less mature than Venture condensates; however, condensates are formed within the 'Oil Window'. Some of the Cohasset and Panuke light oils are possibly derived from the aquatic source rock of possible lacustrine origin, (b) According to aromatic gc-ms none of the source rock extracts are correlatable with any petroleum. On the other hand, based on stable carbon istope data, Cohasset extracts are correlatable to some of the Cohasset light oils.

TABLE OF CONTENTS

INTRODUCTION

Administrative Aspect

This research proposal was requested by Supply and Services Canada, Dartmouth, Nova Scotia on August 14, 1990 at the initiation of the Basin Analysis Subdivision of the Atlantic Geoscience Centre, Geological Survey of Canada, Bedford Institute of Oceanography. Global Geoenergy Research Ltd. of Halifax, Nova Scotia, submitted a financial and work schedule for the research proposal on August 20, 1990. The proposal was accepted on August 28, 1990. The research work was started September 1, 1990. Canada Nova Scotia Offshore Petroleum Board (CNSOPB), Halifax, Nova Scotia, on our request, permitted us to collect thirty crude oil and condensates, seven unwashed cuttings, and nine core samples from selected Scotian Shelf wells at the CNSOPB-COGLA Repository at BIO, Dartmouth, Nova Scotia. According to the contract, liquid chromatography of thirty crude oil and condensate samples was done by Dr. P. K. Mukhopadhyay at the ISPG Laboratory at Calgary, Alberta. All samples for the liquid chromatography work, were taken from the ISPG storage facility.

Basin Analysis Subdivision approached LASMO Nova Scotia Limited, Calgary, Alberta, to participate in the cost of this research project. LASMO Nova Scotia Ltd. of Calgary, Alberta, provided $10,000.00 which was used specifically for the isotope and aromatic GC-MS analyses in order to complete a composite organic geochemical database and facilitate interpretation using some new geochemical parameters.

Bitumen extraction and liquid chromatography of 5 source rock samples was subcontracted to SeaTech Ltd., Halifax, Nova Scotia, SGS Supervision Ltd, Montreal, Quebec provided API gravity of 30 crude oil and condensate samples, Coastal Science Laboratories, Austin, Texas, USA provided Stable Carbon Isotope of saturate and aromatic fractions of oils and source rock extracts, and Dr.

Michael Kruge, Southern Illinois University, Carbondale, Illinois, USA did special aromatic GC-MS analyses.

This report incorporates some of the data and interpretations which were generated during earlier research contracts on Scotian Shelf oils and source rocks funded to Geofuel Research Inc., Sydney, Nova Scotia and Global Geoenergy Research of Halifax, Nova Scotia (during 1990-1988) by SSC, Dartmouth, Nova Scotia at the initiation of Basin Analysis Subdivision of AGC-GSC-BIO, Dartmouth, Nova Scotia.

Scientific Aspect

Twenty-three significant discoveries of crude oil, condensate and natural gas have been made in the general Sable Island area of the Scotian Shelf. Since 1976, a number of publications recorded various aspects of organic geochemical studies such as source rock potential and maturation, oil quality, possible migration avenues, and possible oil-oil and oil-source rock correlation (Barss et al., 1980; Bujak et al., 1977; Cassou et al., 1977; Rashid and McAlary, 1977; Powell and Snowdon, 1979; Powell, 1982, 1985; Purcell et al., 1979). Although these studies did little to solve the regional complexity of hydrocarbon source rock questions, they opened up new dimensions of advanced knowledge on source rock and crude oil geochemistry including fluorescence microscopy and aromatic biomarker GC-MS techniques.

Some major problems still unsolved include:

(a) the possible source rock types in various stratigraphic intervals,

(b) a proper database of organic geochemical properties for the various crude oil and condensate samples,

(c) the possible relation between hydrocarbon generation and overpressuring,

(d) oil/condensate and oil-source rock correlation using aromatic

biomarkers and isotopes, because of complications with aliphatic biomarkers resulting from biodegradation and high levels of maturation.

In order to resolve some of these problems, three projects have recently been initiated by the Basin Analysis Subdivision of AGC, Dartmouth, Nova Scotia. This report will incorporate some of these data. The earlier studies did not include the detailed basic chemical and organic geochemical analyses (API, liquid chromatography, selected GC of the saturate fraction, stable carbon isotope of the saturate and aromatic fractions, and aromatic gc-ms of crude oil and condensate samples) and correlation of crude oil/condensate with the candidate source rocks from the Logan Canyon Formation, Missisauga Formation, Misaine (Abenaki Formation) Member, and Verrill Canyon Formations.

Objectives

The objectives of this current research project are to determine:

(a) The relationship between fluorescence and vitrinite reflectance in the overpressured source rock shales,

(b) The maturity (as defined by the aromatic biomarker and stable carbon istope parameters) of the various source rock extracts and light oil/condensates. A special emphasis will be given to the Cohasset/Panuke and Sable Island light oils.

(c) Genetic types of various oils and condensate samples and their possible correlation with the source rocks.

GEOLOGICAL SETTING

Regional Geology

The Scotian Basin, which lies south of Nova Scotia and Newfoundland, consists of a number of interconnected depocentres (subbasins) and a series of flanking, more positive elements. Separating the two is a basement hinge zone. Studies to delineate the source rocks for the discovered hydrocarbons have concentrated on the Sable Subbasin which underlies the general Sable Island area and the adjacent edge of the LaHave platform (Figure 1).

The Scotian Basin developed as a result of the breakup of Pangaea and the separation of North America and Africa. Initial (synrift) sedimentation occurred during the Late Triassic and Early Jurassic into grabens formed during the rifting phase of breakup. These fluvial, lacustrine and aeolian sediments are the Eurydice Formation (Figure 2). In the deeper grabens the Eurydice Formation contains an evaporite facies and is overlain by large thicknesses of Argo Formation salt which has mobilized with burial to form the many diapirs shown as black areas on Figure 1.

The drifting phase of breakup is dated in the sedimentary record on the Scotian shelf as begining during the Early Jurassic. It is expressed as an erosional unconformity (the Breakup Unconformity) on top of the Argo and Eurydice formations. The first post-rift units are the clastic Mohican Formation and a local dolostone facies the Iroquois Formation. Seismic data indicates that the Mohican Formation is several kilometres thick in this area of the basin where subsidence across the hinge was very rapid.

The Mohican is overlain by a variety of continental to marine facies of Middle to Upper Jurassic age. These include the Mohawk (sandstone and shale); the Mic Mac (sandstone, shale and limestone); the Abenaki (carbonate bank); and the Verrill Canyon (basinal shale). Generalized relationships are illustrated in Figures 2 and 3. The Mohawk and part of the Mic Mac Formation form a continental and shallow marine back-bank facies north of the carbonate bank. East of the bank, the Mic Mac Formation occurs as a paralic wedge across the entire shelf. The Abenaki carbonate bank

developed along the hinge zone at the edge of the LaHave Platform and, in the western part of the area formed a paleo-shelf edge. However, as the bank trends northeast toward Sable Island, the carbonate interfingers with the Mic Mac facies to the east. Seaward, both formations are replaced by basinal shales of the Verrill Canyon Formation (Figure 3).

In the Scotian Basin, sedimentation during the Early Cretaceous was dominated by two very thick formations. A generally regressive, (progradational) sandstone and shale sequence, the Missisauga Formation and the transgressive/regressive Logan Canyon Formation. Both units have their basinal shale equivalents - the Verrill Canyon Formation and the Shortland Shale. A series of thin limestone beds within the upper part of the Missisauga Formation, the "O" Marker, provide a semi-regional seismic marker (Figure 1). These formations are characterized by very thick sequences of alluvial to deltaic clastics deposited over a broad area of the present day shelf. Growth faults are common along the outer shelf resulting from the accumulation of very thick clastic facies with unstable salt at depth.

The Late Cretaceous global rise in sea level resulted in two deeper water formations, the Dawson Canyon marine shale and the Wyandot chalk. The sands and shales of the Tertiary are included in the Banquereau Formation which completes the stratigraphic succession.

Twenty-three wells have discovered hydrocarbons in the Scotian Basin. Of these two are light oil, two are oil and gas, and 19 are gas and condensate. All of the discoveries are within 100 km of Sable Island. Hydrocarbons occur in all formations from the Wyandot to the Mic Mac (Figure 4). Of specific interest in this study is the source of the light oil in the Cohasset and Panuke discoveries and similarities or differences with the oil and condensates in other wells.

Reservoir Setting

Cohasset and Panuke fields

The Cohasset and Panuke fields are located approximately 50 km southwest of Sable Island along the edge of the Abenaki carbonate bank. The light oil is reservoired in the Logan Canyon and Missisauga formations. The Logan Canyon Formation consists of four members representing regional cycles of transgression and regression (Figure 2). Cohasset field reservoirs are in the lower part of the Cree Member (Wade and MacLean, 1990) in a stacked series of thin, generally coarsening upward bar sands separated by intervals of marine shale and siltstone. Depositional environment is broadly interpreted to be lower delta plain. Panuke field reservoirs are stratigraphically older, occuring in the uppermost sands of the Missisauga Formation which are complex channel sands. Trapping mechanism is interpreted to be uplift resulting from Late Cretaceous movement by diapiric Argo Formation salt.

Venture and South Venture fields

The Venture field lies, immediately east of Sable Island and South Venture is 5 km to the southeast. The Venture area gas and condensate reservoirs are in a 1500 m thick sequence of deltaic clastics in the upper part of the Mic Mac Formation and the lower member of the overlying Missisauga formation. Generally, the sequence is regressive, in several cycles from delta front/prodelta at depth to distributary channel sands and bars and occasional back barrier and lagoon facies. As in most deltaic environments, the facies are in close association. The trapping mechanism for both fields is large rollover anticlines.

CRUDE OILS/CONDENSATES AND SOURCE ROCKS

Table 1a lists the analyzed 30 crude oil and condensate samples from the 22 boreholes along with their stratigraphic

position, depth, and reservoir temperature and facies. Table 1b lists the 5 source rock samples from 5 boreholes analyzed for this contract. It also include another five source rock data which were studied in an earlier contract. Table 3 shows the list of 34 samples from 10 different boreholes (eight core samples and 26 cuttings) for which vitrinite reflectance and fluorescence characteristics have been determined.

Analytical Procedures

For the determination of kerogen type by organic petrography, three types of sample preparation were used: kerogen smear slide, whole rock polished pellet, and kerogen polished pellet. We used incident and transmitted white and blue light excitation. The terminologies used for maceral composition and kerogen type determination, are from Stach et al. (1982, Mukhopadhyay et al., (1985), Senftle et al., (1986), Teichmuller (1986), and Mukhopadhyay (1989). Details on source-rock characterization using organic facies are shown in Mukhopadhyay and Wade (in press). Vitrinite reflectance was measured using both whole rock and kerogen pellets and Zeiss Axioskop with MPM 21 Controller for MPM 03 Photomultiplier.

API gravity was determined using standard formula (API gravity = 141.5/density at 15°C - 131.5). API gravity of crude oil and condensates presented in Table 1 are either from (1) those determined during drillstem testing or (2) determined by the subcontractor (SGS Supervision Inc.) on the samples collected recently from CNSOPB Repository at Dartmouth, Nova Scotia.

Rock-Eval pyrolysis was done on selected washed cuttings, washed/hand-picked cuttings, and from the conventional cores using Rock-Eval II instrument at the ISPG laboratory at Calgary, Alberta. Some Rock-Eval data used here, are determined using an Oil-Show Analyzer, which does not generate S_3 or oxygen index.

Bitumen extraction was done using Soxhlet for 24 hours with dichloromethane. Column chromatography was done using 1:1 silica:alumina column and pentane, pentane+dichloromethane, and methanol as solvent for saturate, aromatics, and heterocomponents. The data on the gas chromatography of the saturate fraction of the oil/condensates and whole oil light hydrocarbon fractions were received from the ISPG laboratory at Calgary, Alberta.

The stable carbon isotope of the saturate and aromatic fractions of the oil/condensate/source rock extracts were determined under a subcontract by Coastal Science Laboratories at Austin, Texas, USA. They used V. G. Micromass Mass Spectrometer. All values reported here are relative to PDB (Pee Dee Belemnite) standard. The analytical method for the aromatics GC-MS will be discussed in the 'Biomarker' chapter of this report.

The temperature data shown in Table 1a and 1b were calculated according to predicted geothermal gradient of Nantais (1983). Some true measured temperature were also incorporated.

RESULTS AND DISCUSSIONS

Figure 5 shows the location of all the analyzed samples. According to stratigraphy, the analyzed samples can be arranged as follows (Table 1a and 1b): one sample of oil and condensate each from the Wyandot Formation and Cap Rock Facies; seven crude oil/condensate samples and four source rock samples from Logan Canyon Formation or its equivalent; seven oil/condensate samples from the upper member of the Missisauga; eight oil/condensate and one source rock from the lower Member of the Missisauga; one oil/condensate from Missisauga; two oil/condensate and one source rock from the Mic Mac Formation; two source rock samples from the Misaine Member of the Abenaki Formation.

Reservoir Temperature/Facies and API gravity/GOR of Petroleum

Reservoir temperature of the oil/condensate samples varies between 50°C (Sable Island 3H-58) to 150°C (Venture B-43) (Table 1a). Formation temperature of the source rocks varies between 70°C (Cohasset A-52) to 170°C (Glenelg J-48 at 5186.7 m and S. Venture O-59 at 6105 m). The sedimentary facies of the reservoir rock from the various boreholes show a wide selection from fluvial channel sand (Panuke B-90, DST #1) to marine distal channel (Alma F-67, DST #2) (Table 1a).

Table 1a lists the API gravity of 30 samples. These data show a strong decrease in API gravity between API's determined earlier (during drilling) compared to recent analysis of storage samples. This suggests a possible evaporation loss of lighter fractions and/or possible oxidation and condensation due to biodegradation. The definition and physical nature of some of the so-called crude oils from Cohasset and Panuke structure are questionable. These crude oils contain very little NSO or asphaltene and according to their physical appearance, they can be grouped as either condensate or light oil.

Comparing the reservoir temperature and API gravity, it is observed that there is no correlation between these two parameters. At 68°C, 49.2 gravity condensate (Cohasset D-42, DST #7) is seen, whereas at 135°C, 39.0 API oil is observed at Chebucto K-90.

Gas to oil ratio or GOR is one of the basic parameter used to differentiate typical oil-reservoirs from gas-reservoirs. Gas to oil ratio associated with an oil reservoir is below 10,000. Oil generated from a source rock of Kerogen Type IIA or IIA-IIB (Kerogen Type II and II-III of Tissot and Welte, 1984), at its peak oil window, has GOR values generally less than 1,000. According to GOR, most of the Cohasset, Panuke and some Sable Island oils should have generated within the oil window. Condensates from the Arcadia J-16, Chebucto, Glenelg J-48, N. Truimph B-52 and G-43 wells are

oversaturated with gas. They are possibly derived from a matured terrestrial source rock (beyond 1.0% R_o). Condensates from Venture wells, according to GOR, can be termed as gas-reservoirs.

Source Rock Evaluation

Kerogen Type By Microscopic Methods

Figure 6-8 illustrates the petrographic characters of some of the samples from various boreholes (Alma F-67,Cohasset A-52, Cohasset D-42, Evangelene H-98, Glenelg J-48, Sable Island E-48, and S. W. Banquereau F-34). For details of the petrographic composition (in volume %), see Mukhopadhyay (1989) and Mukhopadhyay (1990). For the petrographic features and Kerogen Type of Louisbourg J-47, S. Venture O-59, and Venture B-43, see Mukhopadhyay and Wade (in press) or Mukhopadhyay and Birk (1989). Except for a few samples in Cohasset D-42, Alma F-67, Glenelg J-48, and S. W. Banquereau F-34, the overwhelming majority of the analyzed samples show abundance of terrestrial macerals like vitrinite, (both autochthonous and allochthonous), inertinite (inertodetrinite, fusinite, macrinite etc.), sporinite, cutinite, and amorphous liptinite IIB and III. As a result, most of the black shales form either Kerogen Type IIB-III and III (major gas-and minor condensate-prone source rocks (Mukhopadhyay, 1989) (Kerogen Type III of Tissot and Welte, 1984) (Figs. 6e, 6f, 7c, 7d, 7g, 7h, and 8c) or Kerogen Type IIB (major condensate- and minor gas-prone source rocks) (Kerogen Type II-III of Tissot and Welte, 1984) (Figs. 6a, 6b, 6g, 6h, 7a, 7b, 7f, 8b, 8e, and 8g). Only a few analyzed black shales contain major marine macerals like particulate liptinite A, amorphous liptinite IIA and alginite forming Kerogen Type IIA-IIB (oil & condensate-prone source rocks (Figs. 6c, 6d, 7e, 8a, 8f, and 8h) (kerogen Type of II-III of Tissot and Welte, 1984). Some rare samples show abundance (>80%) amorphous liptinite IIA forming Kerogen Type IIA (typical oil-source rock) (Type II of Tissot and Welte, 1984) (Fig. 8d). However, none of the analyzed samples show features of total anoxic environments (prolific oil-source character).

Some of the samples in Cohasset D-42 and S. W. Banquereau F-34, show an abundance of solid bitumen within the matrix amorphous liptinite (Figs. 8f and 8g). These solid bitumens are generally nonfluorescent to brown fluorescent, which are possibly formed due to later gas injection into an oil reservoir.

Kerogen typing by microscopic methods are complicated by the formation of secondary macerals due to advanced maturation. These macerals (such as rank-inertinite, solid bitumen, clustered micrinite, and micrinite; Fig. 6a and 8h) are formed at the expense of oil-generating liptinites (such as amorphous liptinite IIA, alginite, cutinite, etc.). This problem is resolved by comparing different types of microscopic preparation using advanced microscopic techniques (Dow et al., 1988; Mukhopadhyay et al., 1985; Senftle et al., 1986; Teichmuller, 1986).

Drilling mud additives (lignite, asphalt, etc.), pipe dopes, oil-base drilling fluid, and cavings from the younger horizons created further problems for kerogen typing by microscopic methods. This problem was partially resolved by hand-picking the cutting samples and using fluorescence characteristics of these contaminants.

Kerogen Type By Rock-Eval pyrolysis

A plot of hydrogen index (mg HC/g TOC) versus oxygen index (mg CO_2/g TOC) illustrates the position of sixty-one selected samples from the eight wells (Fig. 9). Similarly, Figure 10, shows a plot of hydrogen index versus T_{max}°C of selected samples from eleven boreholes. The maturation path of Kerogen Types I, II, III, and IV in Figure 9. and Kerogen Type I, II, and III in Figure 10 are from Tissot and Welte (1984) and Espitalie et al., (1985). In Figure 9, most of the Verrill Canyon samples from Alma F-67 and S. W. Banquereau F-34, lie either close to Type II or within the Type II-III maturation paths of oil-prone source rocks. A vast majority of

the Cohasset D-42 and Evangeline H-98 Logan Canyon and Missisauga Formation samples lie within Kerogen Type III gas-prone source rocks. Some of the Missisauga shales from Sable Island O-47 and Logan Canyon shales from Cohasset A-52, lie within Kerogen Type II and III oil and condensate-prone source rocks. The low oxygen index of most of the samples from the Missisauga, Abenaki, and Verrill Canyon Formations suggest possible advanced maturation. On the other hand in Figure 10, most of the analyzed samples lie in the Kerogen Type III gas-prone source rocks. Only a few samples from Verrill Canyon Formation of Alma F-67, Glenelg J-48, and S. W. Banquereau F-34 lie within Type II oil-prone source rock maturation path. The maturity determined by T_{max}, suggests that most of the samples lie within the "oil window" (430 to 465°C). Comparing both Figures 9 and 10, it is obvious that there are only a few oil-prone source rock in the Logan Canyon, Missisauga, and Abenaki Formations within our selected data set. Distal Verrill Canyon shales are obviously more oil-prone (Mukhopadhyay, 1990).

Maturation by Vitrinite Reflectance and T_{max}

Table 3 and Figure 11 shows the vitrinite reflectance and fluorescence data of 26 washed cutting samples (kerogen plugs from M. P. Avery) from S. Venture O-59 and S. W. Banquereau F-34 and 8 selected core samples (whole rock plugs) from 8 boreholes. Based on the present and earlier data (Mukhopadhyay and Wade, in press; Mukhopadhyay, 1989), the oil window (0.5% R_o) in the Sable Subbasin and surrounding area starts around 2500 to 2600m, but ends (1.4% R_o) between 4,400 to 5,600 m depending on the occurrence of overpressure. The maturation data based on vitrinite reflectance and T_{max} (Rock-Eval pyrolysis) generally corrlate well when Kerogen Type II-III and III are used. Using T_{max}, the oil window lies between 430 and 465°C. Comparing the T_{max} and vitrinite reflectance, it is observed that these two parameters correlate well when core or hand-picked cuttings samples are used. A core sample from

Cohasset A-52 (2275 m) shows a T_{max} of 430°C, which has a reflectance of 0.5%. Another hand-picked cuttings sample from Cohasset D-42 at 4425 m (14520') shows a T_{max} of 461°C, which has a reflectance of 1.36%. Most washed cuttings, which are not hand-picked, show anomalously low T_{max} due to the presence of contaminants.

Source-Rock Potential

Comparing both Rock-Eval pyrolysis and microscopic analyses of these selected samples, the source rock potential can be assigned to the following:

(a) Presence of multiple mature source rocks of Kerogen Type IIA (oil-source), IIA-IIB (oil-condensate-source), IIB (condensate-gas-source), IIB-III (gas-condensate source), III (gas-source), and IV (non-source rock) below 2,200 m. However, in the distal Verrill Canyon Formation, the overwheming majority of the analyzed mature source rocks are of Kerogen Type IIB, IIB-III, and III.
(b) Possible presence of thin and local oil prone, mature Kerogen Type IIA-IIB in the Logan Canyon, Missisauga, Abenaki (Misaine Member) Formations, which could be the source for Cohasset and Sable Island light oils.

THE RELATION BETWEEN OVERPRESSURING AND MATURATION PARAMETERS

An extensive area with very high overpressures has been encountered within thick, normally compacted, sandstone and shale sequences in the Abenaki and Sable Subbasins (Fig. 12). More than 40 wells have drilled into this system. Analyses of the Scotian Shelf occurrences indicate that rapid burial or shale diagenesis is not the sole cause of the overpressure. The top of the overpressured system is generally shallowest and youngest to the southwest (Aptian/Barremian at 3000-3500 m) and deepest and oldest to the northeast (Callovian and older at >4800 m). This pattern is attributed to the propagation of the overpressure through the many

listric normal faults which cut the section.

In most wells, the top of the overpressure is manifested by a sharp increase in pressure gradient through a transition zone and then a return to a lower gradient once the top of full overpressure is reached. In the Venture Field the total overpressure zone is more than 1200 m thick and its base has not been encountered. The maximum overpressure encountered in this area is 118,000 kPa at a depth of 5700 m.

In most of the boreholes, which encountered overpressuring, vitrinite reflectance profile shows a kinky appearance with a sharp increase in reflectance gradient. This abnormality in vitrinite reflectance is possibly caused due to perturbation of the thermal gradient caused by heat transfer processes associated with the development of abnormal pressure. Conductive heat transfer may be considered as the major processes of the vitrinite reflectance gradient kink, which is related to the top of the overpressuring (Law et al., 1989). Figure 13 shows the relationship between vitrinite reflectance, depth (m), and pressure (KPa) from two boreholes on the Scotian Shelf (S. Venture O-59 and Louisbourg J-47); in both boreholes, the kink in vitrinite reflectance gradients are quite obvious. However, in Louisbourg J-47, the top of the overpressure is directly related to the sharp increase in vitrinite reflectance, whereas, in S. Venture O-59, the change in vitrinite reflectance gradient started 300-400 m deeper than the top of the overpressure. This may suggest that in S. Venture O-59, the top of the overpressure was deeper and propagated through time. This supports the view of Wade and MacLean (1990), who assumed that original top of the overpressured system was deeper and subsequently forced upward.

The cause of overpressuring in the Scotian Shelf is not yet been resolved. Mudford and Best (1989) emphasized that disequilibrium compaction is responsible for much of the

overpressuring at least in the Venture Gas field. On the other hand, Wade and Maclean (1990) suggested that recent active gas generation would result overpressuring. Wade and Maclean (1990), however, also interpreted that hydrocarbon generation from Middle Jurassic source rocks associated with rapid burial could have caused excessive thermal expansion of fluids and increased the level of overpressuring. This view was supported by Jansa and Urrea (1990), who emphasized that the formation of dynamic diagenetic barriers within the zone of peak gas generation helps retard the diffusive migration of hydrocarbons and other fluids expelled during shale diagenesis resulting in pressure build up.

Considering a possible relationship between gas generation and overpressuring in the Scotian Shelf, we plotted the depth of 1.0% R_o (starting of the peak gas generation, Tissot and Welte, 1984) and the depth of the overpressuring from some selected boreholes (Fig. 14). In most of boreholes in the Sable Island area, the top of the overpressure zone is shallower than the 1.0% R_o. In the eastern part of the Sable Subbasin, the top of the overpressure zone is deeper than 1.0% R_o. This possibly suggests that overpressuring is older in the eastern part than the Subbasin. We did not observe any overpressuring where 1.0% R_o is shallower than 4000m. The relationship between these two parameters (top of overpressure zone and vitrinite reflectance) is still unknown and at present is under study.

Earlier studies on organic facies and maturation show fluorescence of organic matter both in the kerogen concentrate and some core samples, which are close to and beyond 1.4% R_o (Mukhopadhyay and Wade, in press). These sediments are either overmature or near the end of the "oil window" and should not show any exinite fluorescence (Stach et al., 1982). Since most of the earlier analyzed samples were cutting samples and can be contaminated by cavings or drilling mud additives, we studied fluorescence on eight core samples collected from depths below 5000

m. Table 3 shows the fluorescence characteristics of 34 samples; 8 are core samples. According to the reflectance data, only two samples (S. Desbarres O-70: R_o = 1.61 - overmature; W. Chebucto K-20: R_o = 1.37 - near end of oil window) are suitable for this special study. The sample from S. Desbarres O-76, which has the highest reflectance, shows distinct yellow to red groundmass fluorescence. Some degraded phytoplanktons (amorphous liptinite) also shows red fluorescence. The W. Chebucto K-20 sample shows very strong yellow (oil-like) fluorescence of the groundmass. It definitely shows at least one large alginite grain with red fluorescence. These data suggest a retardation of alginite fluorescence and possible extension of the oil window due to overpressuring. The groundmass bitumen was not changed to pyro-bitumen, which suggests that overpressured rocks possibly retain the "live oil-like substance" still in their matrix. The alginite fluorescence can also be caused by secondary infitration of these "live bitumens" into the alginite.

GENESIS OF THE LIQUID HYDROCARBONS AND OIL-SOURCE CORRELATION

Liquid and Gas Chromatography of Crude/Condensates and Source-Rock Extracts

The gross composition of all the analyzed light oils and condensates shows that all these samples contain more than 95% hydrocarbons and mostly less than 5% nonhydrocarbons. This is substantially lower than the average composition of crude oils (Tissot and Welte, 1984) and may suggest that either these oils are derived from mature source rocks, whereby most of NSO and asphaltenes are cracked, or that all of these "oils" can only be termed as condensates. However, for our general use, we call them light oil and condensate.

Liquid chromatographic data of the light oils and condensates

suggest that these samples can be genetically classified into three groups: (a) samples which have more than 70% saturate fraction; typical examples are Cohasset and Sable Island light oils, (b) samples which have more than 60% aromatic hydrocarbons and very low saturate aromatic ratio; typical examples are Chebucto K-90, Banquereau C-21, N.Truimph B-52 condensates, (c) samples which have more or less equal amounts of saturate and aromatic fractions; typical examples are S. Venture O-59, DST#10, Primrose N-50, DST#1, Sable Island E-48, DST#16. This abundance of aromatic hydrocarbons in some petroleum may be caused by either biodegradation (selective removal of saturates) or generation from terrestrial organic matter.

Figures 16a through 16g show gas chromatograms of the saturate fraction of some of the selected oil samples. The n-alkane distribution pattern of all samples show a very similar trend. All the light oil or condensate samples have predominantly low-molecular weight hydrocarbons (less than C_{20}) and peak of the n-alkane distribution lies either at C_{14} or C_{15}. These n-alkane distribution patterns suggest their possible origin from a marine organic matter. High pristane/phytane ratios (>2.5) in the same samples (Cohasset A-52, DST#2 & 3; Panuke B-90, DST #1; Thebaud C-74, DST # 4) suggest oxidation due to either biodegradation in the reservoir or derivation from a source rock which was partially oxidized. Saturated hydrocarbon biomarkers like triterpane or sterane between C_{27} and C_{33} are either absent or present in very minor amount.

Stable Carbon Isotope of Saturate and Aromatic Fractions

Stable carbon isotopes have been widely used as a tool for oil-oil and oil-source rock correlation (Tissot and Welte, 1984; Sofer, 1984; Sofer et al., 1986). Tables 2a and 2b show the stable carbon isotope data of the saturate and aromatic fractions of the light oil/condensate and source-rock extracts. These data are

plotted in the Figures 17a, 17b and 17c. The dividing line drawn in Figure 17a and 17c is from the linear equation evolved by Sofer (1984) to distinguish between waxy (terrestrial) and nonwaxy (marine) oils, which is as follows:

$$del^{13}C_{aro} = 1.14\ del^{13}C_{sat} + 5.46.$$

Figure 17b plotted the isotopic data only from the analyzed light oil and condensate samples. The best-fit linear equation for these samples is as follows:

$$del^{13}C_{aro} = 1.078\ del^{13}C_{sat} + 3.54$$

Sofer (1984) from the "Y" intercept defined two distinct linear equations, one for waxy (terrestrial) and another for nonwaxy (marine) crude oils. The best-fit linear equation from the Scotian Shelf light oil and condensate samples (Fig. 17b) is very close to the nonwaxy oils as defined by Sofer (1984).

The position of the samples in Figure 17b, shows a broad variation of isotopic composition between -28‰ to -26‰ for the saturate fraction and between -28‰ to -24‰ for the aromatic fraction. The plot suggests two possible clusters indicating presence of two oil families. The first group contains samples 1, 6, 7, 8, 16, 20, 25, 28, and 29. Most of the oil samples from Cohasset & Panuke, one sample each from Sable Island, Olympia, and Thebaud belong to this group. The second group contains samples 2, 3, 9, 14, 15, 18, 24, and 26, which are from N. Truimph B-52, S. Venture O-59, Arcadia, and Venture B-43. Two samples from Primrose and Sable Island are not clustered in any of these groups, so also one sample each from Olympia and Citnalta. This third group of samples occurs more towards the positive part of the saturate isotope suggesting more marine or non-waxy origin of these oils or condensates. Sample 11 (Cohasset A-52, DST#5) is totally different from all other samples. Sofer (personal communication, 1990)

suggested that maturation trend points toward the positive part of the isotope data. Accordingly, Cohasset A-52, DST#5 is the least mature and Glenelg J-48, DST#9 shows the highest maturity.

Figure 17c shows the isotopic composition of the source rock extracts from the analyzed five samples and our earlier data (Mukhopadhyay, 1989). The vitrinite reflectance data of these samples also corroborates the maturation trend as suggested by Sofer (personal communication, 1990). However, they do not match the possible maturation of the oils. According to these data, only sample 'b' (Cohasset D-42, 4410 m) may support some correlation with the oils in Cohasset and Panuke field. Sample 'd' (Alma F-67, 4500m) is isotopically totally different from any of the petroleum or source rock extracts. This abnormality is possibly caused by contamination of base-oil during drilling with oil-base mud.

In summary, the isotope and liquid chromatography data indicate: (a) the presence of two oil families separating Cohasset-Panuke oils from the Venture condensates, (b) A part of these oils are possibly derived from nonwaxy source rocks (lacustrine and marine), (c) the analyzed source rocks do not correlate properly with the oil or condensates.

Biological Markers: Aromatic Hydrocarbons

In the last two decades, great advances have been made in the application of biological marker compounds to the determination of maturity and organic facies of sedimentary organic matter. However, these compounds, generally polycyclic alkanes, cannot always present a complete picture. For example, maturation indicators based on the saturate hydrocarbons are ineffective in samples at mid to late oil window maturity levels.

The aromatic fractions in fossil fuels provide many additional clues. A wide variety of polyaromatic compounds has been documented

in fossil fuels (Later et al., 1981; Radke et al., 1984b; Rowland et al., 1984; Whitehurst et al., 1982; White and Lee, 1980). Distribution of these compounds have been shown to be sensitive to maturation (Alexander et al., 1983; Radke, 1987; Radke et al., 1980; 1982a; 1982b; 1984a; 1986). In particular, the methylphenanthrene Index (MPI) of Radke and Welte (1983) has been proven useful in maturity assessment, particularly in the middle to late oil window range. More recently, Kruge and others (1989; 1990a; 1990b) have documented the maturation and organofacies sensitivity of a series of polyaromatic molecular markers in marine shale extracts, coal extracts, and coal pyrolysates.

Some of the probable Scotian Shelf source rocks and condensate lie or derived in/from the late catagenetic stage (>1.0% <2.0% R_o) (source rock data, this report; Snowdon and Powell, 1979; Powell, 1983; Mukhopadhyay and Wade, 1990). Aromatic biomarkers of selected Scotian Basin oils, condensates, and source-rock extracts were, therefore, analyzed by gas chromatography/mass spectrometry (GC/MS) to determine levels of thermal maturation and, as far as possible, to correlate the oils and condensates with one another and with candidate source rocks.

The analyzed aromatic fraction of five oils, five condensates and four source rock extracts are listed in Table 4 . The location of these fractions are shown in Figure 18.

Instrumentation

The aromatic fractions were analyzed by a Hewlett Packard 5890A gas chromatograph, coupled to an HP 5070B Mass Selective Detector at the Geochemistry Laboratory of the Southern Illinois University at Carbondale. The GC was held at 100°C for 10 min., then raised to 300°C at 3°/min., where it was held for 5 minutes. A 25 m OV-1 column with 0.2 mm inside diameter and 0.33 μm film thickness was employed. The mass spectrometer was run in selective ion monitoring mode, collecting data on the following ions: m/z 91,

156, 162, 168, 169, 170, 182, 184, 192, 196, 198, 202, 206, 212, 216, 220, 228, 230, 231, 242, 252, 253, 256, 268, 282, 296, and 310, which are either the molecular ions of the most common polyaromatic compounds or are principal fragment ions of aromitized biomarkers, such as steriods. Two samples were rerun using full scan mode, to confirm that all principal aromatic peaks were being recorded. Quantitations were done on the molecular ions of the compounds of interest, using the selected ion monitoring data and the Hewlett Packard data system.

A total of 79 GC peaks representing polyaromatic compounds were recognized and quantified individually in each of the fourteen samples, along with ca. 25 additional peaks (varying from sample to sample), which were quantified collectively on m/z 206, 242, and 256 mass chromatograms. The polyaromatic peaks are often clusters of isomers that cannot be specifically identified due to the similarity of their mass spectra and the lack of commercially available authentic standards. However, most of the members of each cluster can easily be separated by GC. For example, we can recognize 10 principal C4-substituted naphthalene peaks, but absolute structural assignments cannot be made. Variations in peak distributions from sample to sample can nevertheless provide much useful information. A variety of peak ratios were computed, principally to illustrate maturation differences.

Due to great number of chromatograms generated from this large data set, visual comparisons were not sufficiently effective for petroleum-to-petroleum or petroleum-to-source rock correlation. To develop signatures for each sample, the main peaks of each of the principal isomer clusters were chosen (Figures 19-21). These peaks were then quantitated and raw peak area data was normalized to the most intense peak in each cluster. The normalized data for each ion cluster could then be presented in simple graphic form. Figure 22 illustrates these first three steps in data reduction. The curves for each of the isomer groups can then be chained together in a

single plot, the composite polyaromatic Trace (CPT), serving as an aromatic "fingerprint" for each sample (Figure 23).

For purposes of sample correlation, we employ a method which combines graphical and computational techniques. The CPT diagram of any sample can be subtracted from that of any other, since each of the constituent cluster curves are normalized to a maximum value of 1.0. If a cluster curve of one sample is similar to that of the other, the curve remaining after subtraction will be near zero (Figure 24a). The remainder from the subtraction of dissimilar cluster curves will show high amplitude fluctuations (Figure 24b). Entire CPT diagrams can be readily compared to one another by the subtraction method.

Maturity Determinations

The Methyl Phenanthrene Index (MPI) of Radke and Welte (1983), a well established maturity parameter, can be computed as follows:

$$\frac{1.5\ (3\text{-mPH} + 2\text{-mPH})}{(\text{Phenanthrene} + 9\text{-mPH} + 1\text{-mPH})}$$

where "mPH" stands for methylphenanthrene, such that the parameter increases with increasing maturity. Phenanthrene is quantitated on m/z 178 mass chromatograms and the methylphenanthrenes, on m/z 192. Our results show that most of the Nova Scotian samples fall into the range of 0.7 to 0.9, the exceptions being Sample 8 (1.25) on the upper end of the MPI-scale (Table 4).

At post-oil generation levels of maturation, the MPI values actually decrease (Radke and Welte, 1983), even though 2- and 3-mthylphenanthrenes continue to increase relative to the 1- and 9-methyl isomers, due to the increase predominance of phenanthrene at the high levels of maturity. Thus, the ratio of 2-methyl to 1-methylphenanthrene was computed to have an additional maturity parameter and to be able to check for the retrograde MPI condition.

The results of the calculation of this ratio are in basic agreement with the MPI, except that oil sample 5 is added to the low maturity group and extract samples 12 and 13 are placed in the high maturity group. The core of the moderately mature petroleums is still present. Figure 25a is a crossplot of the MPI with the 2-/1 methylphenanthrene ratio. Samples 11 and 4 are clearly the in the low maturity field according to both ratios and Samples 14 and 8 are high. Samples 1, 2, 3, 6, 7, 9, and 10 (Table 4) are indisputably in the middle range, corresponding to near peak or peak oil window levels of maturation (equivalent vitrinite reflectance of ca. 0.8%, Radke et al., 1984a). The designation for Samples 5, 12, and 13 are less straightforward, but they are probably also not far off from a mid oil window range.

For yet a third maturation parameter, the ratio of chrysene to benzo(α)anthracene is used, shown to be an effective parameter which increases with maturation within the oil window from ca 0.5 to 1.0 (Kruge et al., 1989). The tetraaromatic chrysene has a ring offset in the middle of its structure, whereas benzo(α)anthracene has 3 rings in a straight row with an offset between the third and fourth rings, giving it greater instability. Thus, benzo(α)anthracene is preferentially lost relative to chrysene as maturation increases. The ratio confirms that Sample 11 is the least mature and Samples 14 and 8 are the highest. The Samples 1, 3, 6, and 12 are shown to be at intermediate maturity levels, whereas samples 7, 9, and 13 are moderately higher and samples 2, 4, 5, and 10 are lower than the core mid-range group. Cross-plotting this ratio with the MPI (Figure 25b) shows that among the mid-range group, oil samples 2, 3, 4, and 5 are overall lower than petroleum samples 1, 6, 7, 9, and 10 and extract samples 12 and 13. Extract sample 11 is clearly the lowest maturity of all samples, in the early stages of oil generation. Extract sample 14 and condensate sample 8 are indisputably the highest, at late or post oil window maturity levels.

Polyaromatic Heteroatomic Compound Content

The concentrations of dibenzothiophene and its homologous are extremely variable in the suite of samples. This is exemplified by the ratio of dibenzothiophene (peak labelled DBT on the m/z 184 trace in figure 19) to the sum of dibenzothiophene and all tetramethylnaphthalenes (peaks labelled C1 to C10, m/z 184). Dibenzothiophene is the dominant m/z 184 peak in extract Samples 12 and 14 and is also strong in Sample 13. In contrast, dibenzothiophene is not detectable in oil Samples 2, 3, 4 and 5. The remaining petroleum samples and rock Sample 11 have intermediate dibenzothiophene contents, as indicated by values of the ratio around 0.1.

Another heteroatomic compound group is the dibenzofuran homologous series. There is again considerable variation in relative concentrations of the dibenzofurans. This may be expressed by the ratio of the three methyldibenzofuran peaks (labelled MDBF on the m/z 182 chromatogram in Figure 21) to the dimethybiphenyl isomers shown in the same chromatogram as peaks D1 through D6. Condensate Sample 8 has a value of 0.09 for this ratio, the lowest in the sample set. Samples 2, 3, 4, and 5 have values between 0.2 and 0.3. The remaining petroleums and the extracts have higher values, ranging between 0.4 and 0.6.

Figure 26 is a crossplot of dibenzothiophene and dibenzofuran ratios. Several groupings are apparent on this chart. Oil Samples 2, 3, 4, and 5 plot closely together, defining a non-thiophenic, moderately furanic sample type. Among the samples richer in furans, extract Samples 12 and 14 stand out as being exceptionally thiophenic. Petroleum Samples 1, 6, 7, 9, and 10 also plot closely together with high furan content, but moderate organo-sulfur contents. Extract Sample 13 and low maturity extract Sample 11 plot near this last petroleum group, but somewhat enriched in methyldibenzofurans and dibenzothiophene. The high maturity

condensate Sample 8 plots alone, with moderate furan and thiophene contents. These heteroatomic parameters reflect the degree of incorporation of sulfur and oxygen into the organic matter of the petroleum source rocks, which in turn reflects the depositional environment and the diagenetic history of the organic matter.

On the basis of these data, we can provisionally group the petroleums into a thiophenic (i.e moderately sulfur-rich) and furanic group (Samples 1, 6, 7, 9, and 10) and into a non-thiophenic (low-sulfur) and low furanic classification (Samples 2, 3, 4, and 5). Condensate Sample 8 matches the sulfur content of the higher sulfur group, but lacks their high furan content. It still may be included in the sulfur group with its lack of furans explained by its extraordinarily high maturation level. The extract Samples 12 and 14 are exceptionally rich in thiophenic sulfur in spite of their elevated maturity levels and as such resemble high sulfur marine organic matter. Extract Samples 11 and 13 more closely resemble the thiophenic petroleum samples in their thiophene and furan contents. The moderately thiophenic petroleum can be designated as "Group 1" and the non-thiophenic as "Group 2".

Since there is the possibility of an early Mesozoic rift basin in the area of the wells (Lorenz, 1988), it is interesting to compare the Nova Scotian crude oil and condensates with extracts of organicrich syn-rift lacustrine rocks of the Newark Supergroup. Group 1 oils are indeed similar in thiophene distribution to the Jurassic lacustrine black shales of Connecticut. Group 2 oils are not similar, but could conceivably be source from low sulfur nonmarine source rocks. Group 2 oils do not resemble land plant-derived material (i.e. they are not coal like), since their m/z 178 and 192 traces show vary little, if any, anthracene and methylanthracene. Anthracenes are present in coal extracts with ranks ranging from pre to mid oil window and as such are excellent molecular markers for terrestrial organic matter (Kruge et al. 1990a). The S. Venture O-59 and Cohasset D-42 extracts are also

dissimilar to the Connecticut specimens, instead resembling marine source rocks in the sulfur content.

Distribution of Polyaromatic Hydrocarbon Isomers

To further test the validity of this classification, the distributions of eight polyaromatic hydrocarbon isomer groups were examined. These include diaromatic compounds, namely six dimethylnapthalene peaks (m/z 156), ten peaks of trimethyl and other possible C3-substituted naphthelene (m/z 170), ten peaks of tetramethyl and other possible C4-substituted naphthalenes (m/z 184), and six dimethylbiphenyl isomers (m/z 182). Also there are the condensed tetraaromatics pyrene and fluoranthene (m/z 202), along with eight unidentified, but consistently appearing peaks on the same chromatograms, seven m/z 216 peaks, collectively identified as methylfluorene, methylpyrene, and/or benzofluorene isomers, and eleven dimethylfluorene, dimethylpyrene and/or methylbenzofluorene peaks on m/z 230. Four m/z 252 peaks, probably isomers of the pentaaromatic hydrocarbon benzo(a)pyrene complete the list. All these peaks are illustrated on appropriate partial mass chromatograms in Figure 1-3. Triaromatic hydrocarbons such as the isomers of methyl and dimethylphenanthrene were not used due to the known sensitivity of the isomer distributions to maturation, particularly the methyl homologues (Radke and Welte, 1983). Linear tetraaromatic hydrocarbons (chrysene isomers) were discussed above as maturation indicators and so were not used for correlation purposes, although in future studies, higher chrysene homologues may be employed.

For each of the 14 samples, as stated in the Instrumentation Section, these 54 peaks were quantitated and their peak areas were normalized, so that the most intense peak in each of the eight isomer clusters was assigned a value of 1.0. All 8 normalized

cluster curves of a sample can be displayed on one Composite Polyaromatic Trace (CPT), as with the example in Figure 4. To facilitate correlation, it is expedient to go one step further. The CPT of one sample can be subtracted from that of another and the remainders plotted. If the correlation is a good one, the remainders will be closed to zero. Graphically, the trace will meet the horizontal axis. If the match is poor, the subtracted trace will deviate widely from the zero line. Figure 24 illustrates this principle, using the trace of only one ion, m/z 170 for simplicity. When the m/z 170 cluster trace of Sample 1, a member of petroleum Group 1, is subtracted from that of Sample 10, also part of Group 1, the remainder trace is so close to zero across its length, that it is difficult to distinguish it from the horizontal axis. In contrast, subtracting the same cluster trace of Sample 1 from that of extract Sample 14 yields high amplitude deviations on the zero line, indicating a lack of correlation. The fit can also be expressed mathematically, with the parameter, α (alpha), defined as the average of the absolute values of all points in a subtracted trace. For the simple example in Figure 24a, $\alpha = 0.02$, indicative of an excellent correlation, whereas in figure 24b, $\alpha = 0.29$ demonstrating a poor match.

The CPT of Sample 1, as a representative of Group 1 petroleum, was subtracted from the CPT of all other petroleum samples. The resulting remainders are displayed graphically in Figure 27. The other Group 1 petroleums (Samples 6, 7, 8, 9, and 10) show CPT remainders that for the most part, rest close to the zero mark. Samples 7 and 10 are especially good matches with Sample 1. With Sample 6 there is significant devaition only for two m/z 230 peaks (curve G). Samples 8 and 9 show particular divergent from null value in curve E, the m/z 202 trace. This trace has a somewhat lower confidence level, due to presence of unknown compounds, not normally seen in the aromatic fractions processed in this laboratory. For Samples 6 through 10, α values are 0.06, 0.05, 0.09, 0.08 and 0.06, all indicating reasonable correlation.

The results of the subtraction of the CPT of Sample 1 from those of the Group 2 oils show considerably more divergent (figure 27). Moderate amplitude are present in all curves, except for curve D m/z 182. It is interesting to note that the shape of the sibtracted curve D is about the sample in the Group 2 profiles, suggesting the correctness of maintaining the Group distinction - they all diverge from Sample 1 in the same fashion. There are high amplitude digengences as well in traces E and H (m/z 202 and 252). Numerically the deviation of Samples 2, 3, and 4 from Sample 1 ranges from α values of 0.13 to 0.14. Sample 5 is somewhat more divergent, as $\alpha = 0.17$.

To test the validity of Group 2 designation, the CPT of its Sample 4 was subtracted from that of other (Figure 28). The CPT remainder of Sample 2 shows only low amplitude deviation from the zero line. Its D trace (m/z 192) matches so well that it nearly indistinguishable from the axis. With $\alpha = 0.06$, it correlates well overall with sample 4. Most of the variability of sample 3 is with four peaks in the E trace (m/z 202) and two in the H trace (m/z 252). The high amplitude divergence of these six peaks is sufficient to drive the α value up to 0.11. Sample 5 exhibits a broad-based moderate divergence, especially among the naphthalenes (A, B, and C traces) and again m/z 202 and 252, accounting for the moderately high α value of 0.12. Dimethylbiphenyls and the substituted tetraaromatics (traces D, F, and G) though are quite close to the axis, indicating that Sample 5 bears both significant differences and similarities to Sample 4. Discounting the suspect m/z 202 trace, it can be concluded that Samples 2, 3, and 4 are reasonably similar to one another and Sample 5 is somewhat more distant related.

The subtractive technique can also be applied to oil-source correlation. The CPT of oil Sample 1 was subtracted from that of the four candidate source rock extracts (Figure 29a). The CPT remainder of Sample 11 shows high amplitude divergence across its

length, with α = 0.23. The variability is moderated in the naphthalene and pentaaromatic traces in Samples 12, 13, and 14 perhaps reflecting maturation-related isomer redistribution. However, Samples 13 and especially 14 show increased amplitude in the tetraaromatic traces, giving both high α scores of 0.21. Sample 12 with a moderately high α value of 0.16, still correlate poorly with oil Sample 1. In correlating the extracts with Group 2 oils, through subtraction of the CPT of Sample 4, the resulting α scores are also high, ranging from 0.17 to 0.23, indicating poor correlation, not unexpected from due to their vastly different organo-sulfur contents.

Examination of Figure 29a reveals similarities in the shapes of the constituent curves of the composite traces remainders of the extracts, for example, curves B and F in Samples 13 and 14. The CPT of Sample 13 was subtracted from those of the other extracts to evaluate these similarities more directly (Figure 29b). Moderate to high amplitude variations in the remainder trace of Sample 11 and α score of 0.018 indicate a lack of correlation, probably exacerbated by the low maturity of this sample. Sample 12 and especially Sample 14 show only moderate amplitude deviations across their length and have correspondingly moderate a (scores) of 0.14 and 0.10 respectively indicating some similarity with Sample 13. This assessment is made without knowledge of the stratigraphic relations of these samples or of any similarities their depositional environments may have had.

CPT diagrams were not made for the Newark Supergroup lacustrine rocks discussed above, but visual comparison were made of their chromatograms with those of the Nova Scotia Offshore samples. The Group 1 petroleums match only in some categories and the Group 2 oils match poorly. This is not a thorough comparison and the concept should be persued further, ideally using the molecular markers in the saturate fractions as well.

Light Hydrocarbon Gas Chromatography

Figure 30 shows the distribution of light hydrocarbons from three selected crude oil and condensate samples from three boreholes. One of them (S. Venture DST #11) does not belong to to our studied sample set. These data was received from Dr. M. G. Fowler, ISPG, GSC, Calgary, Alberta. These data shows the presence of several saturate and aromatics light hydrocarbons such as toluene, nC_7, methylcyclohexane in these three samples. Toluene is generally derived and dominant in the terrestrial organic matter and is generally absent in lacustrine or marine aquatic organic matter. Figure 30 shows the absence of toluene in Cohasset D-42 (DST #7) sample suggesting possible aquatic origin of this oil; N. Truimph B-52 (DST #4) sample, in contrary, shows an abundance of toluene suggesting terrestrial origin of this oil. S. Venture condensate with a mixed toluene and methylcyclohexane is possibly derived from a mixed marine and terrestrial organic matter.

SUMMARY AND CONCLUSIONS

Source-Rock-Characterization

According to our existing data based on advanced microscopic techniques, Rock-Eval pyrolysis, and Elemental Analysis of various organic-rich sediments, the following characteristics on the various source rocks could be established.

(a) There are multiple mature source rocks of Kerogen Type IIA (oil-source), IIA-IIB (oil-condensate prone), IIB (condensate-gas prone), IIB-III (gas-condensate prone), III (gas prone), IV (non-source), below a depth of 2200 m. However, except in the distal Verrill Canyon Formation, the overwhelming majority of the analyzed samples are Kerogen Type IIB, IIB-III, and III (Kerogen Type IIA, IIA-IIB, IIB, IIB-III are equivalent to Kerogen Type II, II-III, III respectively of Tissot and Welte, 1984).

(b) Thin and local oil-prone mature source rock of Kerogen Type IIA-IIB in the Logan Canyon (or its equivalent Shortland Shale), Upper Missisauga, and Abenaki (Misaine Member) Formations, could be the source for light oils in Cohasset, Panuke and Sable Island Structures.

(c) The base of the 'Oil Window' (1.4% R_o) varies between 4400 m at Cohasset D-42 to 5700 m at S. Venture O-59. Vitrinite reflectance is related to lithologic association and thermal conductivity/heat flux related to overpressuring.

Relation between Overpressuring and Maturation Parameters

(a) Below the top of the overpressure zone, vitrinite reflectance shows sudden increase in gradient ('kinky' appearance). Conductive heat transfer may be considered as the major process associated with the development of abnormal pressure. The relation between top of overpressure and vitrinite reflectance 'kink' suggests that in some boreholes the overpressure is older than the present 'top' and migrated through time.

(b) The relation between 1.0% R_o (onset of major gas generation) and the top of the overpressure suggests a possible relationship between gas generation and overpressuring.

(c) In the overpressure zone, organic matter (especially the groundmass) preserves fluorescence suggesting the presence of 'live oil or bitumen' in the so-called overmature zone or near the base of the oil window (1.3 to 1.7% R_o). This suggests the possible presence of more condensate and light oil between 4500 to 6000 m depth in the Scotian Basin, if suitable reservoir and seal are present.

Quality, Maturation and Genesis of Petroleum

The limited analysis of various light oil and condensate samples suggest the following:

(a) There is no relationship between the API gravity and reservoir temperature. According to the overwhelming dominance of hydrocarbons (>95%), all the liquid hydrocarbon samples should be considered as condensate or light oil. This may also suggest a possible gas injection at a later phase into an oil reservoir, which reduces the asphaltene and heterocomponents in the petroleum.

(c) Based on liquid chromatography and stable carbon isotope data, the petroleum samples can be divided into two families. Family I is high aliphatic-rich and possibly less mature; most of the Cohasset-Panuke oils, and some of the Sable Island oils belong to this family. Family 2 contains high aromatics and possibly more mature; S.Venture O-59, Glenelg J-48, Chebucto K-90, Arcadia J-16, Venture B-43, N. Truimph B-52, belong to this family. Two Sable Island and Primrose oils belong to neither of these families. At this stage, it is not evident whether they can be grouped into another Family or not. According to the maturity trend based on isotopes, Cohasset A-52, DST #5 is the least mature and Glenelg J-48, DST #9 is the most mature.

(d) The methylphenanthrene Index and the ratio of chrysene to benzo(α)anthracene from the aromatic GC-MS indicate that most of the petroleum samples have a maturity level corresponding to the middle of the oil window (MPI: 0.7 to 0.9). Accordingly, Cohasset-Panuke-Sable Island petroleums are less mature than the S. Venture, Venture, and other samples. Cohasset A-52, DST #5 has the lowest maturity and the South Venture O-59 (DST#5) condensate has the highest maturity.

(e) Based on aromatic GC-MS data, the petroleum may be classified as "moderately thiophenic" Group 1 (Chebucto K-90; N. Truimph B-52; Olympia A-12, DST#5; Glenelg J-48, DST#8; and both S. Venture O-59

samples) and as "non-thiophenic" Group 2 (Cohasset D-42, DST#7, Cohasset A-52, DST#5, Sable Island 3H-58, DST#5, Panuke B-90, DST#1). Group 1 classification is supported by the similarity in the distribution of polyaromatic hydrocarbon isomers among its members. Group 2 shows more variability, although the two Cohasset petroleums correlate very well. Some of the Group 2 petroleums are possibly derived from lacustrine source rocks, which can be developed with the Logan Canyon and Missisauga lower delta plain environments.

(f) Light hydrocarbon gas chromatography data clearly differentiate the Cohasset D-42 light oil from N. Truimph B-52 condensate based on the ratio of toluene and methylcyclohexane. Cohasset oil is most probably originated from aquatic source rock and N-Truimph is from terrestrial source.

ACKNOWLEDGMENTS

The author acknowledges John A. Wade of Basin Analysis Subdivision, Atlantic Geoscience Centre, Bedford Institute of Oceanography, Dartmouth, Nova Scotia for his contribution to the geology part of the report and several fruitful discussions for this report. The author acknowledges M. P. Avery of Atlantic Geoscience Centre for kerogen plugs and some computer drafting. The author acknowledges Steven Bigelow of CNSOPB and Mary-Jean Verrall of COGLA for their permission and assistance for sample collection. The author acknowledges Dr. Michael A. Kruge of Southern Illinois University, Carbondale, Illinois, USA for the aromatic gc-ms part of this report. The author acknowledges the help of M. G. Fowler and Sneh Achal of I. S. P. G., Calgary, Alberta for their help at the laboratory and the gas chromatography data. The author acknowledges Zvi Sofer of Amoco Research Center at Tulsa for the fruitful discussion on the isotope data.

REFERENCES

Alexander, R., Kagi, R. I., and Sheppard, P. N. 1983. Relative abundance of dimethylnaphthalene isomers in crude oils. Jour. Chrom. v. 267, p. 367-372

Alexander, R., Cumbers, K. M. and Kagi, R. I. 1986. Alkylbiphenyls in ancient sediments and petroleums. Org. Geochem. v. 10 (1-3), p. 841-845.

Barss, M. S., Bujak, J. P., Wade, J. A., and Williams, G. L., 1980, Age, stratigraphy, organic matter type and color, and hydrocarbon occurrences in forty-seven wells offshore eastern Canada. Geo. Surv. Can. Open File Report 714; 6p.

Bujak, J. P., Barss, M. S., and Williams, G. L. 1977. Offshore eastern Canada - Part I and II: Organi type and color and hydrocarbon potential, Oil and Gas Journal, v. 75 (15), p. 96-100 and p. 198-202.

Cassou, A. M. Connan, J., and Borthault, B., 1977. Relationships between maturation of organic matter and geothermal effect, as examplified in Canadian East Coast Offshore wells. Bull. Can. Pet. Geol. v. 25, p. 174-194.

Dow, W. G., Mukhopadhyay, P. K., and Jackson, T., 1988. Sourcerock potential and maturation of deep Wilcox from south-central Texas. Bull. Amer. Assoc. Petrol. Geol. v. 72 (2), p. 179.

Espitalie, J., Deroo, Cr., and Marquis, F. 1985. Rock-Eval pyrolysis and its applications. Report Institut Francais du Petrole No. 33878, 72 p.

Jansa, L. F. and Urrea, V. H. N. 1990. Geology and diagenetic history of overpressured sandstone reservoirs, Venture Gas Field, Offshore Nova Scotia, Canada. Bull. Amer. Assoc/ Petrol. Geol. v. 74 (10), p.1640-1658.

Jones, R. W. 1987. Application of organic facies for hydrocarbon potential. In. Advances in Petroleum Geochemistry (Brooks, J., ed.)v. 2, p. 1-90.

Kruge, M. A., Bensley, D. F., and Crelling, J. C. 1989. An organic geochemical and petrologic study of a suite of sporinite-rich coals from the Lower Kittanning Seam, Upper Carboniferous, USA. Int. Conf. Coal Formation, Occurrence and Related Properties, Orleans, Abs. no. 9.

Kruge, M. A. Bensley, D. F. and Adams, J. P. 1990a. Comparison of the behavior of molecular maturity parameters in coal and marine shale extracts. 199th American Chemical Society National Meeting,

Boston, Div. of Geochemistry. Abs. no. 10.

Kruge, M. A., Crelling, J. C., Pascone, J. M., Palmer, S. R. and Hippo, E. J. 1990b. Confined pyrolysis of Illinois Basin coals and maceral concentrates. 200th American Chemical Society National Meeting, Washington, D. C. Divn. of Geochemistry. Abs. No. 43.

Law, B. E., Nuccio, V. F., and Barker, C. E. Kinky vitrinite reflectance well profiles: evidence of paleopore pressure in low-permeability, gas-bearing sequences in Rocky Mountain Foreland Basins. Bull. Amer. Assoc. Petrol. Geol. v. 73 (8), p. 999-1010.

Later, D. W., Lee, M. L., Bartle, K. D., Kong, R. C. and Vassilaros, D. L. 1981. Chemical class separation and characterization of organic compounds in synthetic fuels. Anal. Chem., v. 53: p. 1612-1620.

Lorenz, J. C. (1988) Triassic-Jurassic Rift-Basin Sedimentology: History and Methods. Van Nostrand, New York.

Mudford, B. S. and Best, M. E. 1989. Venture Gas Field, Offshore Nova Scotia: Case study of overpressuring in region of low sedimentation rate. Bull. Amer. Assoc. Petrol. Geol. v. 73 (11)., p. 1383-1396.

Mukhopadhyay, P. K. and Wade, J. A. in press. Organic facies and maturation of sediments from the three Scotian Shelf Wells. Bull. Can. Petrol. Geol. v. 38 (4).

Mukhopadhyay, P. K. 1990. Evaluation of organic facies of the Verrill Canyon Formation, Sable Subbasin, Scotian Shelf, SSC Report No. OSC89-00482-(010).

Mukhopadhyay, P. K. 1989. Characterization of amorphous and other organic matter types by microscopy and pyrolysis-gas chromatography. Org. Geochem. v. 14 (3), p. 269-284.

Mukhopadhyay, P. K. and Birk, D. 1989. Organic facies in the Sable Subbasin, Scotian Shelf. Geo. Surv. Canada, Open File # 2027.

Mukhopadhyay, P. K. 1989. Cretaceous organic facies and oil occurrence, Scotian Shelf. SSC Report No. OSC89-00136-(008)

Mukhopadhyay, P. K. Hagemann, H. W., and Gormly, J. R. 1985. Characterization of kerogens as seen under the aspect of maturation and hydrocarbon generation. Erdol und Kohle-Erdgas-Petrochemie, v. 38 (1), p. 7-18.

Nantais, P. T. 1983. A reappraisal of the regional hydrocarbon potential of the Scotian Shelf. Geological Survey of Canada Open File Report No. 1175, 76 p.

Powell, T. G. 1985. Paleogeographic implications for the distribution of upper Jurassic source beds: Offshore Eastern Canada, Bull. Can. Petrol. Geol. v. 33 (1), p. 116-119.

Powell, T. G. 1982. Petroleum geochemistry of Verrill Canyon Formation, a source for Scotian Shelf hydrocarbons. Bull. Can. Petrol. Geol. v. 30. (2), p. 167-179.

Powell, T. G., and Snowdon, L. R. 1979. Geochemistry of crude oils and condensates from the Scotian Basin, Offshore Eastern Canada. Bull. Can. Petrol. Geol. v. 27 (4), p. 453-466.

Purcell, L. P., Rashid, M. A., and Hardy, I. A. 1979. Geochemical characteristics of sedimentary rocks in Scotian Basin. Bull. Amer. Assoc. Petrol. Geol., v. 63 (1), p. 87-105.

Radke, M. 1988. Application of aromatic compounds as maturity indicators in source rocks and crude oils. Mar. Petrol. Geol. v. 5. p. 224-236.

Radke, M. 1987. Organic Geochemistry of aromatic hydrocarbons. In Brooks, J. and Welte, D. H. (eds.), Advances in Petroleum Geochemistry, v. 2, p. 141-207, Academic Press, London.

Radke, M., Schaefer, R. G., Leythaeuser, D., and Teichmuller, M. 1980. Composition of soluble organic matter in coals: relation to rank and liptinite fluorescence. Geochim. Cosmochim. Acta, v. 44, p. 1787-1800.

Radke, M., Welte, D. H., and Willsch, H. 1986. Maturity parameters based on aromatic hydrocarbons: influence of organic matter type. Org. Geochem. v. 10 (103), p. 51-63.

Radke, M. Leythaeuser, D., and Teichmuller, M. 1984a. Relationship between rank and composition of aromatic hydrocarbons for coals of different origins. Org. Geochem. v. 6, p. 423-430.

Radke, M., Willsch, H., and Welte, D. H. 1984b Class separation of aromatic compounds in rock extracts and fossil fuels by liquid chromatography. Anal. Chem. v. 56, p. 2538-2546.

Radke, M. and Welte, D. H. 1983. The Methylphenanthrene Index (MPI): A maturity parameter based on aromatic hydrocarbons. In. Bjoroy, M. et al. (eds)., Advances in Organic Geochemistry 1981,, p. 504-512.

Radke, M., Welte, D. H. and Willsch, H. 1982a. Geochemical study on a well in the Western Canada Basin: relation of the aromatic distribution pattern to maturity of organic matter. Geochim. Cosmochim. Acta, v. 46, p. 1-10.

Radke, M., Willsch, H., and Leythaeuser, D. 1982b. Aromatic

components of coal: relation of distribution pattern to rank. Geochim. Cosmochim. Acta, v. 46, p. 1831-1848.

Rashid, M. A. and McAlary, J. D. 1977. Early maturation of organic matter and genesis of hydrocarbons as a result of heat from a piercement salt dome. Jour. Geochem. Expl. v. 8, p. 549-569.

Rowland, S. J., and Alexander, R., and Kagi, R. I. 1984. Analysis of trimethylnaphthalenes in petroleum by capillary gas chromatography. Jour. Chem. v. 249, p. 407-412.

Senftle, J. T., Brown, J. H., and Larter, S. R. 1987. Refinement of organic petrographic methods for kerogen characterization. Int. Jour. Coal. Geol. v. 7, p. 105-118.

Sofer, Z., Zumberge, J. E., and Lay, V., 1986. Stable carbon isotopes and biomarkers as tools in understanding genetic relationship, maturation, biodegradation, and migration of crude oils in the Northern Peruvian Oriente (Maranon) Basin, Org. Geochem. v. 10, p. 377-389.

Sofer, Z. 1984. Stable carbon isotope compositions of crude oils: application to source depositional environments and petroleum alteration. Bull. Amer. Assoc. Petrol. Geol. v. 68 (1), p. 31-49.

Stach, E., Mackowsky, M. Th., Teichmuller, M., Taylor, G. H., Chandra, D., and Teichmuller, R. 1982. Textbook of Coal Petrology. 3rd Ed. 536 p. Borntraeger, Stuttgart.

Teichmuller, M. 1986. Organic petrology of source rocks, history and state of the art. Org. Geochem. v. 10 (1-3), p. 581-599.

Tissot, B. and Welte, D. H. 1984. Petroleum Formation and Occurrence. Springer-Verlag, Berlin, 699 p.

Villar, H. J., Puttman, W., and Wol, M. 1988. Organic Geochemistry and petrography of Tertiary coals and carbonaceous shales from Argentina. Org. Geochem. v. 13 (4-6), p. 1011-1021.

Wade, J. A. and Maclean, B. C. 1990. Aspects of the geology of the Scotian Basin from recent seismic and well data. In. Geology of the Continental Margin of Easten Canada, M. J. Keen and G. L. Williams (eds). Geology of Canada no. 2, p. 190-238.

Wade, J. A. In press. Lithostratigraphy 12: Overpressure; in East Coast Basin Atlas Series: Scotian Shelf; Atlantic Geoscience Centre, Geological Survey of Canada.

White, C. M. and Lee, M. L. 1980. Identification and geochemical significance of some aromatic componenets of coal. Geochem. Cosmochem. Acta, v. 44, p. 1825-1832.

Whitehurst, D. D., Butrill, S. E., Derbyshire, F. J., Farcasiu, M., Odoerfer, G. A. and Rudnick, L. R. 1982. New characterization techniques for coal-derived liquids. Fuel, v. 61, p. 994-1005.

LIST OF TABLES & FIGURES

Table

Figures

Kerogen Type IIB (condensate-gas source rock)

c. Rank-amorphous liptinite IIA, particulate liptinite A, and vitrinite, Cohasset D-42, 4410.5 m. kerogen concentrate, transmitted white light.. X200. Kerogen Type IIA-IIB (oil-condensate source rock)

d. Rank-amorphous liptinite IIA, clay minerals, and bitumen with framboidal pyrite, Cohasset D-42, 4425.7 m. whole rock, incident white light. X500. Kerogen Type IIA-IIB (oil-condensate source rock).

e. Inertodetrinite, macrinite, vitrinite (allochthonous and autochthonous), amorphous liptinite IIB (in the middle), oxidized sporinite, Cohasset A-52, 2138 m., kerogen contrate, incident white light., X500. Kerogen Type IIB-III (gas source rock).

f. Vitrinite, sporinite, alginite, and oxidized framboidal pyrite, Cohasset A-52, 2138 m., whole rock, incident white light. X500. Kerogen Type IIB-III (gas source rock).

g. Vitrinite, oxidized sporinite, oxidized pyrite, Cohasset A-52, 2275 m., whole rock, incident white light. X500. Kerogen Type IIB (condensate-gas source rock).

h. Vitrinite, particulate liptinite A, amorphous liptinite IIB, and inertinite. Cohasset A-52, 2275 m., kerogen concentrate, transmitted white light. X200. Kerogen Type IIB (condensate-gas source rock).

7. Photomicrographs for source rock analysis from the boreholes Evangeline H-98, Sable Island E-48, and Cohasset D-42.

a. Sporinite, partially biodegraded particulate liptinite A (dinoflagellate), vitrinite, and amorphous liptinite IIA. Evangeline H-98, 2335 m, kerogen concentrate, transmitted white light. X200. Kerogen Type IIB (condensate-gas source rock).

b. Particulate liptinite A (acritarch etc.), vitrinite, and amorphous liptinite IIB. Evangeline H-98, 2335 m, kerogen concentrate, transmitted white light. X200. Kerogen Type IIB (condensate-gas source rock).

c. Vitrinite, lignite contamination (large dark grain), and liptodetrinite. Evangeline H-98, 4760 m, kerogen concentrate, transmitted white light, X200. Kerogen Type III (gas source rock).

d. Vitrinite, lignite contamination (trimacerite grain), clay minerals, and oxidized pyrite. Evangeline H-98, 4760 m, whole rock, incident white light, X500. Kerogen Type III (gas source rock).

e. Amorphous liptinite IIA mixed with mineral bituminous groundmass

and partially oxidized framboidal pyrite. Evangeline H-98, 4910 m, whole rock, incident white light, X500. Kerogen Type IIA-IIB (oil-condensate source rock).

f. Vitrinite, sporinite, amorphous liptinite IIB, and inertinite. Evangeline H-98, 5020 m, kerogen concentrate, transmitted white light, X200. Kerogen Type IIB (condensate-gas source rock).

g. Vitrinite, amorphous liptinite IIB, particulate liptinite A (dinoflagellate?; partially biodegraded), Sable Island E-48, 2490.2 m, kerogen concentrate, transmitted white light, X200. Kerogen Type III (gas source rock).

h. Saprovitrinite and partially oxidized framboidal pyrite. Cohasset D-42, 2319.6 m, whole rock, reflected white light, X500. Kerogen Type IIB-III (gas-condensate).

8. Photomicrographs for source rock samples from the Verrill Canyon Formation of three boreholes.

All photomicrographs are in incident white light. Magnification X500.

a. Amorphous liptinite IIA and pyrite. Alma F-67, 4625 m, kerogen concentrate. Kerogen Type IIA-IIB (oil-condensate source rock).

b. Amorphous liptinite IIA and mineral bituminous groundmass and pyrite. Alma F-67, 5040 m, whole rock. Kerogen Type IIB (condensate-gas).

c. Vitrinite, meta-sporinite, and amorphous liptinite IIB, and pyrite. Glenelg J-48, 4620 m, kerogen concentrate. Kerogen Type III (gas source rock).

d. Amorphous liptinite IIA changed to granular vitrinite, amorphous liptinite IIA (without change), mineral-bituminous groundmass, and pyrite. Glenelg J-48, 4940 m, whole rock. Kerogen Type IIA (oil source rock).

e. Meta-alginite, vitrinite, inertinite, rank-sporinite, and pyrite. Glenelg J-48, 5180.7 m, kerogen concentrate. Kerogen Type IIB (condensate-gas).

f. Mineral-bibuminous broundmass with amorphous liptinite IIA, solid bitumen, and pyrite. S. W. Banquereau F-34, 6260 m, whole rock. Kerogen Type IIA-IIB (oil-condensate source rock).

g. Large solid-bitumen with amorphous liptinite IIA, pyrite, and other minerals. S. W. Banquereau F-34, 6305 m, whole rock. Kerogen Type IIB (condensate-gas source rock).

h. Clustered micrinite (secondary maceral) from amorphous liptinite

IIA and pyrite. Thebaud P-84, 4045 m, kerogen concentrate. Kerogen Type IIA-IIB (oil-condensate source rock).

9. A plot of hydrogen index versus oxygen index showing position of selected samples (from eight boreholes) within the various kerogen maturation paths (after Espitalie et al., 1985).

10. A plot of T_{max} (°C) versus hydrogen index showing position of selected samples (from eleven boreholes) within various kerogen maturation paths (after Espitalie et al., 1985).

11. A plot of mean randon vitrinite reflectance (% R°) and depth (m) from two Scotian Shelf boreholes (S. Venture O-59 and S. W. Banquereau F-34).

12. Contour diagram showing the top of the overpressure in the various Scotian Shelf boreholes (after Wade, in press).

13. A plot of mean random vitrinite reflectance, depth (m), and formation pressure from two Scotian Shelf boreholes (S. Venture O-59 and Louisbourg J-47). Data and plot from M.P. Avery (A.G.C.).

14. A plot of various Scotian Shelf boreholes showing the depth (m) of 1.0% R_o (mean randon vitrinite reflectance) (starting of the main phase of gas generation) and the depth (m) of the top of the overpressure.

15. Location map of various Scotian Shelf boreholes, where analysis for stable carbon isotope of saturate and aromatics fractions were done.

16. Gas chromatograms of the staurate fraction of various crude oil and condensate samples: (a) Cohasset A-52, DST #5, (b) Cohasset A-52, DST #2, (c) N. Truimph B-52, DST #4, 3771-3777 m., (d) N. Truimph G-43, DST #1, 3835-3846 m, (e) Panuke B-90, DST #1, (f) Thebaud C-74, DST #9, 3865-3888 m, (g) Thebaud C-74, DST #4.

17. A plot of del^{13}C (stable isotope of carbon) of saturate and aromatics fractions of:

(a) crude oil, condensate, source rock extracts without lebels. The dividing line showing the position of marine and terrestrial source of these extracts (after Sofer, 1984)

(b) crude oils and condensates with lebels. The dividing straight line is the best-fit line for linear equation: y = 1.07826 + 3.54538. The dividing dashed line is the line drawn after Sofer (1984):

$$Y\ (\text{del}^{13}C_{aro} = 1.074\ X\ (\text{del}^{13}C_{sat}) + 5.46$$

(c) crude oil, condensate, and source rock extracts with lebels for

the source rock extracts. The dividing line is the line drawn after the linear equation of Sofer (1984) as given in figure 17b.
18. Location map of various Scotian Shelf boreholes, where analysis for aromatic GC-MS was done.

19. Mass Chromatograms of the isomers of the naphthalene homologues. Peaks used in the study are labelled and molecular structures are shown.

20. Mass chromatograms of the isomers of selected tetraaromatic compounds and their homologues. Peaks used in this study are labelled and molecular structures are shown.

21. Mass chromatograms of the isomers of dimethylbiphenyl, methyldibenzofuran and selected pentaaromatics. Peaks used in the study are labelled and molecular structures are shown.

22. Examples of data preparation. Each individual are shown along with the figure.

23. Example of a Composite Polyaromatic Trace (CPT) of normalized isomer clusters. Each cluster is normalized to a maximum of 1, as shown in Figure 22. See Figure 19 for key peaks in traces A-C, Figure 20 for traces E-G, and Figure 21 for traces D and H.

24. Example of the computation of polyaromatic Trace remainders, (a) From subtraction of traces of like samples, (b) From substraction of dissimilar samples.

25. Maturity crossplots: (a) The ratio of 2-methylphenanthrene to 1-methylphenanthrene and Methylphenanthrene Index; (b) The chrysene/benzo(α)anthracene ratio and the Methylphenanthrene Index. The clarification of the symbols are in the figure.

26. Crossplots of the ratio of the sum of methyldibenzofuran isomers to the sum of dimethylbiphenyl and methyldibenzofuran isomers (quantitated on m/z 182 chromatograms) and the ratio of dibenzothiophene to the sum of tetramethylnaphthalenes plus dibenzothiophene (m/z 184). Symbol keys are in the figure 26.

27. Composite Polyaromatic Trace remainders of "Group 2" oil samples after the subtraction of the trace of Sample 4. Sample numbers are shown to the left of each trace. See Figure 5 for key to curves A through G. Scales are the same for each trace. Horizontal axis is the zero line.

28. Composite Polyaromatic Trace remainders of oil and condensate samples after the subtraction of the trace of Sample 1. Sample numbers are shown to the left of each trace. See Figure 5 for key to curves A through G. Scales are the same for each trace. Horizontal is the zero line. (a) Group 1 petroleums, (b) Group 2 petroleums.

29a. Composite Polyaromatic Trace remainders of rock extract samples after the subtraction of the trace of Sample 1. Sample numbers are shown to the left of each trace. See Figure 5 for key to curves A through G. Scales are the same for each trace. Horizontal axis is the zero line.

29b. Composite Polyaromatic Trace remainders of rock extract samples after the subtraction of the trace of extract Sample 13.

30. Light hydrocarbon gas chromatograms of the whole oil/condensate samples from Cohasset D-42, DST #7, S. Venture O-59, DST #11, N. Truimph B-52, DST #4 (Fowler, personal communication).

Table 1a. List of crude oil/condensate samples showing borehole number, stratigraphy, age, reservoir temperature, facies and API data.

Borehole No. and Test No.	Formation (Age)	Depth (m) (ft)	Reservoir Temp (Celsius)	Reservoir Facies	API 1(*)	API 2(*)	Gas/Oil Ratio (GOR)
Alma F-67 (DST#7)	Upper Mississauga (Barremian)	2872-2890	105	Marine channel - beach	47.8	41.3	63,200
Alma F-67 (DST#2)	Mississauga (Barremian)	3026-3032	110	Marine distal channel	41.6	33.7	-
Arcadia J-16 (DST#9)	MicMac (Bathonian-Tithonian)	4857-4869	135	Delta - shallow marine	34.3	29.7	2,190,474
Banquereau C-21 (DST#2)	Upper Mississauga (Barremian)	3585-3596	105	Delta plain - fluvial channel	42.0	29.7	10,000
Chebucto K-90 (DST#4)	Upper Mississauga (Barremian)	4227-4238	135	Delta front	39.0	29.0	129,753
Citnalta I-59 (DST#2)	Lower Mississauga (Tithonian)	3951-3957	110	Lower delta plain	57.5	-	13,348
Cohasset A-52 (DST#5)	Logan Canyon (Albian)	2149-2153 (TVD - 1888-91)	69	Lower delta plain	49.7	44.6	-
Cohasset A-52 (DST#2)	Logan Canyon (Albian/ Aptian)	2337-2341 (TVD: 2043-46)	73	Lower delta plain	53.7	43.9	36
Cohasset D-42 (DST#7)	Logan Canyon (Albian)	1861-1865 (6107-6121')	68	Lower delta plain	49.2	41.9	123
Cohasset D-42 (PT#3)	Upper Mississauga (Barremian)	2248-2255 (7376-7399')	80	Fluvial	49.2	41.9	115
Glenelg J-48 (DST#9)	Logan Canyon (Aptian-Cenomanian)	3061-3064	104 (98+)	Marine channel or fan	50.0	36.2	72,815
Glenelg J-48 (DST#8)	Upper Mississauga (Barremian)	3491-3495	113	Marine channel	45.8	31.9	175,000

**N.Triumph B-52 (DST#4)	Upper Mississauga (Berriasian-Valanginian)	3771-3777	119	Delta front	41.1	30.9	230,769
N.Triumph G-43 (DST#1)	Upper Mississauga (Barremian)	3835-3846	120	Delta front	45.3	36.3	197,740
Olympia A-12 (DST#8)	Lower Mississauga (Tithonian)	4525-4538	130	Tidal/ lagoonal	36.6	31.2	7,035
Olympia A-12 (DST#5)	Lower Mississauga (Tithonian)	4664-4678	135	Distal channel bar	47.2	31.3	5,610
Panuke B-90 (DST#1)	Mississauga (Upper Mbr.) (Barremian)	2293-2299 (TVD: 2271-77)	81	Fluvial	55.0	42.4	-
Primrose A-41 (DST#2)	Wyandot (Mid Campanian)	1512 (4960')	53	Shallow marine	47.5	36.5	33,923
Primrose N-50 (DST#1)	Cap-rock Facies (?)	1643-1660 (5390-5415')	67	?	33.5	32.3	6,600
Sable Is. E-48 (DST#16)	Logan Canyon (Aptian-Cenomanian)	1460-1461 (4790-4795')	50	Shallow marine	36.8	27.1	410
Sable Is. E-48 (DST#5)	Logan Canyon (Aptian)	2226-2239	70	Lower delta plain	64.0	43.2	-
Sable Is. 3H-58 (DST#4)	Logan Canyon (Aptian)	1632-1633 (TVD:1435-1435.5 (4701-4710')	50	Shallow marine	30.0	26.7	4,657
S.Venture O-59 (DST#10)	Lower Mississauga (Berriasian-Valanginian)	4255-4267	122	Delta front	48.9	33.7	3,338
S.Venture O-59 (DST#5)	Lower Mississauga (Tithonian-Berriasian)	5035-5050	145	Distal channel	50.9	40.7	97,014
Thebaud C-74 (DST#9)	Mississauga (Lr. Mbr.) (Tithonian-Berriansian)	3865-3888	117	Distal channel	45.0	35.3	41,300

Thebaud C-74 (DST#4)	Mississauga (Lr. Mbr.) (?Tithonian)	4508-4521	135	Barrier bar	51.5	39.5	99,358
Venture B-52 (DST#13)	Lower Mississauga (?Tithonian)	4920-4925	135	Distal channel	38.8	30.7	1,000,000
Venture B-13 (DST#11)	Lower Mississauga (Berriasian-Valanginian)	4475-4485	133	Delta front distributary channel	45.7	32.2	46,875
Venture B-43 (DST#2)	MicMac (?Kimmeridgian)	5478-5498	150	Delta front	44.0	40.5	86,238
Intrepid L-30 (PT#3)		3841-3845			36.0	23.6	-

1* = API determined after drilling
TVD = True vertical depth

2* = API determined on samples collected from COGLA, Dartmouth, N.S. in 1990

Table 1b. List of source rock samples showing borehole number, stratigraphy, age, formation temperature, depositional facies, and total organic carbon content (wt%) & vitrinite reflectance

Borehole No.	Formation (Age)	Depth (m) (ft)	Formation Temp (Celsius)	Facies	TOC (wt%)	Ro
a. Cohasset A-52	Logan Canyon (?Albian)	2275.75 (TVD:1992)	70	Shallow marine (partially anoxic)	2.88	0.50
b. Cohasset D-42	Abenaki-Misaine (Bathonian)	4410-4413 (14470-14480')	147	Deep marine (partially anoxic)	0.33	1.31
c. S.Venture O-59	MicMac (?Oxfordian-Kimmeridgian)	6105-6110	170	Prodelta (partially anoxic)	2.25	1.97
d. Alma F-67	Verrill Canyon (Cretaceous)	4500	160	Deep marine (partially anoxic)	2.72	
e. Glenelg J-48	Verrill Canyon (Cretaceous)	5186.7	170 (163)	Deep marine (partially anoxic)	1.29	1.87
**f.Cohasset D-42	Abenaki-Misaine (Bathonian)	4425 (14520')	147	Deep marine shelf (partially anoxic)	0.65	1.36
**g.Cohasset A-52	Logan Canyon (Aptian-Coniacian)	2275 (deviated depth) 2036 (true depth)		Shallow marine (partially anoxic)	4.60	0.50
**h.Evangeline H-98	Shortland Shale (Albian-Turonian)	5020		Deep marine (partially anoxic)	2.06	1.52
**i.Sable Is. E-48	Logan Canyon	2490 (8170')		Shallow marine (partially oxidised)	2.81	0.56
**j.Sable Is. O-47	Lr.Mississauga (Barriasian-Valanginian)	3849 (12630')		Prodelta (partially oxic)	2.02	0.85

** = Data taken from earlier report (Mukhopdhyay, 1989)

Table 2a. Liquid chromatography and carbon isotope data of oil/condensate and source-rock extracts.

Borehole No. and Test No.	Sample Type	Component Analysis % of oil				Del C-13	
		% Sat.	% Arom	%NSO+Asph	Sat/Arom	Sat	Arom
Alma F-67 (DST#7)	Light oil -condensate	83.8	13.4	2.8	6.20	-26.9	-25.2
Alma F-67 (DST#2)	Light oil	72.9	24.3	2.8	3.00	-27.4	-25.9
Arcadia J-16 (DST#9)	Light oil -condensate	-	-	-	-	-26.6	-24.8
Banquereau C-21 (DST#2)	Light oil -condensate (?)	37.3	60.1	2.6	0.62	-26.9	-25.2
Chebucto K-90 (DST#4)	Light oil	33.0	63.1	3.9	0.50	-26.1	-24.4
Citnalta I-59 (DST#2)	Condensate	59.5	36.8	3.7	1.61	-26.7	-25.9
Cohasset A-52 (DST#5)	Light oil -condensate	76.5	19.9	3.6	3.80	-28.4	-27.7
Cohasset A-52 (DST#2)	Condensate -light oil	83.4	13.6	3.0	6.10	-27.1	-25.4
Cohasset D-42 (DST#7)	Light oil -condensate	77.8	17.2	5.0	4.50	-27.0	-25.7
Cohasset D-42 (PT#3)	Light oil	74.1	22.2	3.7	3.30	-27.0	-25.4
Glenelg J-48 (DST#9)	Condensate	78.9	18.1	3.0	4.40	-25.9	-24.2
Glenelg J-48 (DST#8)	Light oil -condensate	55.4	41.7	2.9	1.30	-26.2	-24.4

N.Triumph B-52 (DST#4)	Light oil -condensate	38.1	57.9	4.0	0.66	-26.7	-24.8
N.Triumph G-43 (DST#1)	Light oil -condensate	56.5	37.6	5.9	1.50	-27.4	-25.3
Olympia A-12 (DST#8)	Light oil -condensate	56.1	43.5	0.4	1.29	-26.8	-25.9
Olympia A-12 (DST#5)	Condensate -light oil	56.7	40.5	2.8	1.40	-27.1	-25.6
Panuke B-90 (DST#1)	Light oil -condensate	74.1	22.8	3.1	3.30	-27.2	-25.3
Primrose A-41 (DST#2)	Light oil	67.8	26.6	5.6	2.55	-26.9	-26.4
Primrose N-50 (DST#1)	Light oil	50.8	46.4	2.8	1.09	-26.1	-24.7
Sable Is. E-48 (DST#16)	Light oil	55.2	42.3	2.5	1.30	-26.2	-25.5
Sable Is. E-48 (DST#5)	Condensate	72.9	23.7	3.2	3.10	-26.7	-25.3
Sable Is. 3H-58 (P.Test #4)	Oil	56.7	37.5	5.8	1.50	-26.2	-25.5
S.Venture O-59 (DST#10)	Condensate	54.4	44.9	0.7	1.21	-27.3	-25.6
S.Venture O-59 (DST#5)	Condensate	73.6	22.3	4.1	3.30	-26.5	-24.4
Thebaud C-74 (DST#9)	Light oil -condensate	55.6	40.7	3.7	1.37	-26.9	-25.4

Thebaud C-74 (DST#4)	Condensate	66.9	29.6	3.5	2.26	-26.6	-24.7
Venture B-52 (DST#13)	Condensate	52.4	44.6	3.0	1.17	-26.5	-25.3
Venture B-13 (DST#11)	Condensate	52.1	44.5	3.4	1.17	-27.1	-25.9
Venture B-43 (DST#2)	Light oil -condensate	67.8	31.7	0.5	2.13	-26.4	-24.5

Table 2b. Liquid chromatography and carbon isotope data of source-rock samples.

Borehole No. and Depth (m)	Sample Type	Bitumen Extract (mg/g TOC)	Component Analsis % of oil				Del C-13	
			% Sat.	% Arom	%NSO+Asph	Sat/Arom	Sat	Arom
a.Cohasset A-52 (2275.75)	Core	393.0	40.4	32.7	26.9	1.23	-29.2	-27.5
b.Cohasset D-42 (4410)	Core	19.0	54.8	22.6	22.6	2.42	-27.2	-25.8
c. S.Venture O-59 (6105)	Cuttings	103.0	48.9	31.5	19.6	1.55	-27.5	-26.7
d.Alma F-67 (4500)	Cuttings	824.0	36.7	37.8	25.5	0.97	-28.5	-24.0
e.Glenelg J-48 (5186.7)	Core	143.0	27.0	21.6	51.4	1.25	-28.3	-27.1
f.Conasset(**) D-42 (4425.0)	Cuttings	14.0	23.5	14.7	61.8	1.59	-26.7	-25.0
g.Cohasset(**) A-52 (2275)	Core	27.6	62.9	11.4	25.7	5.50	-26.8	-25.3
h.Evangeline H-98(**)	Cuttings	40.1	68.6	11.2	20.2	6.10	-27.9	-26.4
i.Sable Is. E-48(**) (2490)	Cuttings	13.4	30.8	20.5	48.7	1.50	-26.9	-25.7
j.Sable Is. O-59(**) (3849)	Cuttings	31.1	56.9	17.7	25.4	3.20	-26.9	-26.0

** Data from earlier report Mukhopadhyay (1989)

Table 3. Vitrinite Reflectance and Fluorescence data of Source Rocks

Borehole No and Sample Type		Depth (m)	Vitrinite Reflectance R_o	Std. Dev.	Fluorescence Observations
S. W. Banquereau F-34					
	Cuttings	655.0	0.22	0.02	Greenish yellow for sporinite
	Cuttings	1080.0	0.32	0.04	Golden yellow for alginite
	Cuttings	1595.0	0.44	0.05	Yellow for sporinite
	Cuttings	2610.0	0.48	0.06	Yellow liptodetrinite; few grains
	Cuttings	3205.0	0.52	0.03	Yellow for sporinite
	Cuttings	3725.0	0.54	0.05	Orange for sporinite & alginite
	Cuttings	4085.0	0.62	0.06	Orange for phytoclasts
	Cuttings	4620.0	0.87	0.11	Nonfluorescent
	Cuttings	5160.0	1.01	0.09	Red for groundmass
	Cuttings	5760.0	1.10	0.18	Nonfluorescent to orange phytoclasts
	Cuttings	5960.0	1.80	0.08	Nonfluorescent to red groundmass
	Cuttings	6140.0	1.75	0.23	Nonfluorescent to orange groundmass
	Cuttings	6305.0	1.90	0.23	Nonfluorescent
Louisbourg J-47	Core	5447.2	1.20	0.15	Red liptodetrinite & cutinite; Reddish brown groundmass
Tantallon M-41	Core	5306.8	0.82	0.09	Orange liptodetrinite; yellow to orange groundmass
Venture B-52	Core	5129.5	0.93	0.07	Orange groundmass;yellow rim within dolomite and foraminiferal test
W. Venture N-91	Core	5137.1	0.99	0.07	Intense diffuse orange-brown for groundmass & liptodetrinite
W. Venture C-52	Core	5256.7	1.00	0.12	Orange liptodetrinite; yellow to orange groundmass
S. Desbarres O-76	Core	5955.0	1.61	0.07	Red phytoclast & yellow/orange groundms.
Arcadia J-16	Core	5175.5	1.22	0.11	Orange cutinite & groundmass
W. Chebucto K-20	Core	5367.9	1.37	0.17	Orange phytoclast & yellow - orange groundmass
S. Venture O-59	Cuttings	520.0	0.24	0.04	Yellow to red sporinite
	Cuttings	1060.0	0.29	0.05	Yellow phytoclasts
	Cuttings	1625.0	0.38	0.07	Yellow-orange sporinite
	Cuttings	2195.0	0.40	0.08	Nonfluorescent to yellow sporinite
	Cuttings	3020.0	0.57	0.06	Nonfluorescent to red sporinite
	Cuttings	3770.0	0.64	0.09	Orange alginite
	Cuttings	4240.0	0.80	0.08	Nonfluorescent to yellow sporinite
	Cuttings	4760.0	0.92	0.10	Nonfluorescent phyto + groundmass
	Cuttings	5330.0	1.21	0.08	Nonfluorescent to orange groundmass
	Cuttings	5830.0	1.46	0.44	Nonfluorescent to yellow sporinite? possible contamination
	Cuttings	5690.0	1.69	0.12	Nonfluorescent
	Cuttings	6030.0	1.77	0.24	Nonfluorescent to red groundmass
	Cuttings	6160.0	1.97	0.21	Nonfluorescent

Table4. List of samples studied for aromatic GC-Ms

Sample	Well	DST	Type
1	Chebucto K-90	4	oil
2	Cohasset D-42	7	oil
3	Panuke B-90	1	oil
4	Cohasset A-52	5	oil
5	Sable Island 3H-58	5	oil
6	N. Triumph B-52	4	condensate
7	Olympia A-12	5	condensate
8	S. Venture O-59	5	condensate
9	S. Venture O-59	10	condensate
10	Glenelg J-48	8	condensate
11	Cohasset A-52		extract
12	Cohasset D-42		extract
13	Alma F-67		extract
14	S. Venture O-59		extract

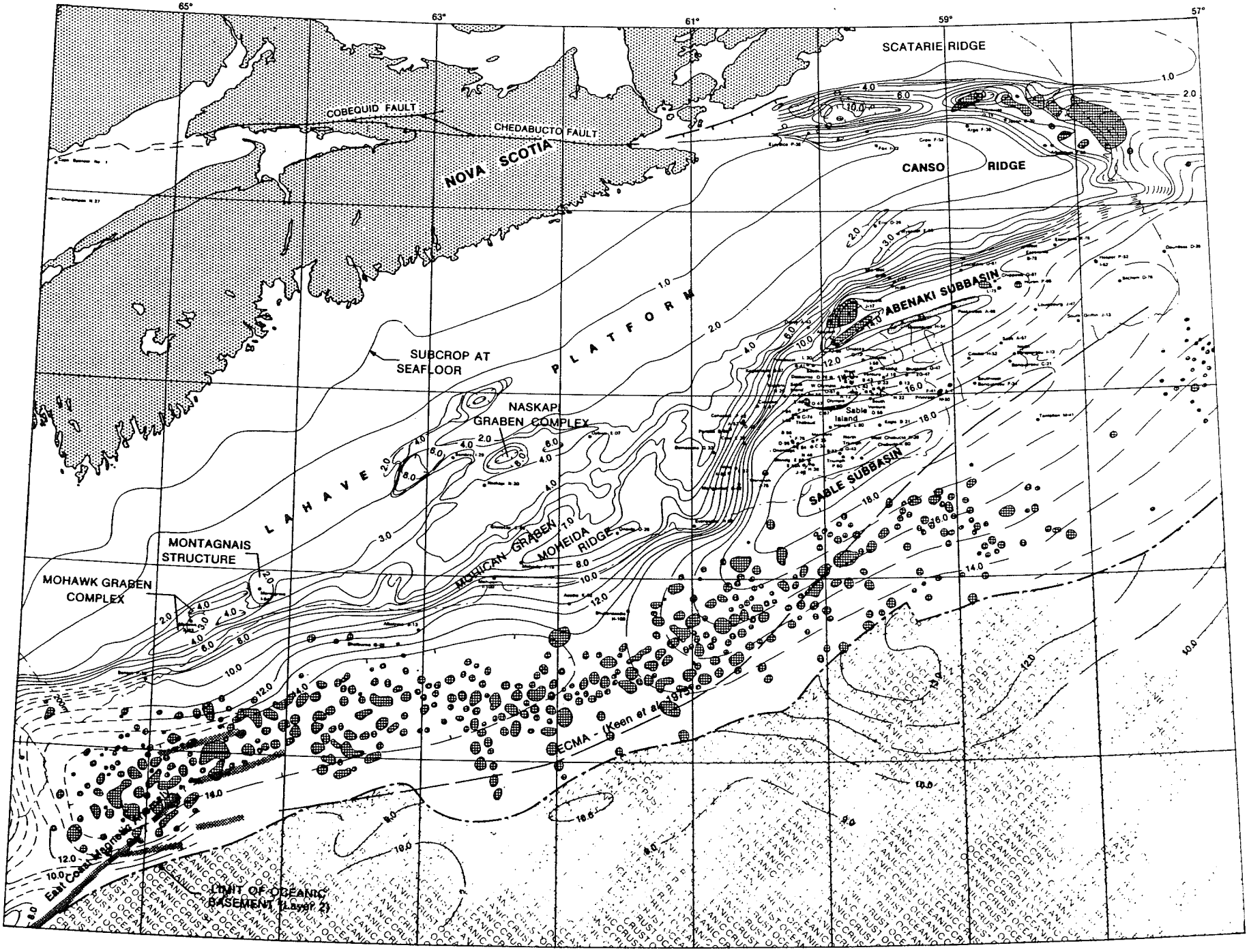
65°
63°
61°
59°
57°
SCATARIE RIDGE
COBEQUID FAULT
CHEDABUCTO FAULT
NOVA SCOTIA
CANSO RIDGE
ABENAKI SUBBASIN
SUBCROP AT SEAFLOOR
NASKAPI GRABEN COMPLEX
LAHAVE PLATFORM
SABLE SUBBASIN
Sable Island
MONTAGNAIS STRUCTURE
MOHAWK GRABEN COMPLEX
MOHICAN GRABEN
MOHEIDA RIDGE
ECMA - (Keen et al 1987)
East Coast Magnetic Anomaly
LIMIT OF OCEANIC BASEMENT (Keen et al)

Figure 1

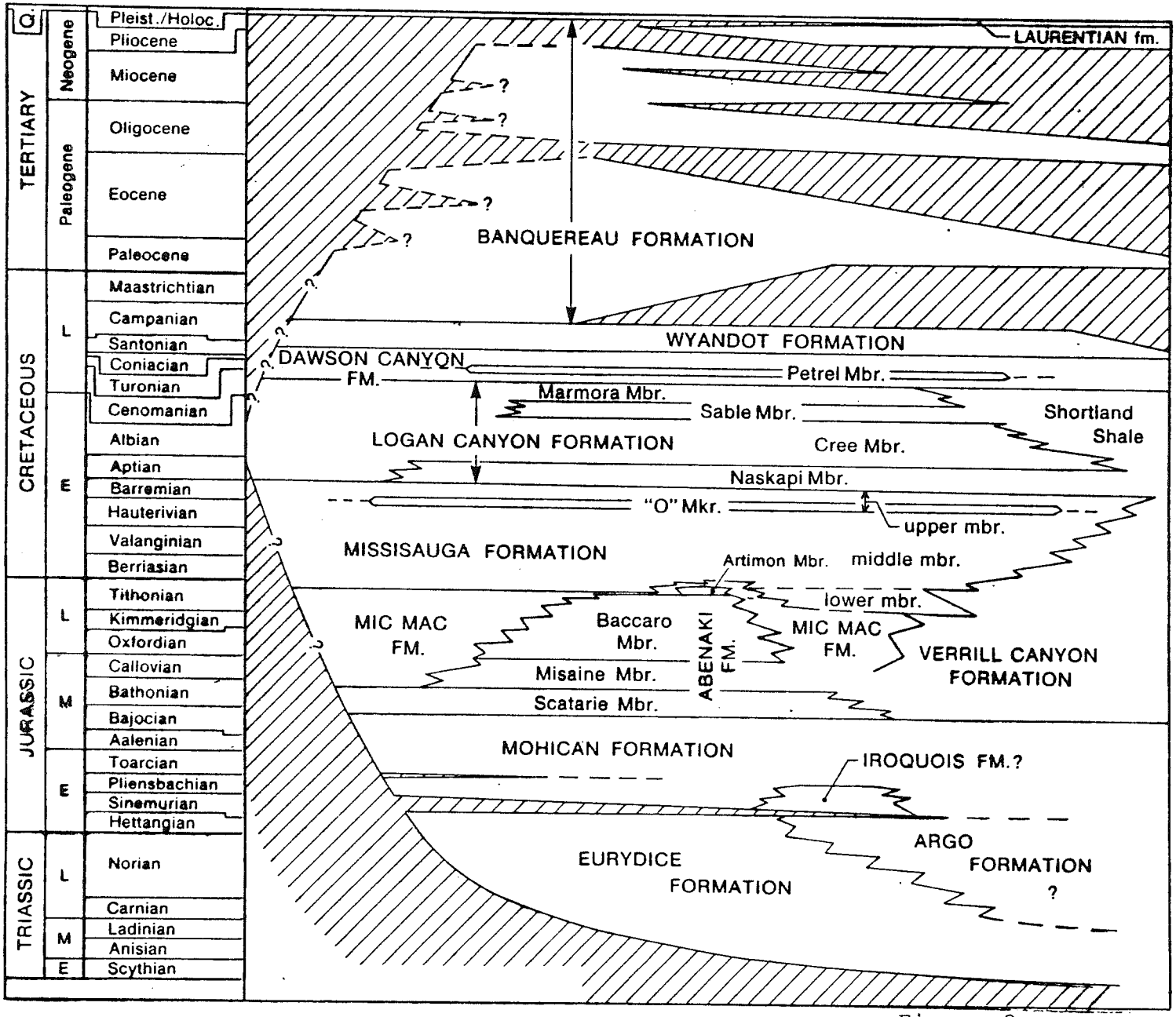
Q.
TERTIARY
Neogene
Paleogene
Pleist./Holoc.
Pliocene
Miocene
Oligocene
Eocene
Paleocene
CRETACEOUS
L
E
Maastrichtian
Campanian
Santonian
Coniacian
Turonian
Cenomanian
Albian
Aptian
Barremian
Hauterivian
Valanginian
Berriasian
JURASSIC
L
M
E
Tithonian
Kimmeridgian
Oxfordian
Callovian
Bathonian
Bajocian
Aalenian
Toarcian
Pliensbachian
Sinemurian
Hettangian
TRIASSIC
L
M
E
Norian
Carnian
Ladinian
Anisian
Scythian
LAURENTIAN fm.
BANQUEREAU FORMATION
WYANDOT FORMATION
DAWSON CANYON FM.
Petrel Mbr.
Marmora Mbr.
Sable Mbr.
Shortland Shale
LOGAN CANYON FORMATION
Cree Mbr.
Naskapi Mbr.
"O" Mkr.
upper mbr.
MISSISAUGA FORMATION
Artimon Mbr.
middle mbr.
lower mbr.
MIC MAC FM.
Baccaro Mbr.
Misaine Mbr.
Scatarie Mbr.
ABENAKI FM.
MIC MAC FM.
VERRILL CANYON FORMATION
MOHICAN FORMATION
IROQUOIS FM.?
EURYDICE FORMATION
ARGO FORMATION ?

Figure 2

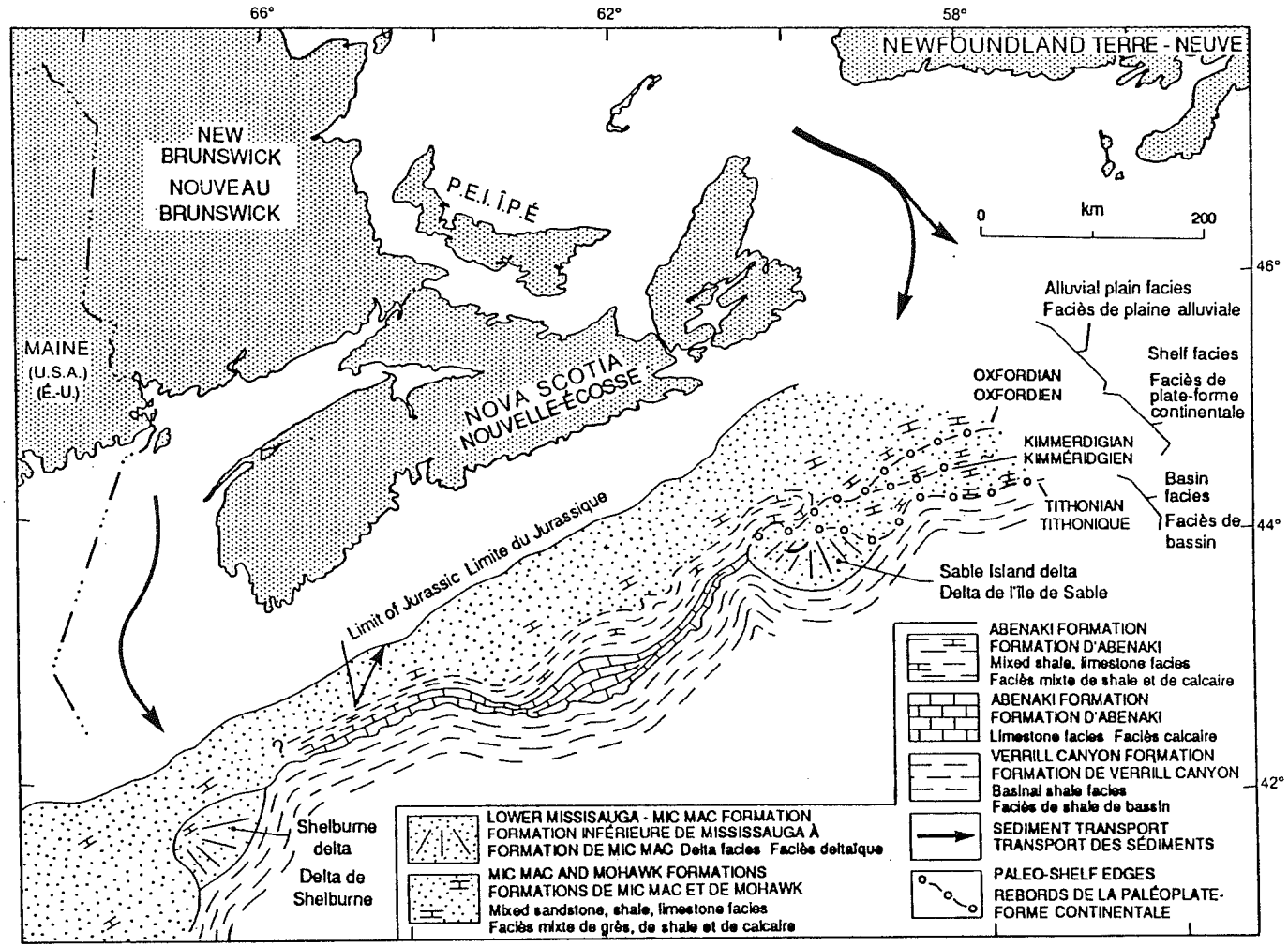
66°
62°
58°
NEWFOUNDLAND TERRE - NEUVE
NEW BRUNSWICK
NOUVEAU BRUNSWICK
P.E.I. Î.P.É.
MAINE (U.S.A.) (É.-U.)
NOVA SCOTIA NOUVELLE-ÉCOSSE
0 km 200
46°
44°
42°
Alluvial plain facies
Faciès de plaine alluviale
Shelf facies
Faciès de plate-forme continentale
OXFORDIAN
OXFORDIEN
KIMMERIDGIAN
KIMMÉRIDGIEN
TITHONIAN
TITHONIQUE
Basin facies
Faciès de bassin
Limit of Jurassic Limite du Jurassique
Sable Island delta
Delta de l'île de Sable
Shelburne delta
Delta de Shelburne
ABENAKI FORMATION
FORMATION D'ABENAKI
Mixed shale, limestone facies
Faciès mixte de shale et de calcaire
ABENAKI FORMATION
FORMATION D'ABENAKI
Limestone facies Faciès calcaire
VERRILL CANYON FORMATION
FORMATION DE VERRILL CANYON
Basinal shale facies
Faciès de shale de bassin
SEDIMENT TRANSPORT
TRANSPORT DES SÉDIMENTS
PALEO-SHELF EDGES
REBORDS DE LA PALÉOPLATE-FORME CONTINENTALE
LOWER MISSISAUGA - MIC MAC FORMATION
FORMATION INFÉRIEURE DE MISSISSAUGA À FORMATION DE MIC MAC Delta facies Faciès deltaïque
MIC MAC AND MOHAWK FORMATIONS
FORMATIONS DE MIC MAC ET DE MOHAWK
Mixed sandstone, shale, limestone facies
Faciès mixte de grès, de shale et de calcaire

Figure 3

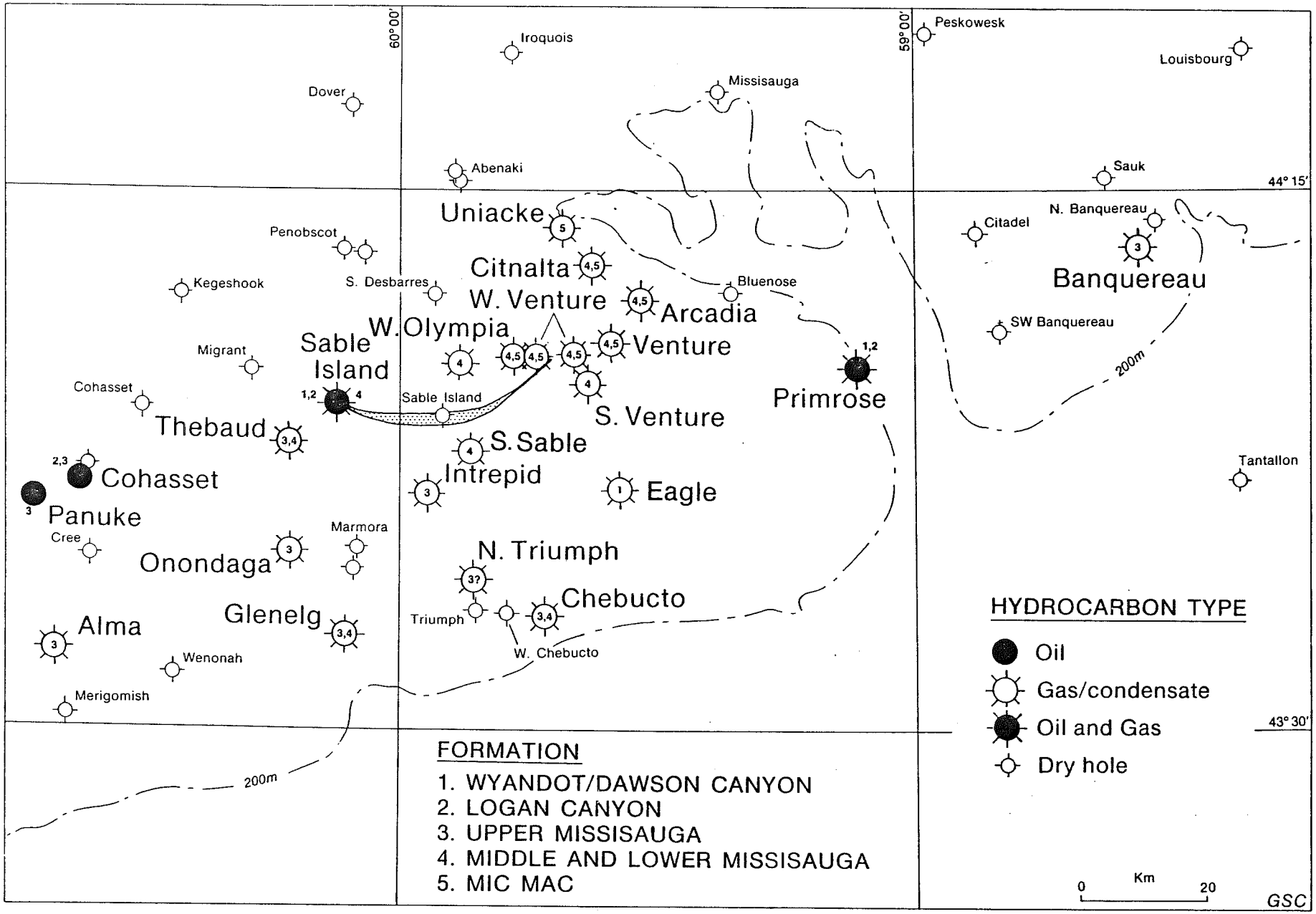
60°00'
59°00'
44°15'
43°30'
Iroquois
Peskowesk
Louisbourg
Dover
Missisauga
Abenaki
Sauk
Uniacke
Penobscot
Citnalta
Kegeshook
S. Desbarres
Bluenose
W. Venture
Arcadia
W. Olympia
Sable Island
Venture
Migrant
Cohasset
Sable Island
Primrose
S. Venture
Thebaud
S. Sable
Intrepid
Eagle
Cohasset
Panuke
Cree
Marmora
Onondaga
N. Triumph
Chebucto
Triumph
W. Chebucto
Alma
Glenelg
Wenonah
Merigomish
200m
N. Banquereau
Citadel
Banquereau
SW Banquereau
200m
Tantallon
HYDROCARBON TYPE
Oil
Gas/condensate
Oil and Gas
Dry hole
FORMATION
1. WYANDOT/DAWSON CANYON
2. LOGAN CANYON
3. UPPER MISSISAUGA
4. MIDDLE AND LOWER MISSISAUGA
5. MIC MAC
0 Km 20
GSC

Figure 4

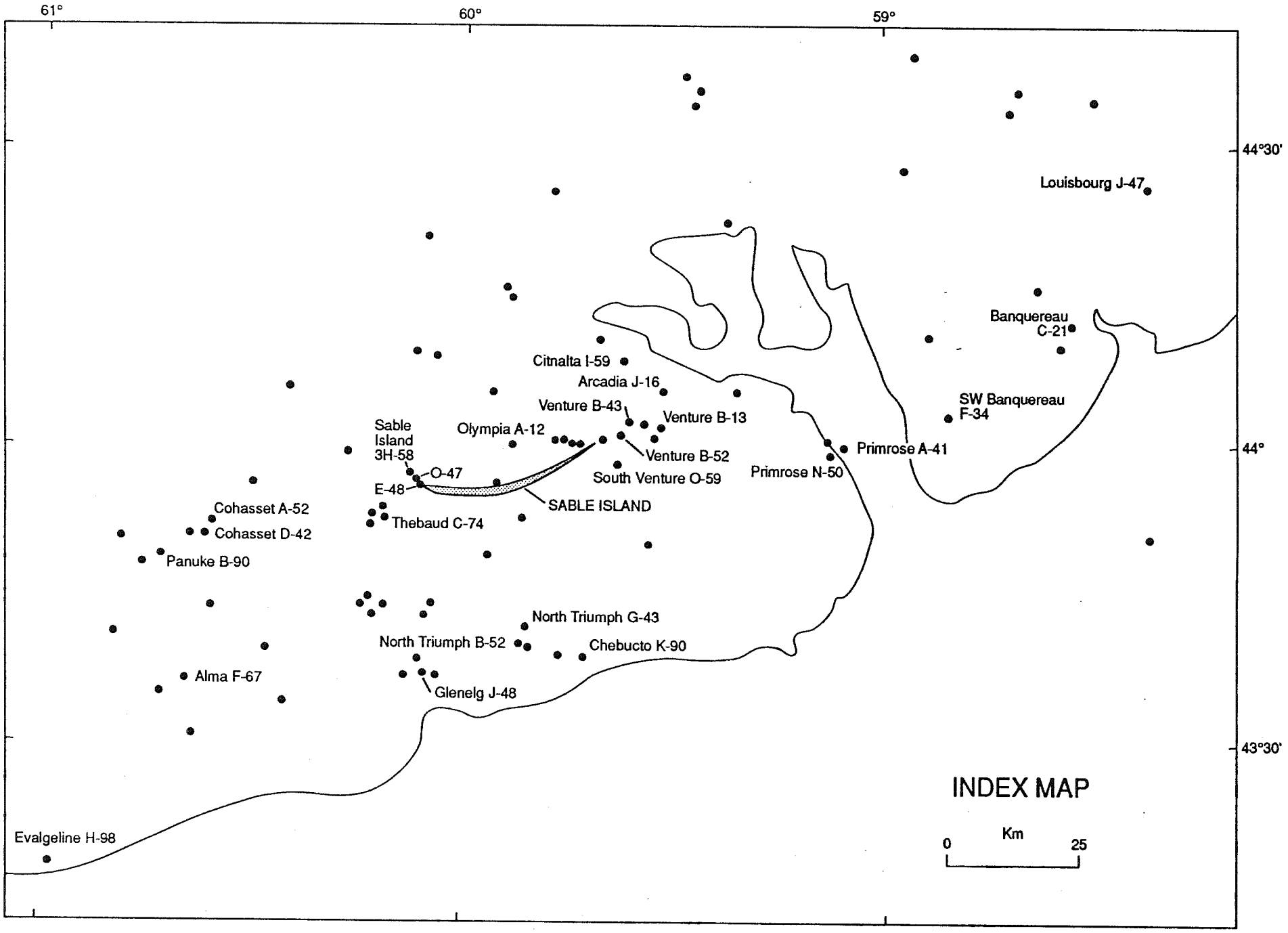
61°
60°
59°
44°30'
44°
43°30'
Louisbourg J-47
Banquereau C-21
SW Banquereau F-34
Citnalta I-59
Arcadia J-16
Venture B-43
Venture B-13
Venture B-52
Sable Island 3H-58
Olympia A-12
O-47
E-48
South Venture O-59
SABLE ISLAND
Primrose A-41
Primrose N-50
Cohasset A-52
Cohasset D-42
Panuke B-90
Thebaud C-74
North Triumph G-43
North Triumph B-52
Chebucto K-90
Alma F-67
Glenelg J-48
Evalgeline H-98
INDEX MAP
Km
0
25

Figure 5

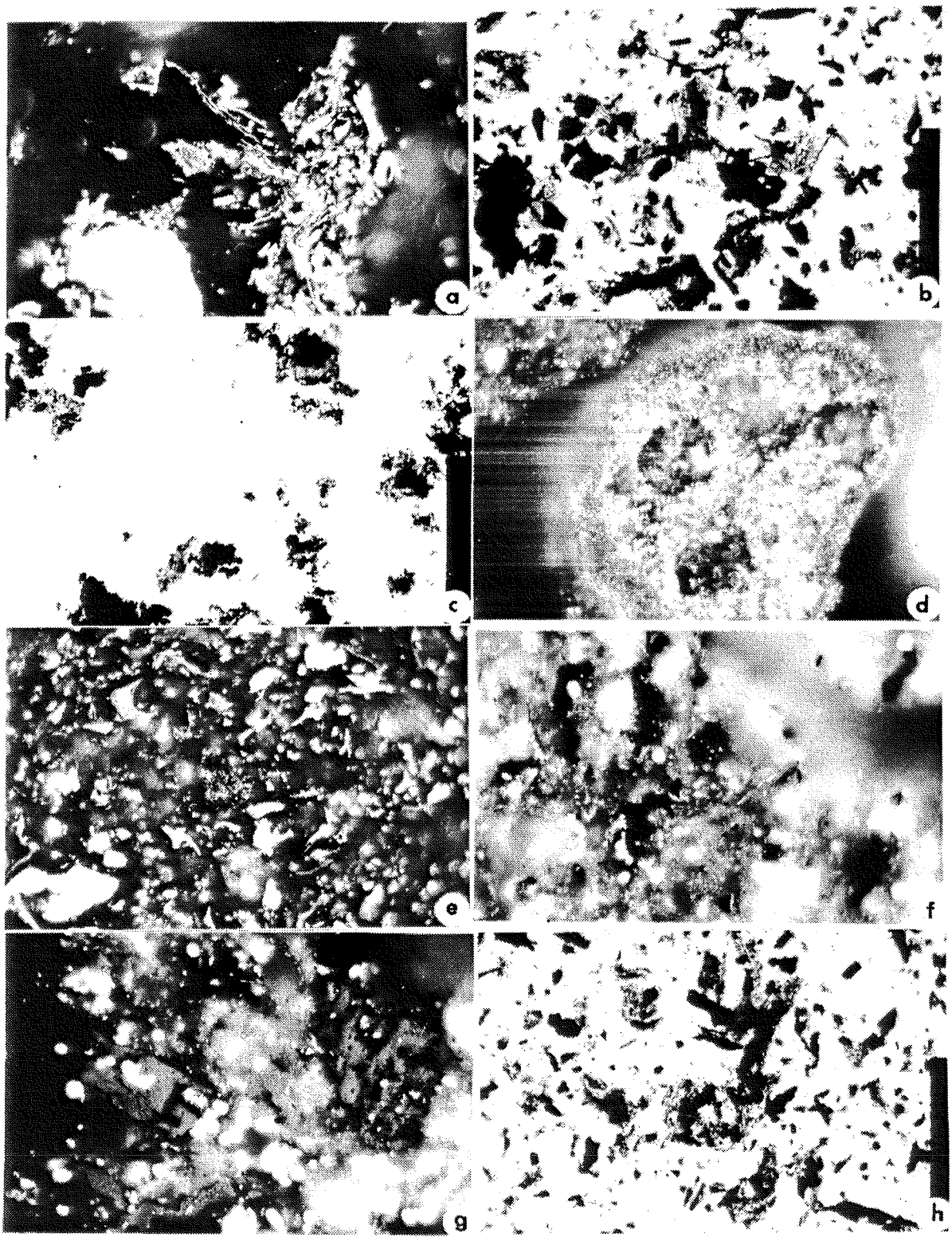

FIGURE 6

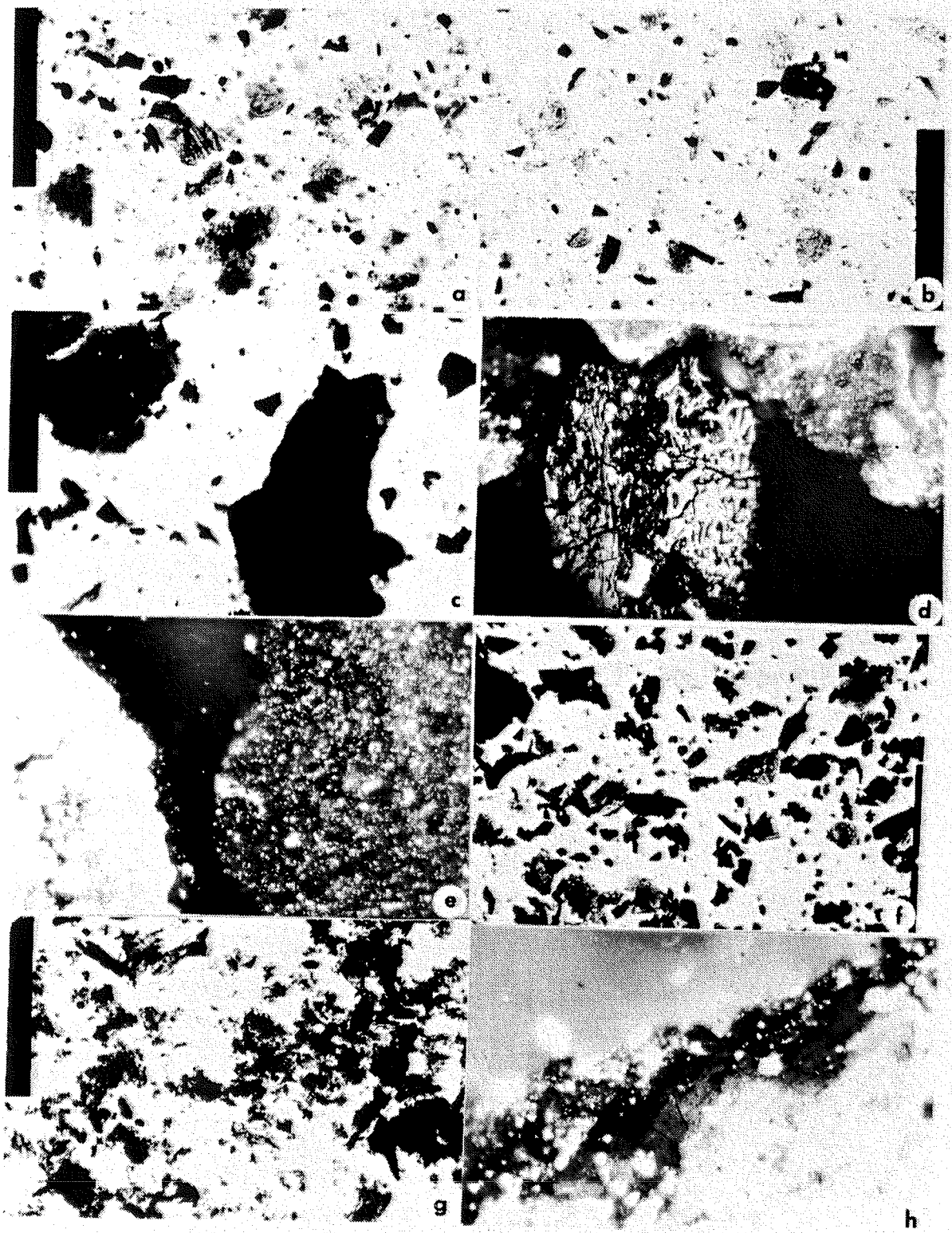

FIGURE 7

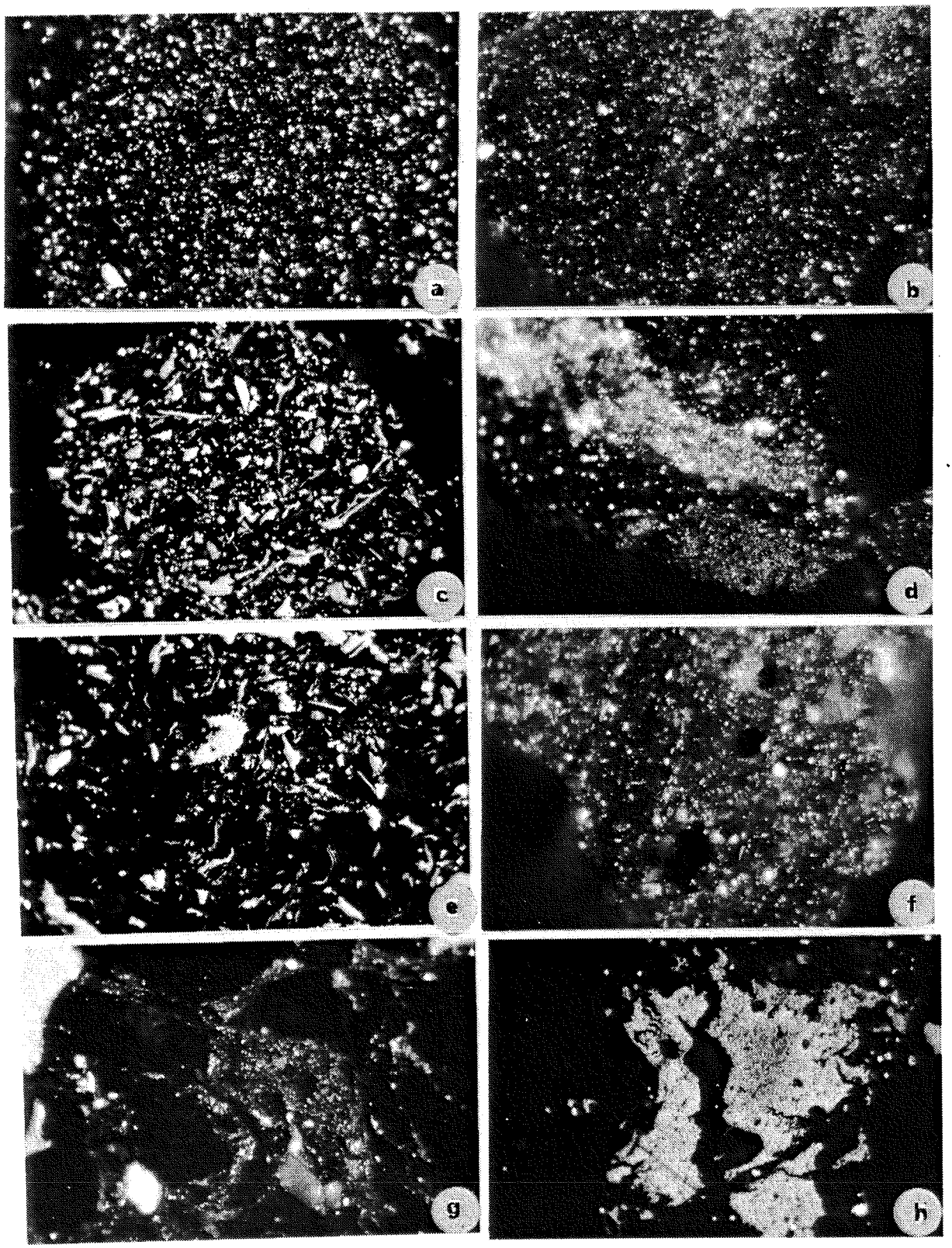

FIGURE 3

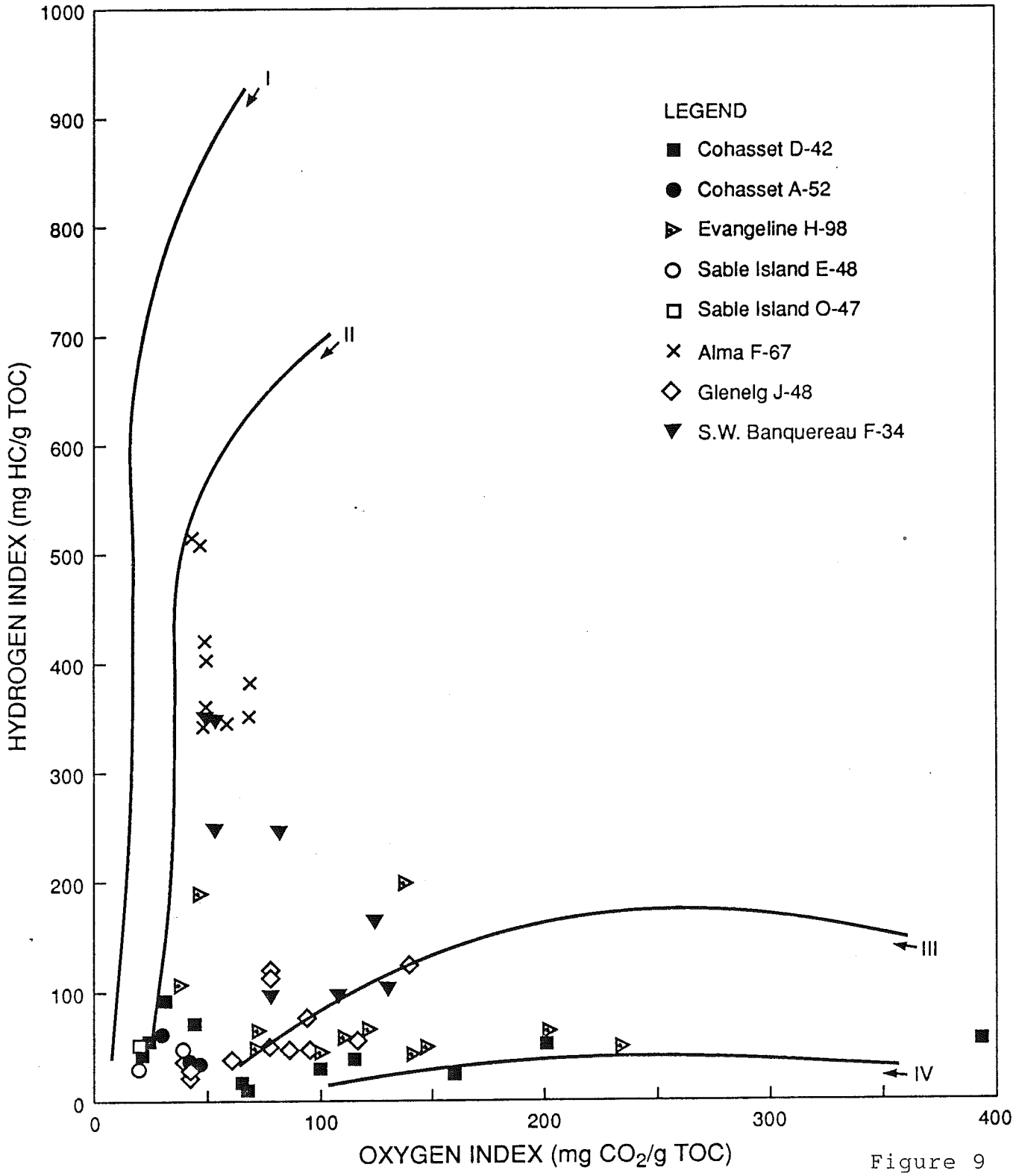
1000
900
800
700
600
500
400
300
200
100
0
HYDROGEN INDEX (mg HC/g TOC)
0
100
200
300
400
OXYGEN INDEX (mg CO_2/g TOC)
I
II
III
IV
LEGEND
Cohasset D-42
Cohasset A-52
Evangeline H-98
Sable Island E-48
Sable Island O-47
Alma F-67
Glenelg J-48
S.W. Banquereau F-34

Figure 9

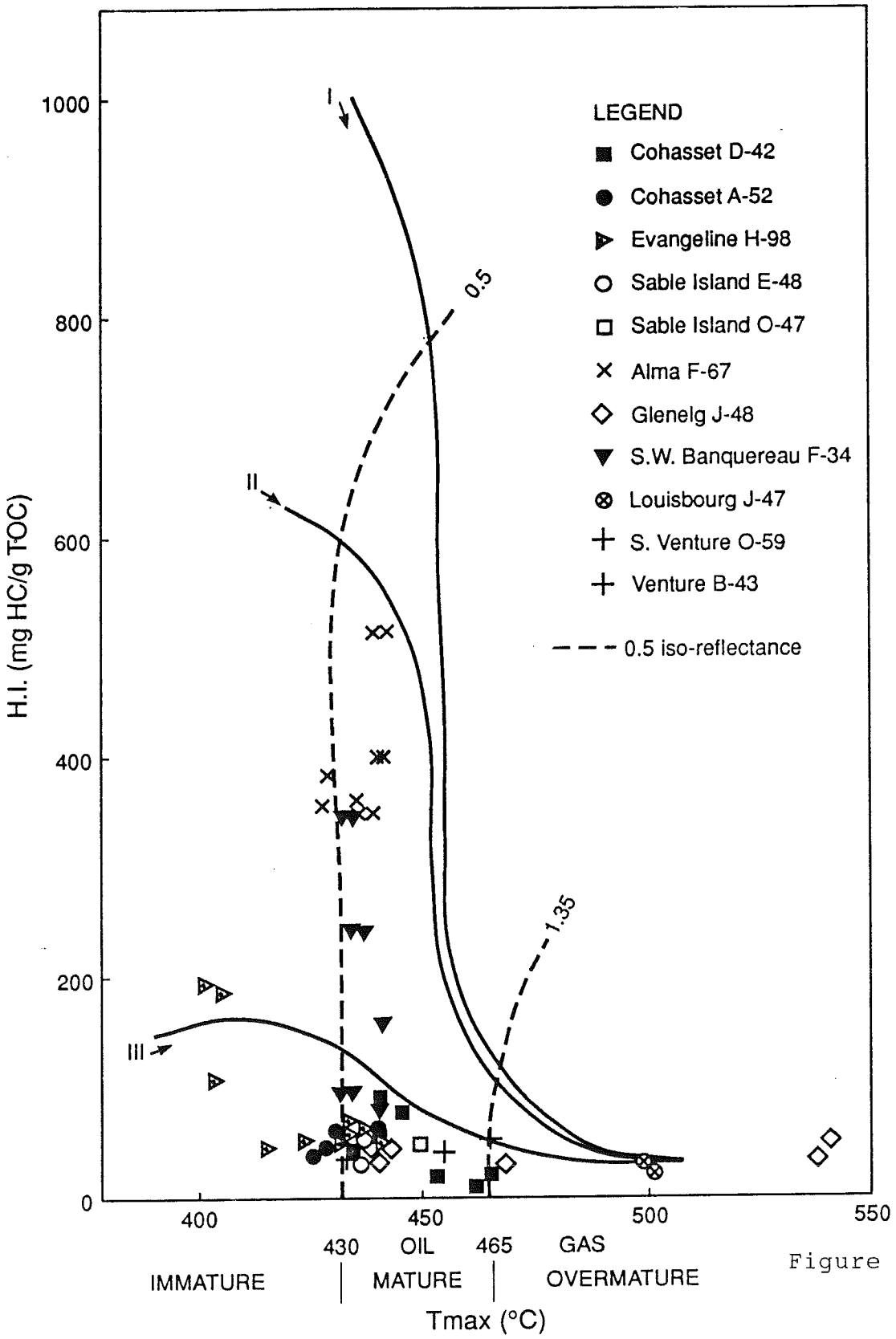
LEGEND
Cohasset D-42
Cohasset A-52
Evangeline H-98
Sable Island E-48
Sable Island O-47
Alma F-67
Glenelg J-48
S.W. Banquereau F-34
Louisbourg J-47
S. Venture O-59
Venture B-43
0.5 iso-reflectance
H.I. (mg HC/g TOC)
Tmax (°C)
IMMATURE
MATURE
OVERMATURE
OIL
GAS
I
II
III
0.5
1.35
0
200
400
600
800
1000
400
430
450
465
500
550

Figure 10

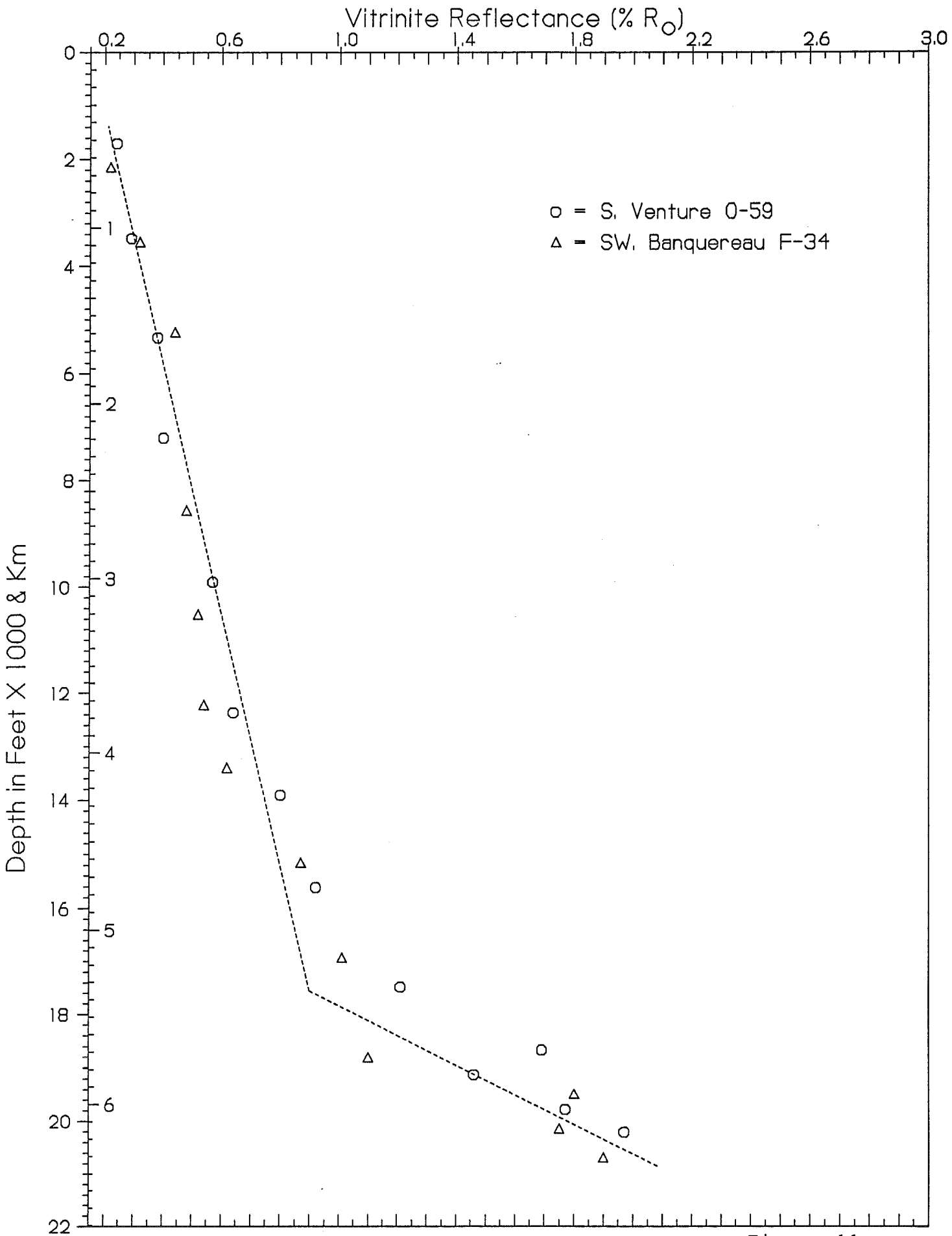

Figure 11

Overlay of VR data from two Scotian Shellf wells

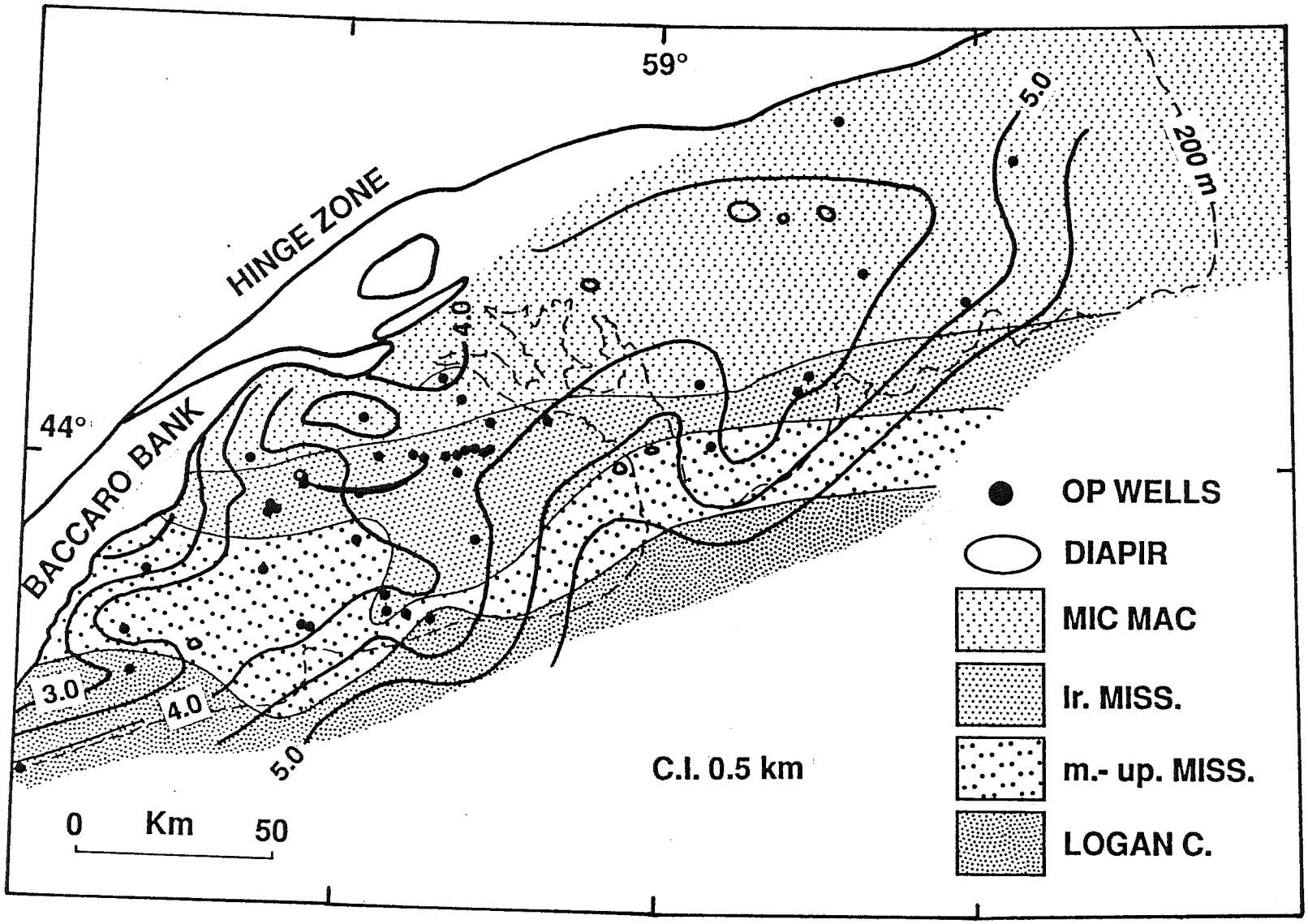
59°
44°
HINGE ZONE
BACCARO BANK
200 m
5.0
4.0
3.0
4.0
5.0
0 Km 50
C.I. 0.5 km
OP WELLS
DIAPIR
MIC MAC
lr. MISS.
m.- up. MISS.
LOGAN C.

Figure 12

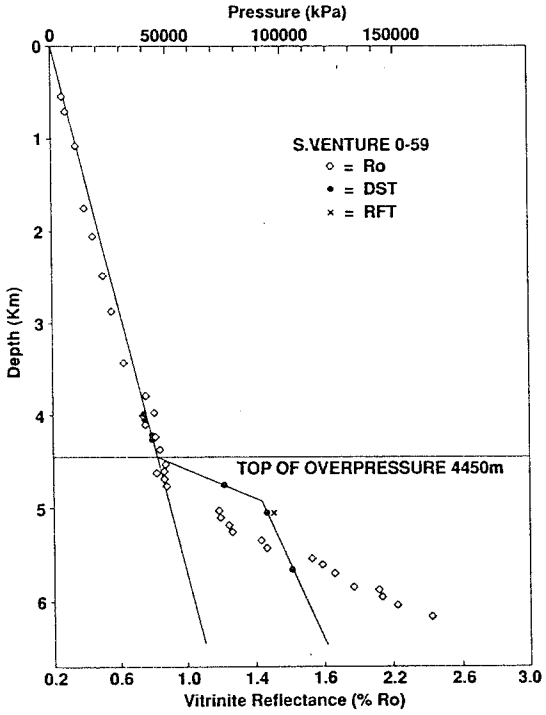
Pressure (kPa)
0
50000
100000
150000
S.VENTURE 0-59
◇ = Ro
• = DST
× = RFT
TOP OF OVERPRESSURE 4450m
Depth (Km)
0
1
2
3
4
5
6
0.2
0.6
1.0
1.4
1.6
2.2
2.6
3.0
Vitrinite Reflectance (% Ro)

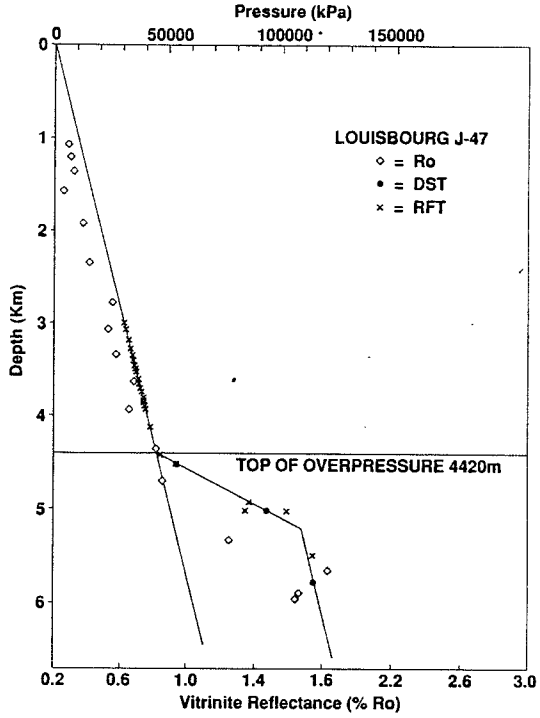
Pressure (kPa)
0
50000
100000
150000
LOUISBOURG J-47
◇ = Ro
• = DST
× = RFT
TOP OF OVERPRESSURE 4420m
Depth (Km)
0
1
2
3
4
5
6
0.2
0.6
1.0
1.4
1.6
2.2
2.6
3.0
Vitrinite Reflectance (% Ro)

Figure 13

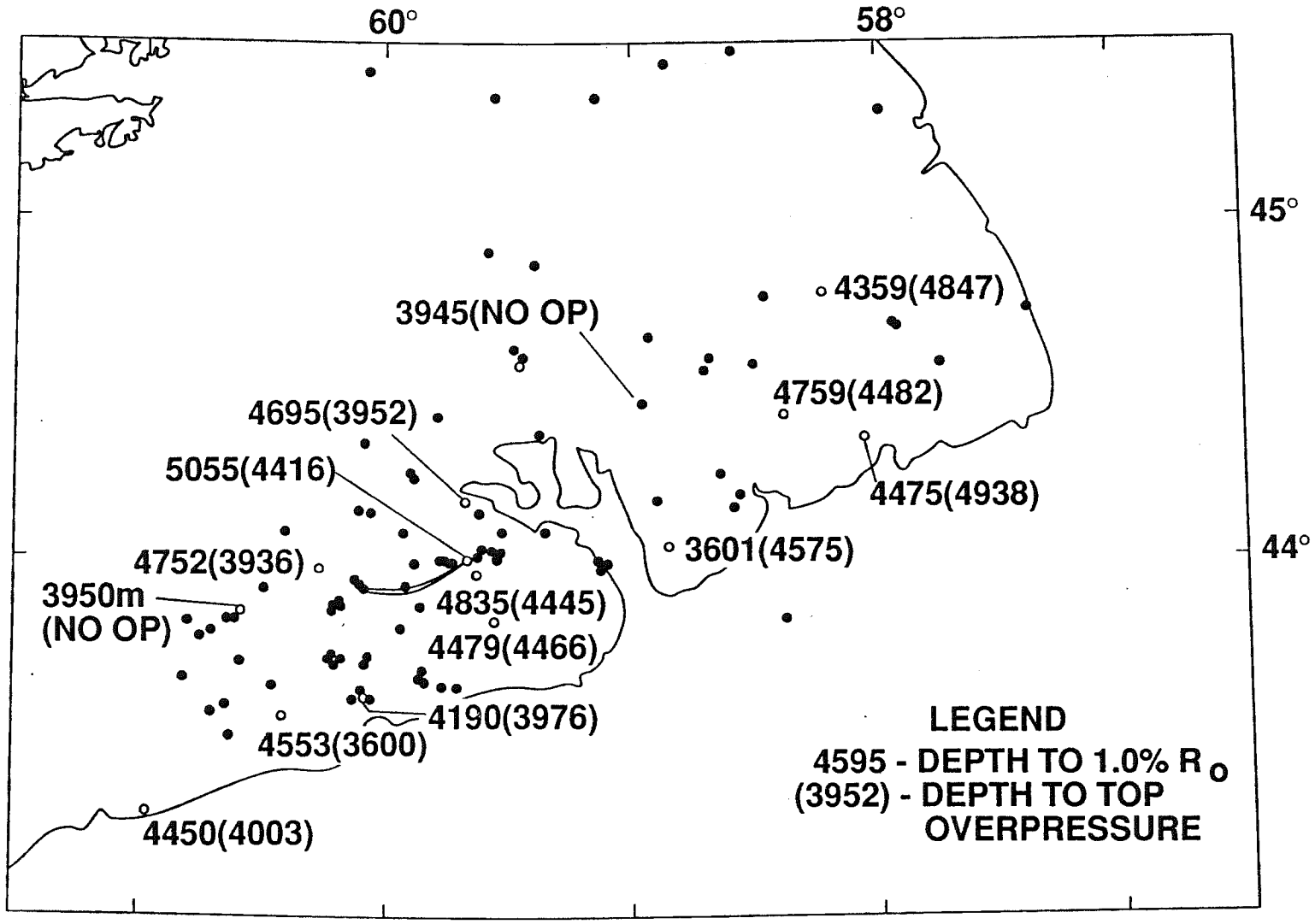
60°
58°
45°
44°
3945(NO OP)
4359(4847)
4759(4482)
4695(3952)
5055(4416)
4475(4938)
3601(4575)
4752(3936)
3950m
(NO OP)
4835(4445)
4479(4466)
4190(3976)
4553(3600)
4450(4003)
LEGEND
4595 - DEPTH TO 1.0% R o
(3952) - DEPTH TO TOP
OVERPRESSURE

Figure 14

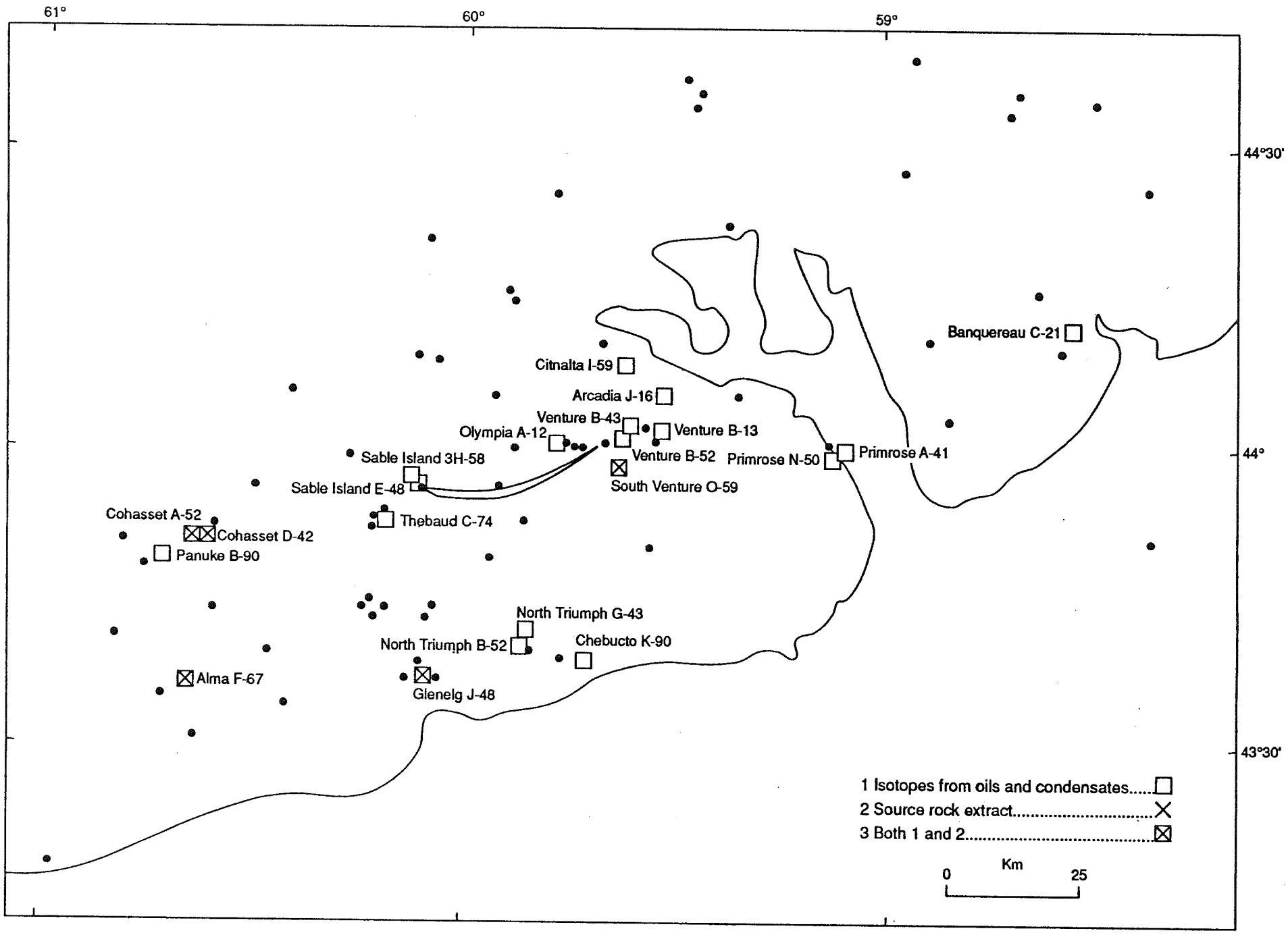
61°
60°
59°
44°30'
44°
43°30'
Banquereau C-21
Citnalta I-59
Arcadia J-16
Venture B-43
Venture B-13
Olympia A-12
Sable Island 3H-58
Venture B-52
Primrose N-50
Primrose A-41
South Venture O-59
Sable Island E-48
Cohasset A-52
Thebaud C-74
Cohasset D-42
Panuke B-90
North Triumph G-43
North Triumph B-52
Chebucto K-90
Alma F-67
Glenelg J-48
1 Isotopes from oils and condensates
2 Source rock extract
3 Both 1 and 2
Km
0
25

Figure 15

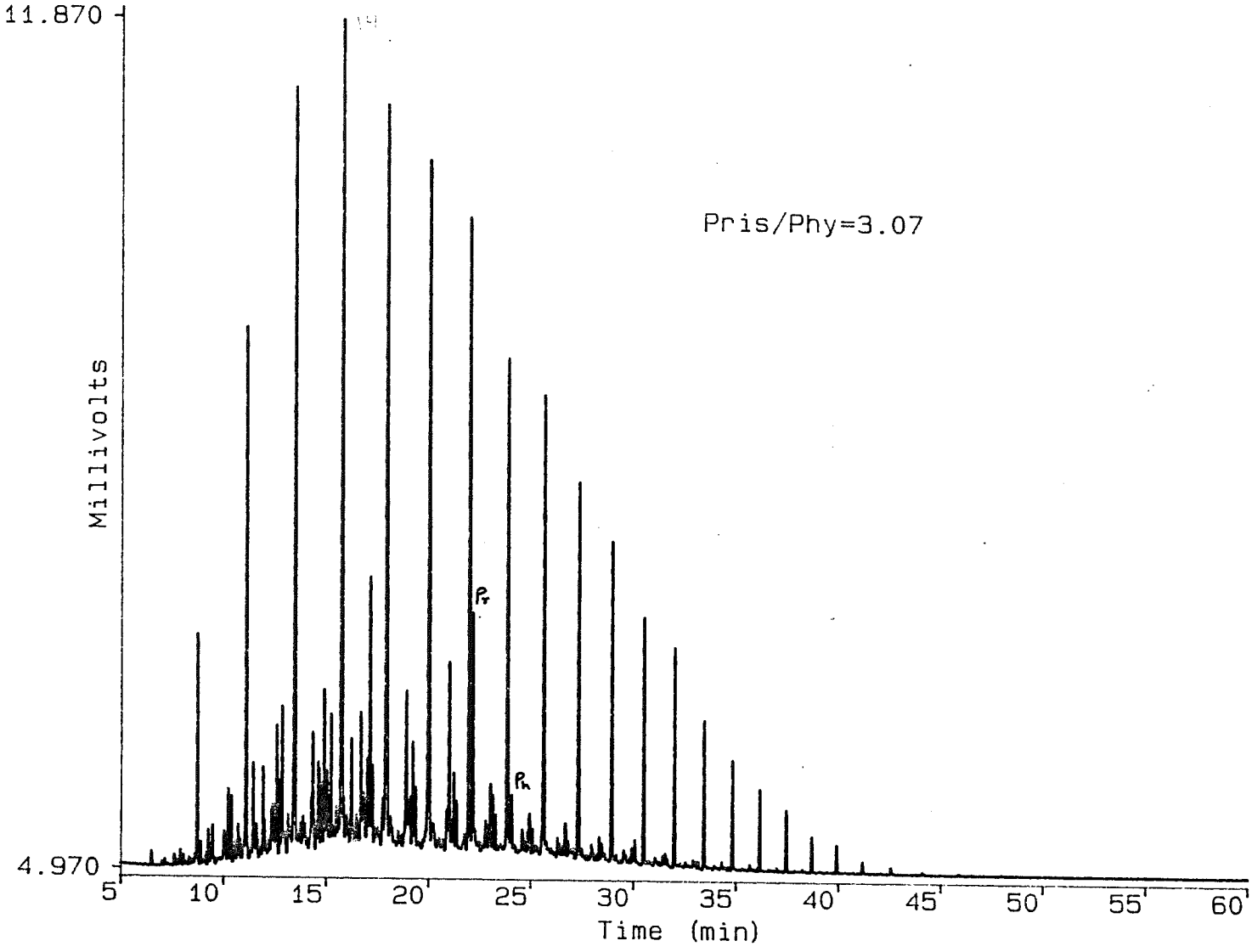

#770 D294 COHASSET A-52 DST#5, ZONE 5

Figure 16a

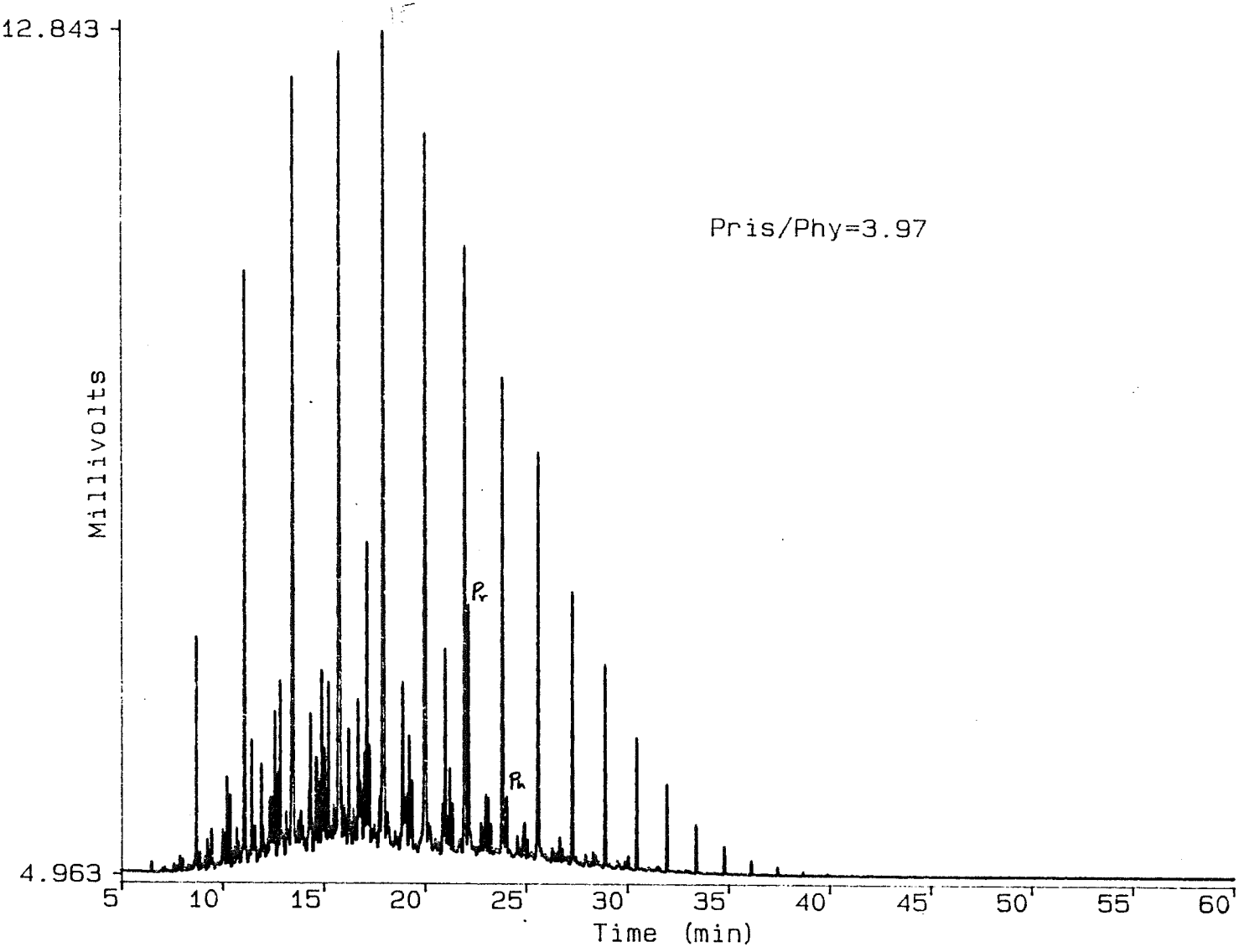

#780 D294 COHASSET A-52 DST#2, ZONE 2

Figure 16b

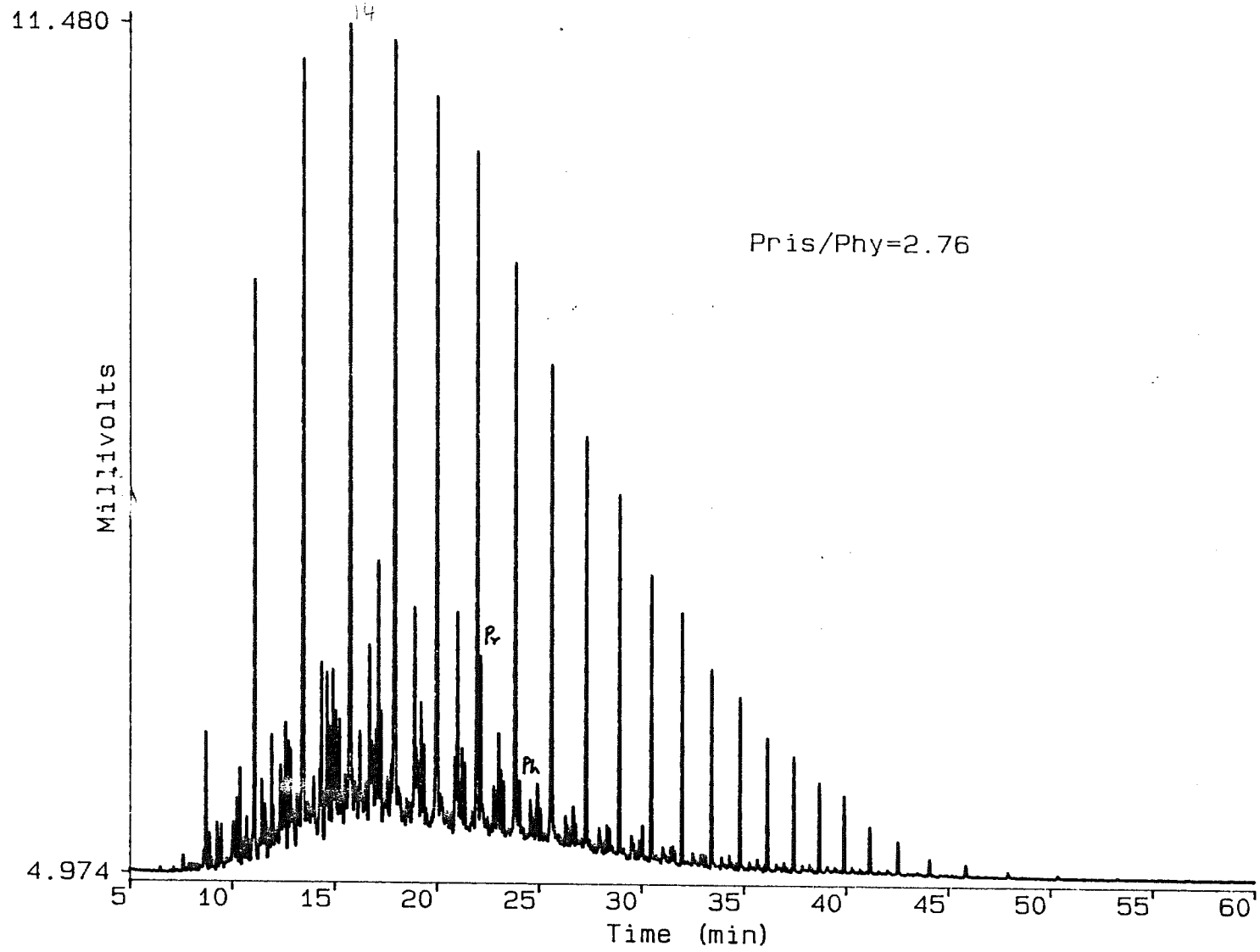
11.480
4.974
Millivolts
Pris/Phy=2.76
Pr
Ph
5
10
15
20
25
30
35
40
45
50
55
60
Time (min)
#763 D289 N.TRIUMPH B-52 3771-3777 m

Figure 16c

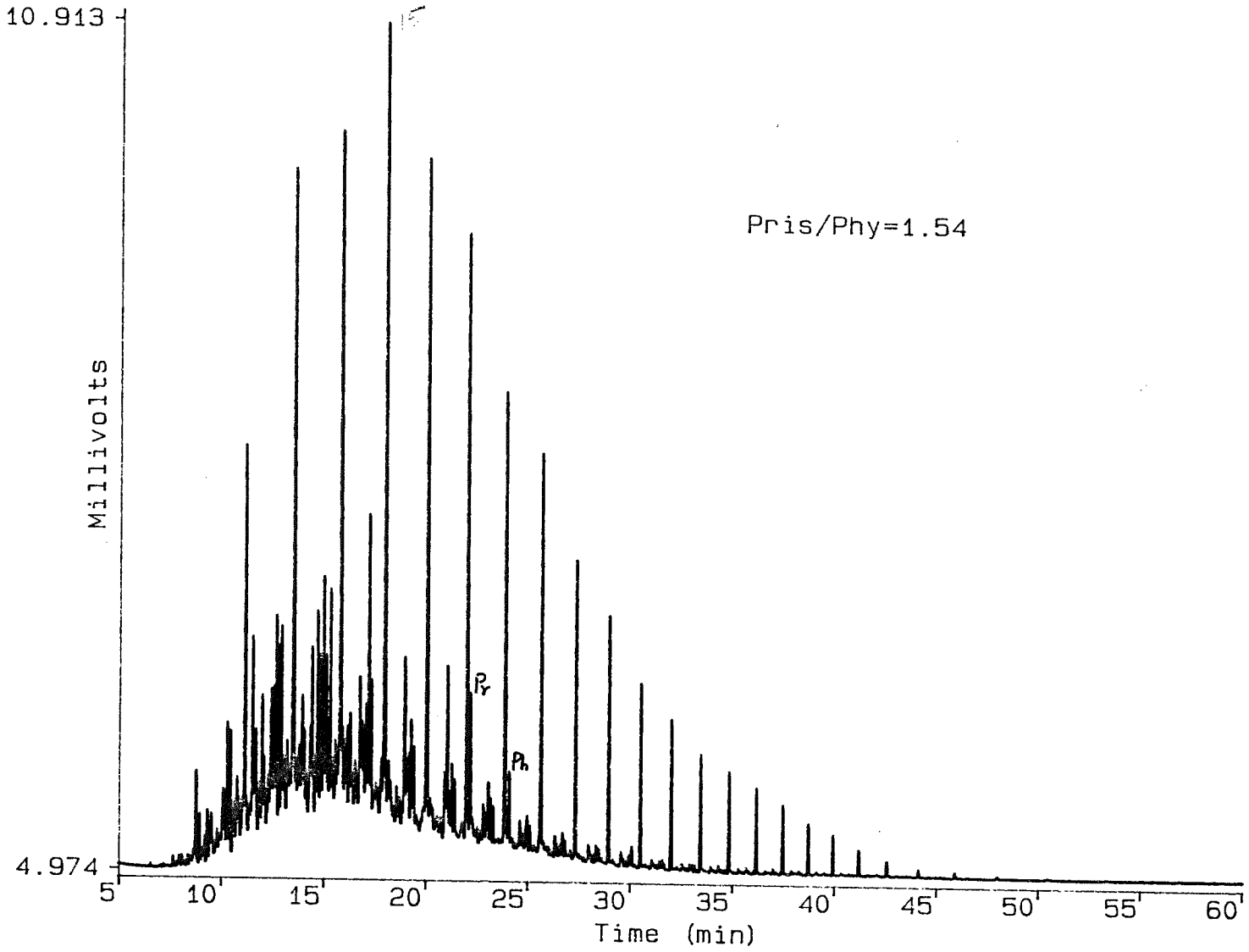

#766 D281 N.TRIUMPH G-43 3835-3846 m

Figure 16d

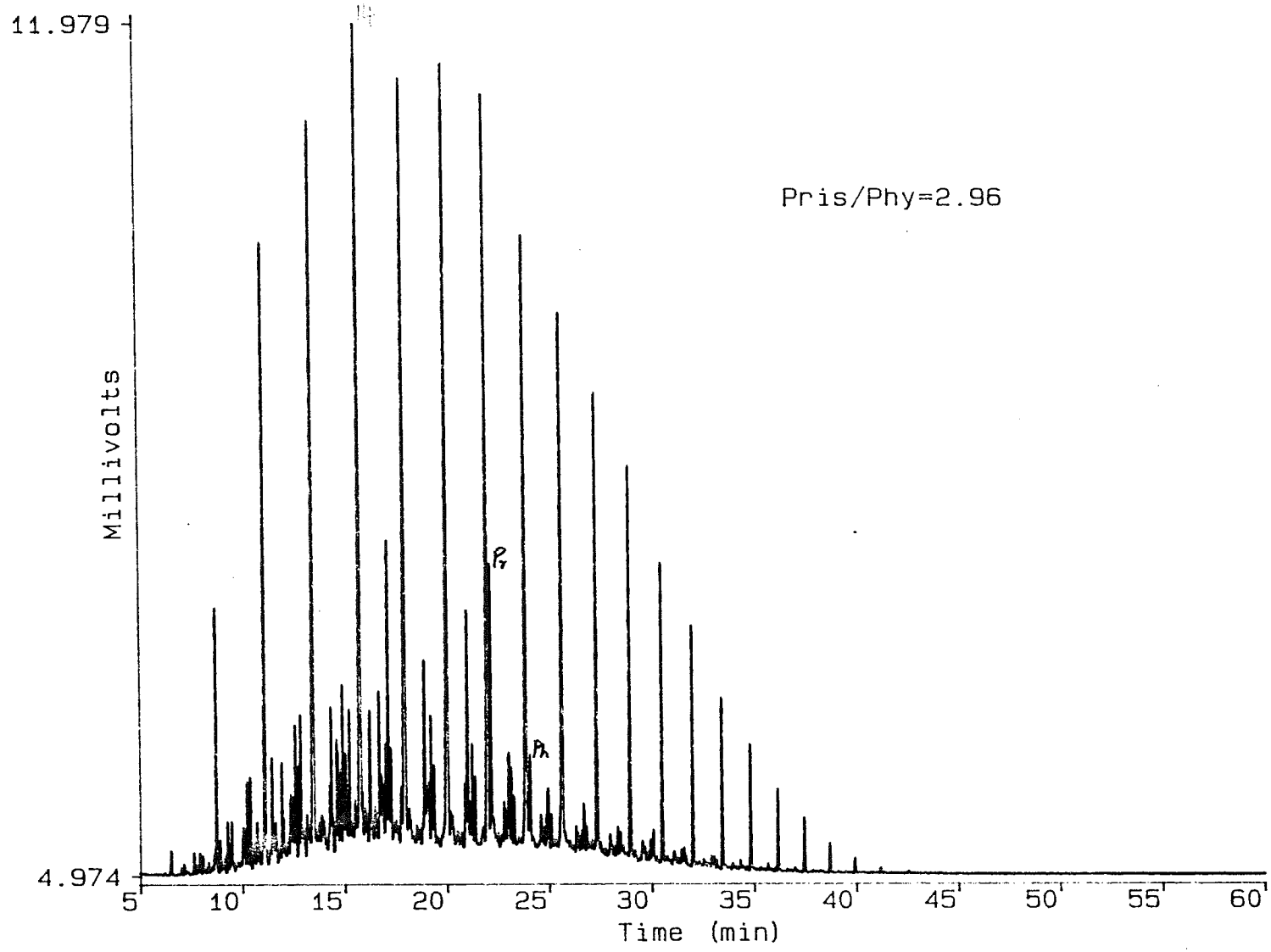

#786 D300 PANUKE B-90 DST#1, ZONE 1

Figure 16e

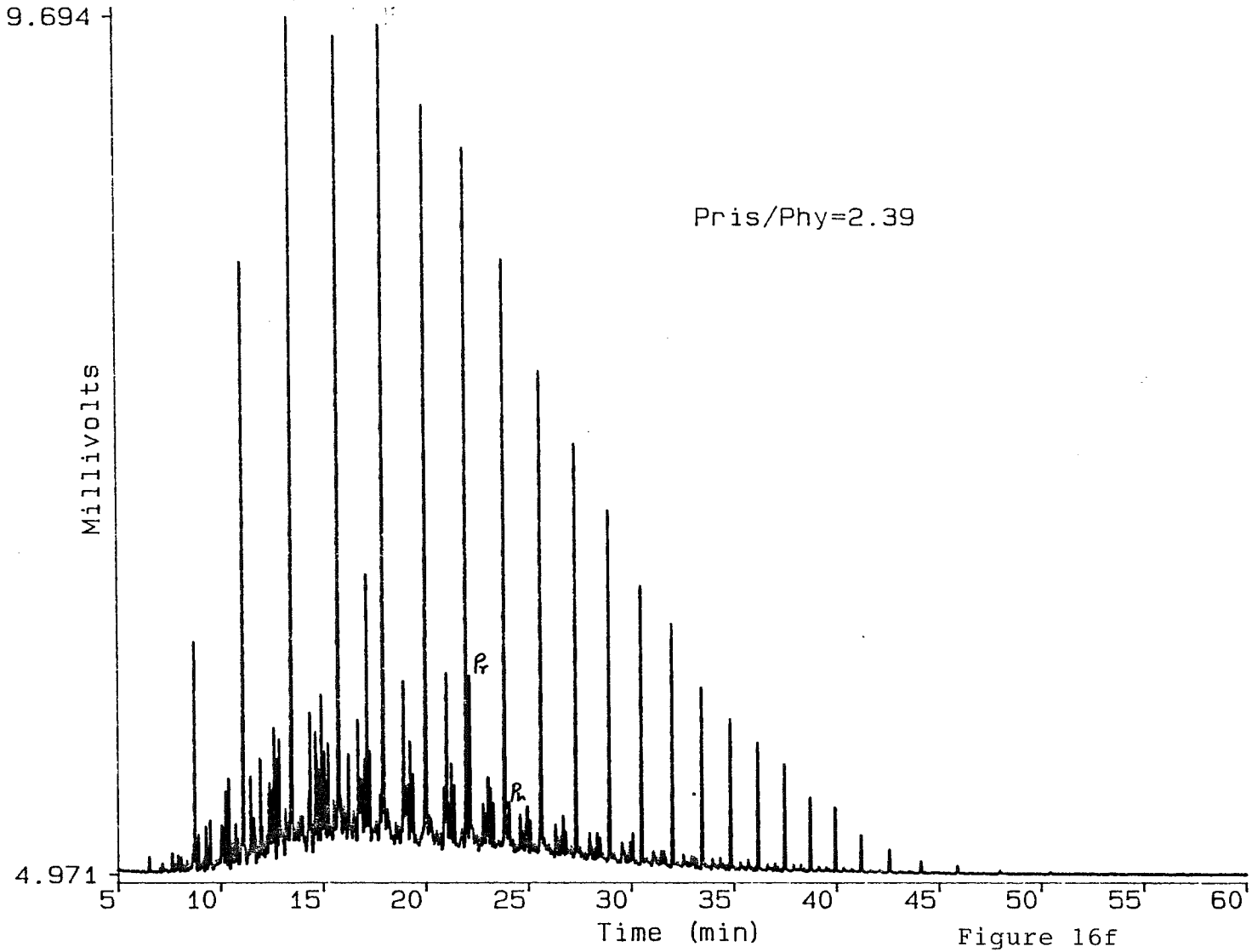

Figure 16f

#771 D295 THEBAUD C-74 3865-3888 m

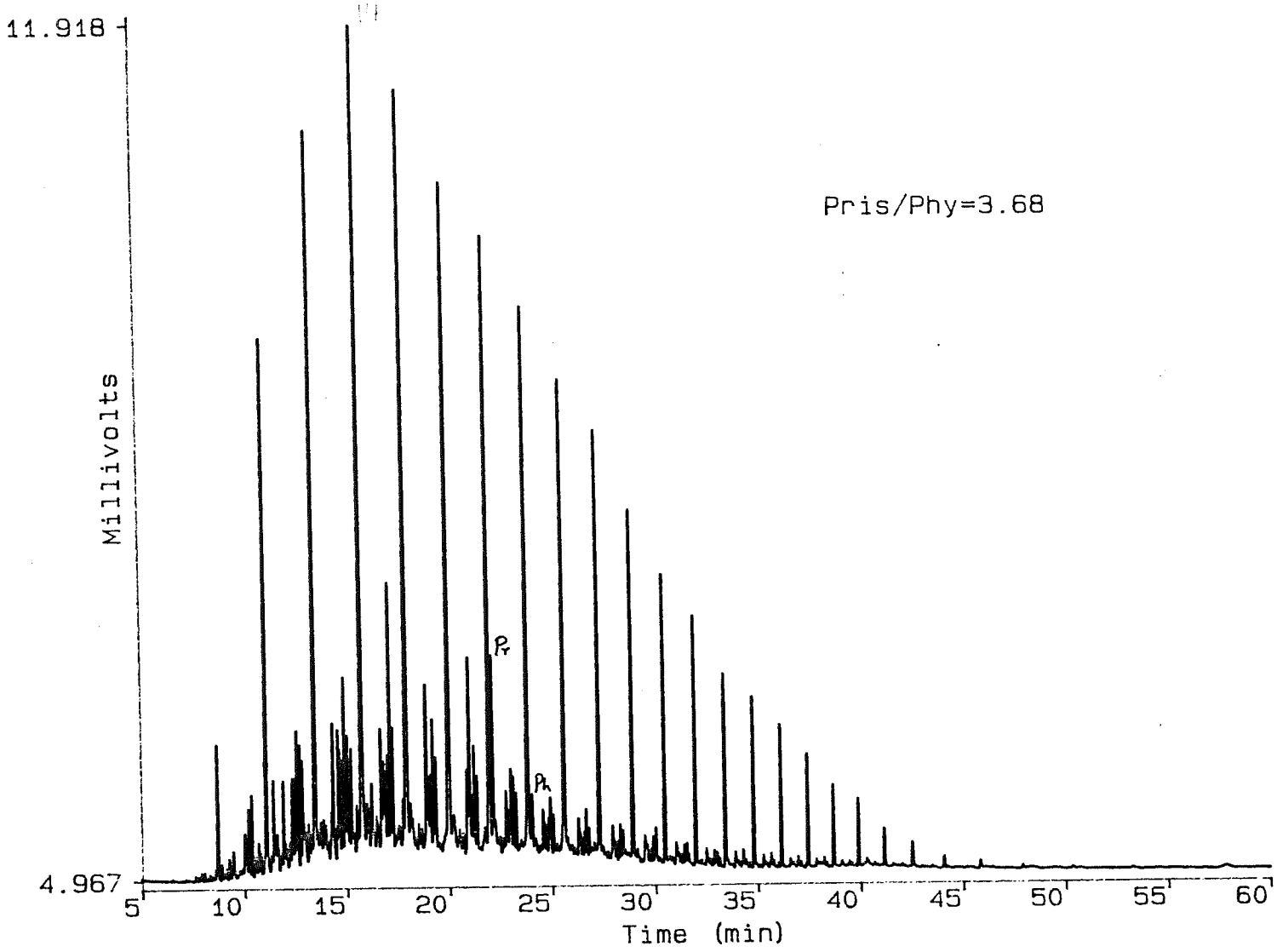

#790 D295 THEBAUD C-74 DST#4, ZONE 4

Figure 16g

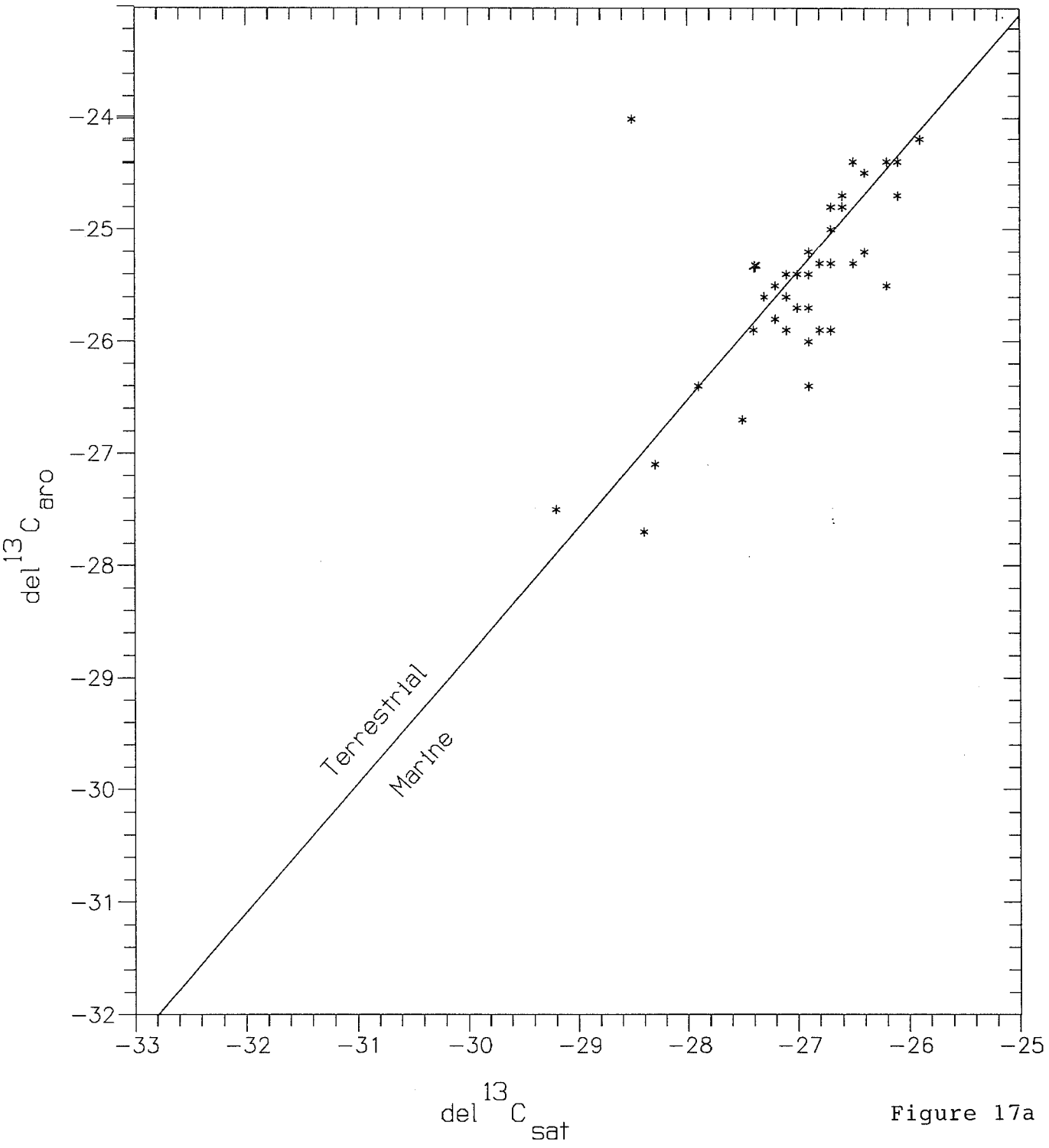
−24
−25
−26
−27
−28
−29
−30
−31
−32
−33
−32
−31
−30
−29
−28
−27
−26
−25
del 13C aro
del 13C sat
Terrestrial
Marine

Figure 17a

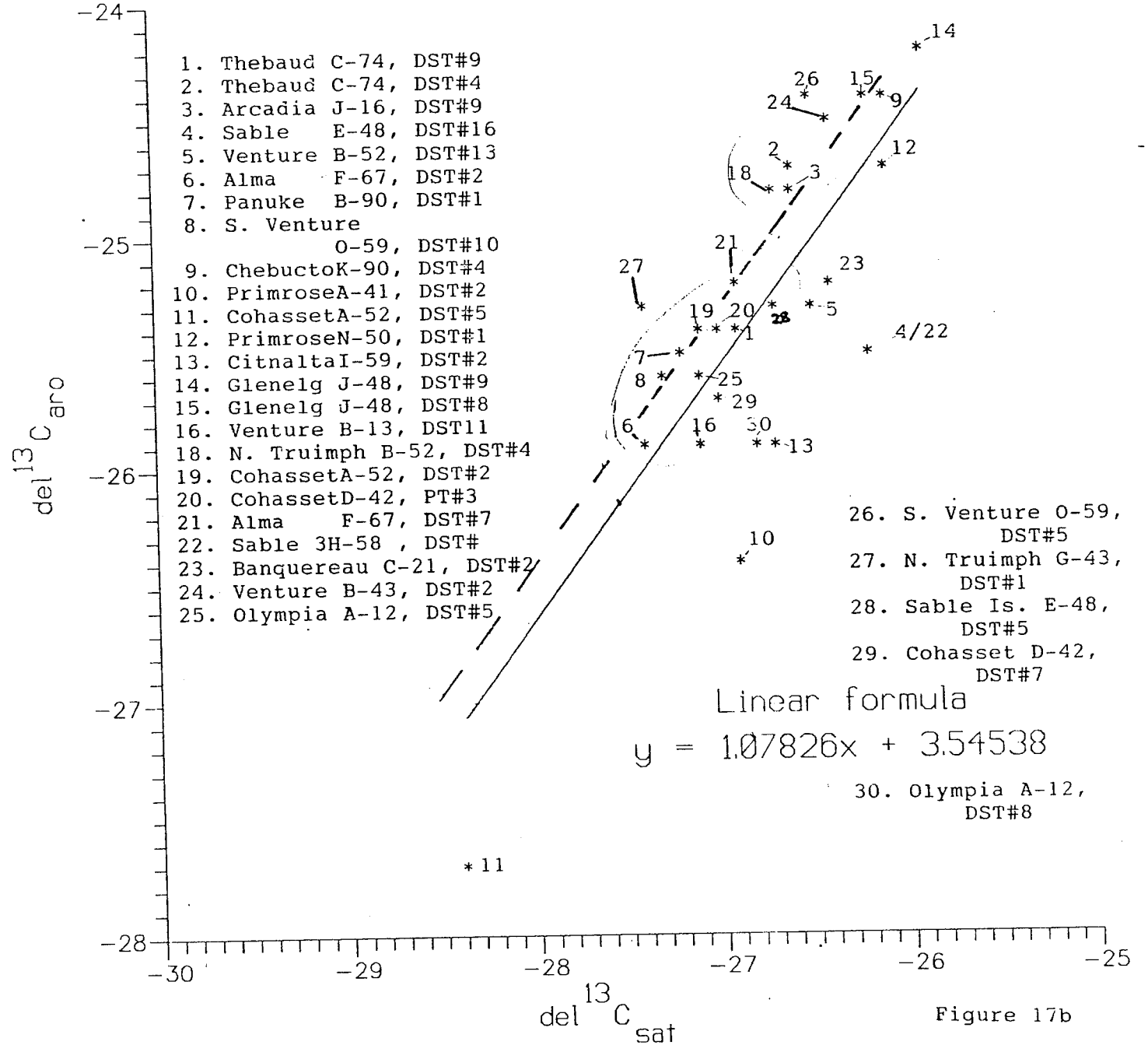
1. Thebaud C-74, DST#9
2. Thebaud C-74, DST#4
3. Arcadia J-16, DST#9
4. Sable E-48, DST#16
5. Venture B-52, DST#13
6. Alma F-67, DST#2
7. Panuke B-90, DST#1
8. S. Venture O-59, DST#10
9. ChebuctoK-90, DST#4
10. PrimroseA-41, DST#2
11. CohassetA-52, DST#5
12. PrimroseN-50, DST#1
13. CitnaltaI-59, DST#2
14. Glenelg J-48, DST#9
15. Glenelg J-48, DST#8
16. Venture B-13, DST11
18. N. Truimph B-52, DST#4
19. CohassetA-52, DST#2
20. CohassetD-42, PT#3
21. Alma F-67, DST#7
22. Sable 3H-58 , DST#
23. Banquereau C-21, DST#2
24. Venture B-43, DST#2
25. Olympia A-12, DST#5
26. S. Venture O-59, DST#5
27. N. Truimph G-43, DST#1
28. Sable Is. E-48, DST#5
29. Cohasset D-42, DST#7
30. Olympia A-12, DST#8
Linear formula
y = 1.07826x + 3.54538
del 13 C aro
del 13 C sat
-24
-25
-26
-27
-28
-30
-29
-28
-27
-26
-25

Figure 17b

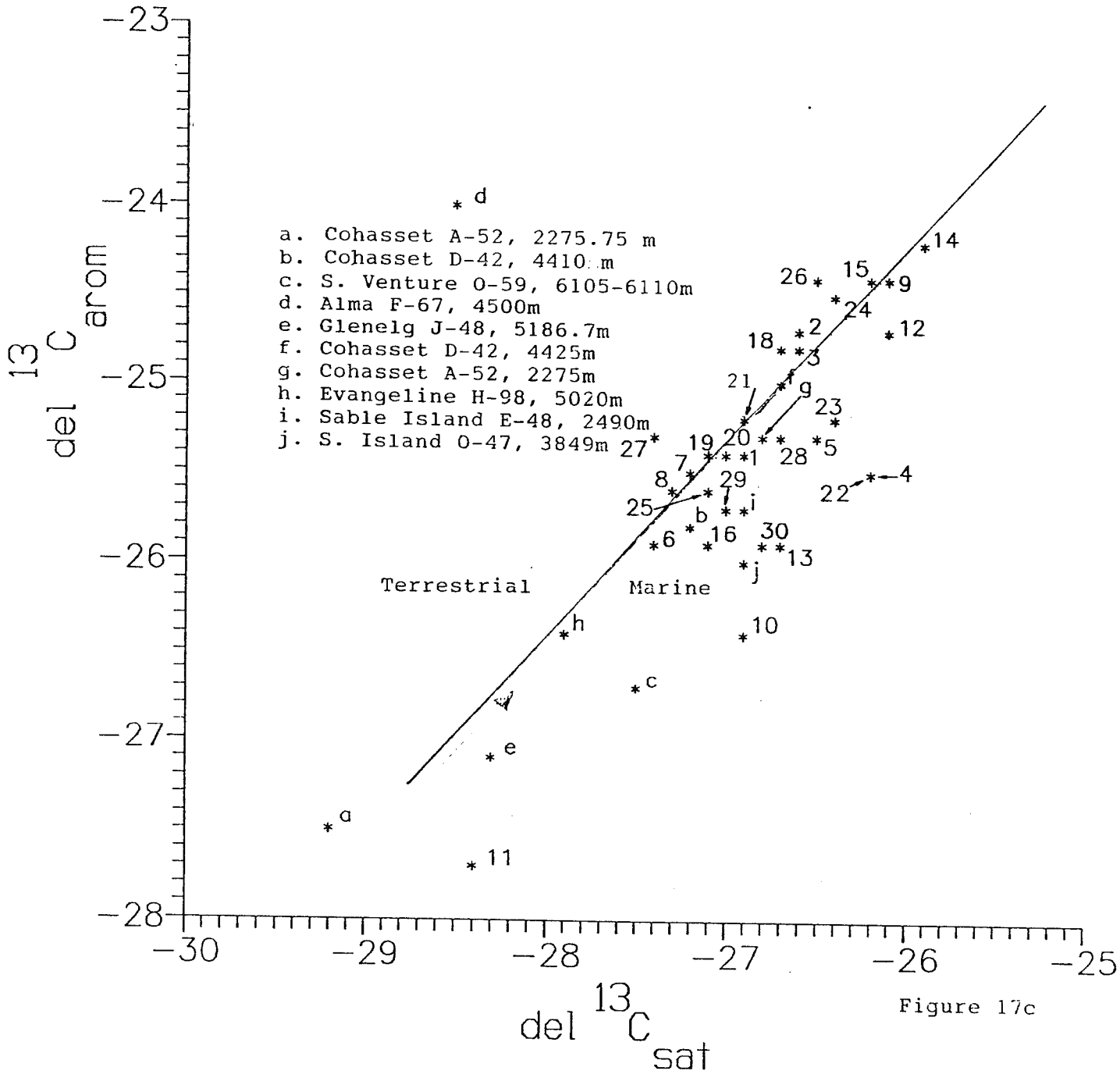
a. Cohasset A-52, 2275.75 m
b. Cohasset D-42, 4410 m
c. S. Venture O-59, 6105-6110m
d. Alma F-67, 4500m
e. Glenelg J-48, 5186.7m
f. Cohasset D-42, 4425m
g. Cohasset A-52, 2275m
h. Evangeline H-98, 5020m
i. Sable Island E-48, 2490m
j. S. Island O-47, 3849m
Terrestrial
Marine
del 13C arom
del 13C sat
−23
−24
−25
−26
−27
−28
−30
−29
−28
−27
−26
−25

Figure 17c

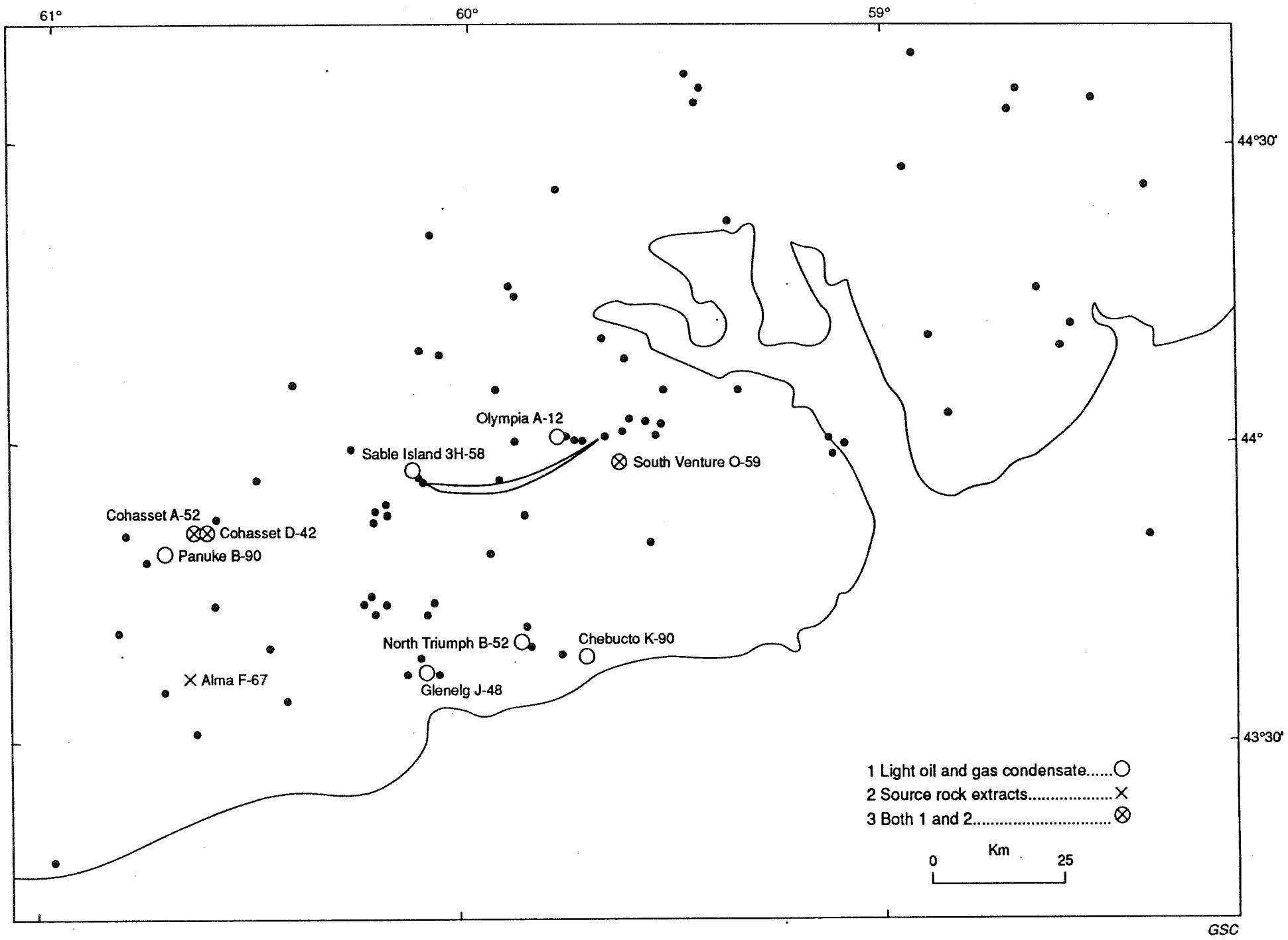

Figure 18

JW2/719/F1

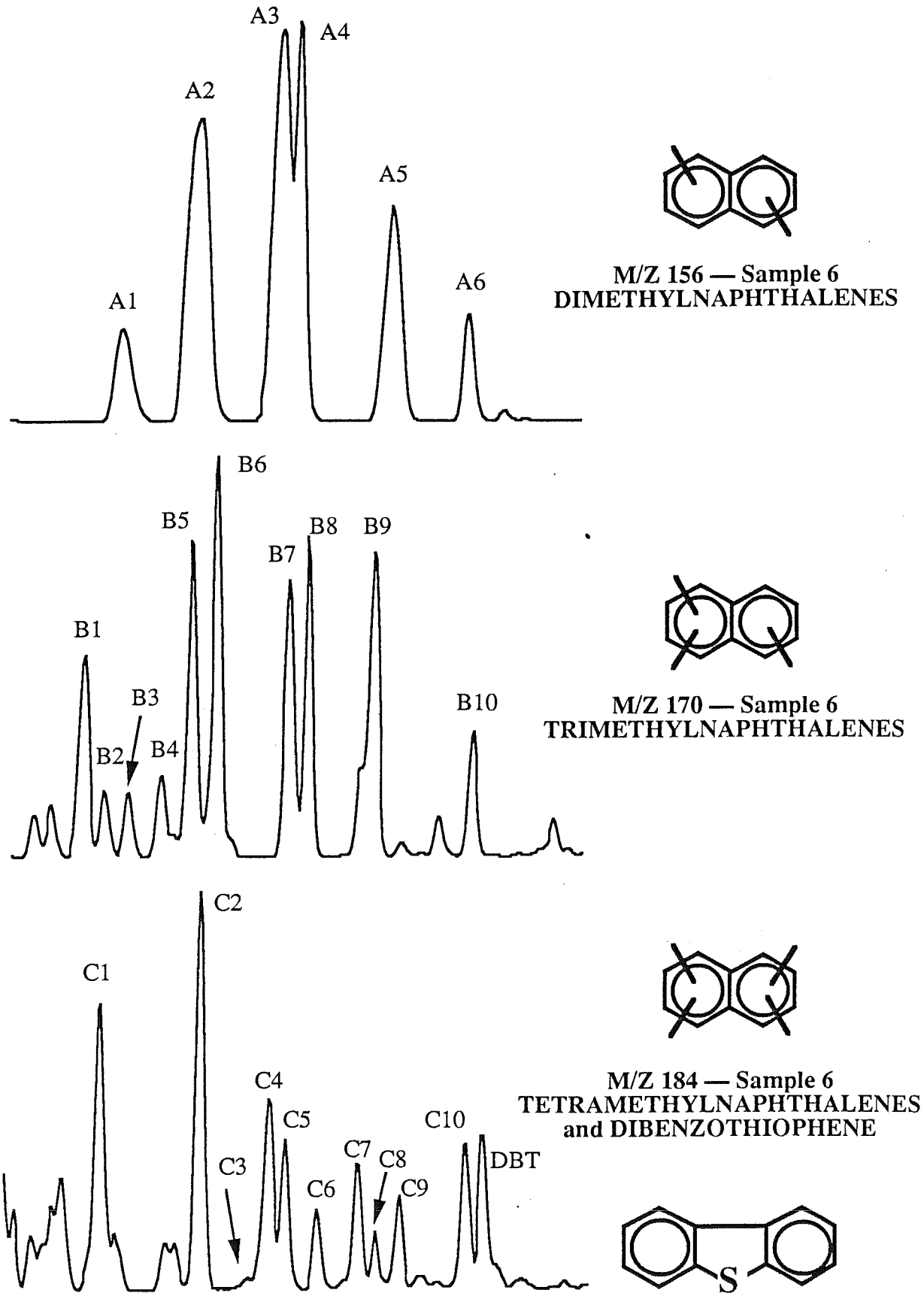

Figure 19 Mass chromatograms of the isomers of naphthalene homologues. Peaks used in the study are labelled and molecular structures are shown.

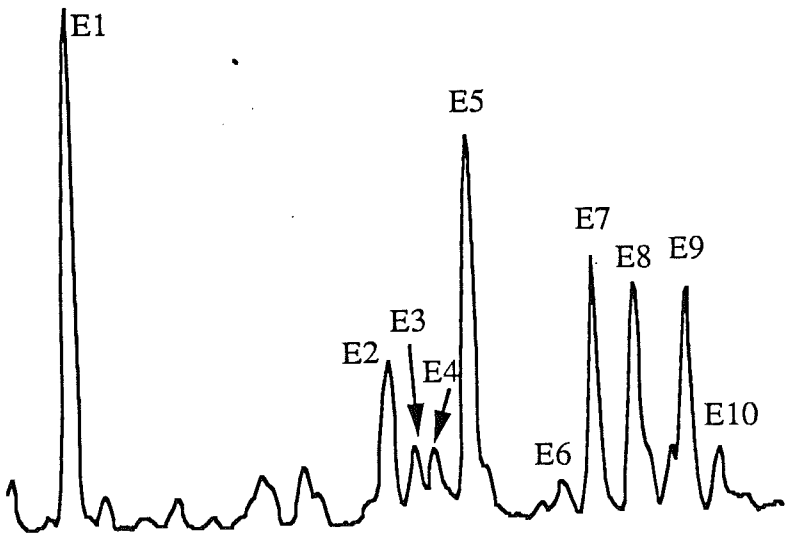

M/Z 202 — Sample 6
PYRENE (E9)
FLUORANTHENE (E5)
AND UNIDENTIFIED PEAKS

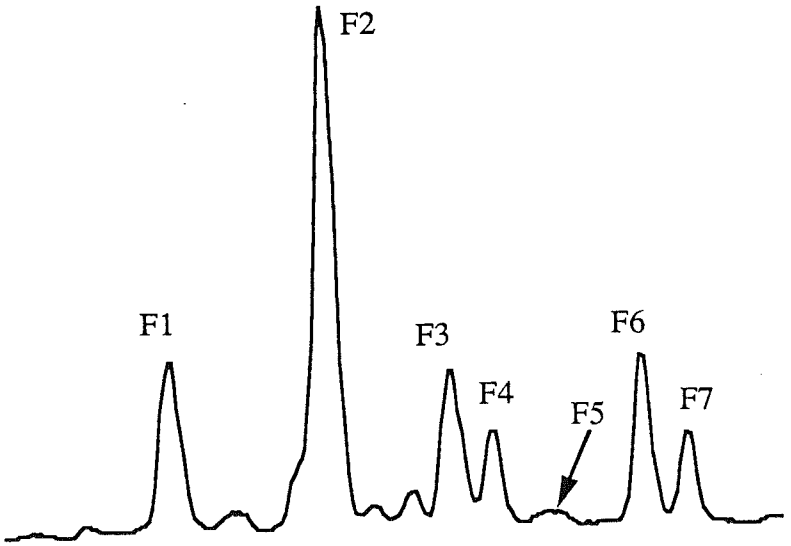

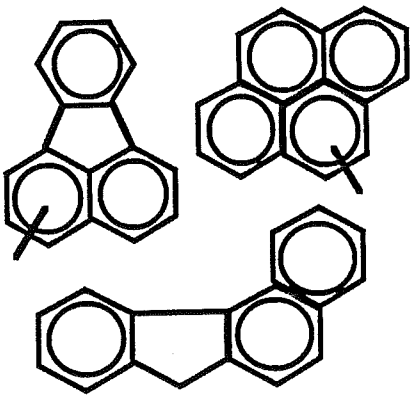

M/Z 216 — Sample 6
METHYLPYRENES
METHYLFLUORANTHENES
BENZOFLUORENE

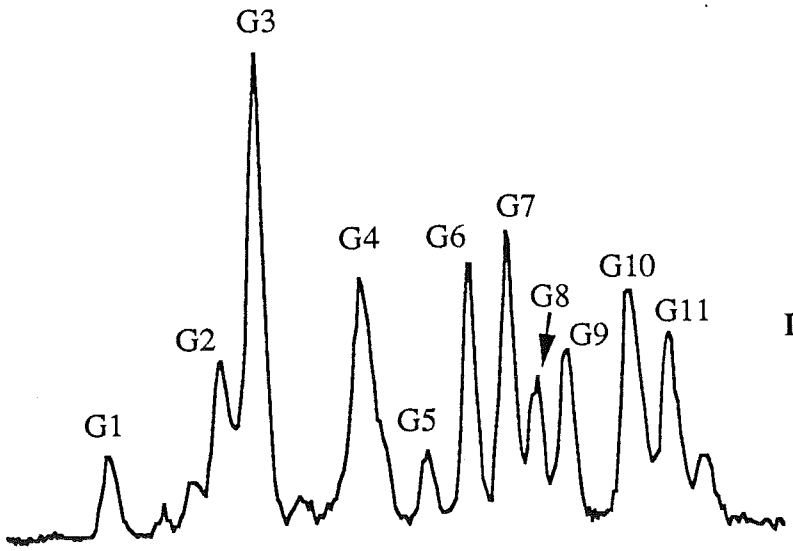

M/Z 230 — Sample 13
DIMETHYLPYRENES
DIMETHYLFLUORANTHENES
METHYLBENZOFLUORENES

Mass chromatograms of the isomers of selected tetraaromaitc compounds and their homologues. Peaks used in the study are labelled and molecular structures are shown.

Figure 20

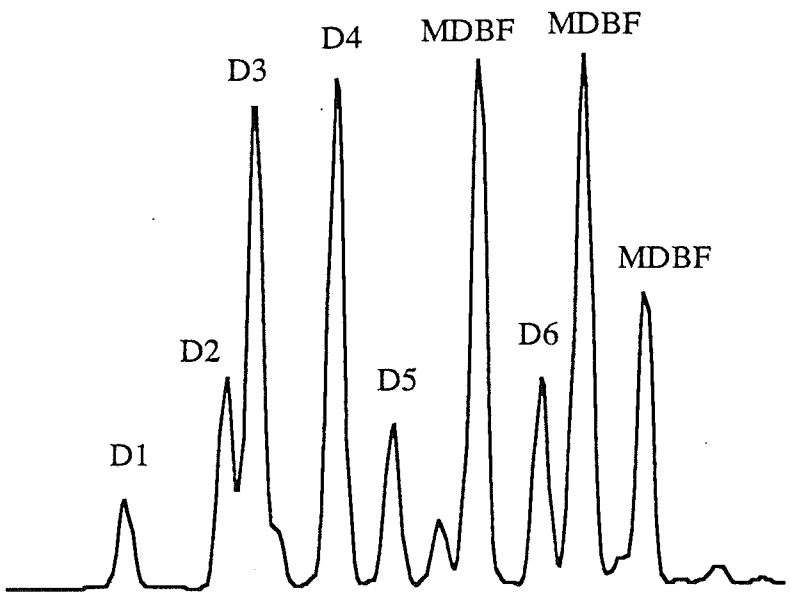

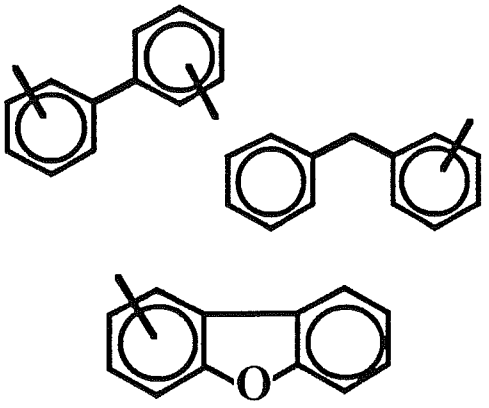

M/Z 182 — Sample 14
DIMETHYLBIPHENYLS
METHYLDIPHENYLMETHANE
METHYLDIBENZOFURANS

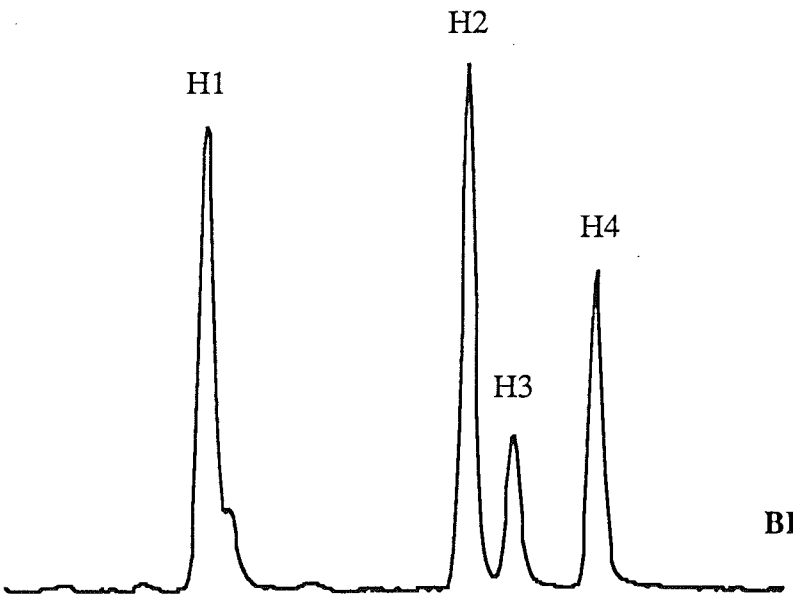

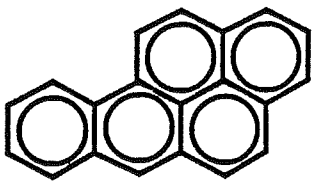

M/Z 252 — Sample 1
BENZO[*a*]PYRENE & ISOMERS

Mass chromatograms of the isomers of dimethylbiphenyl, methyldibenzofuran and selected pentaaromatics. Peaks used in the study are labelled and molecular structures are shown.

Figure 21

Example of data preparation.

a) Original partial mass chromatogram of m/z 170, showing the distribution of trimethylnaphthalene isomers.

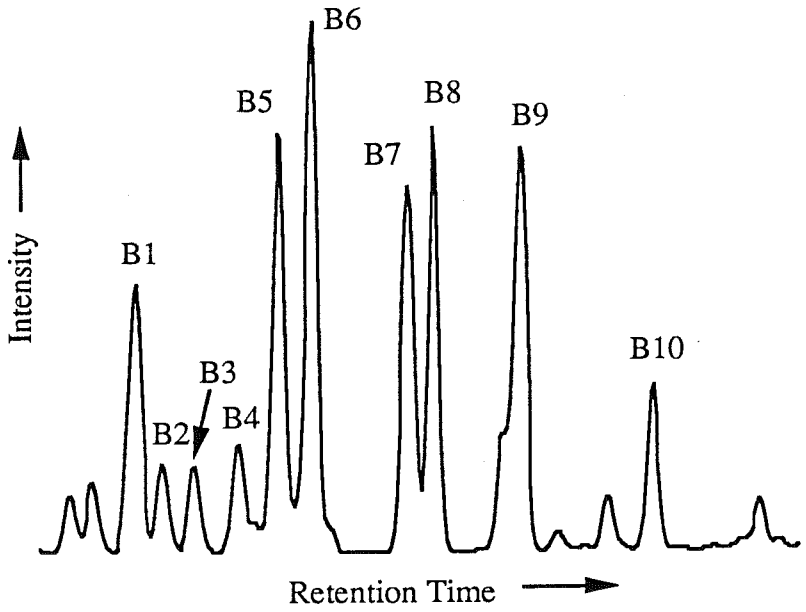

b) Quantitation results of the principal trimethylnaphthalene peaks.

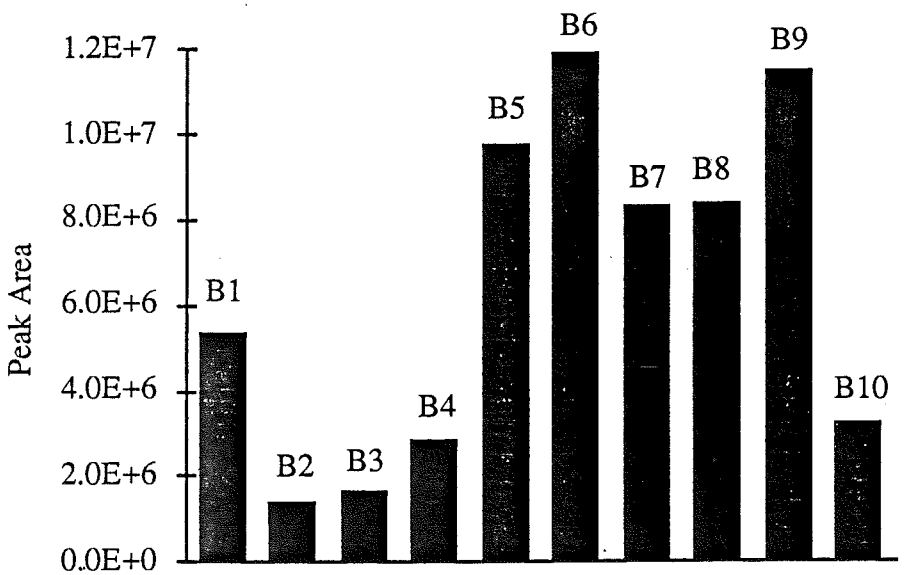

c) Normalized quantitation results (most intense peak is assigned a value of 1).

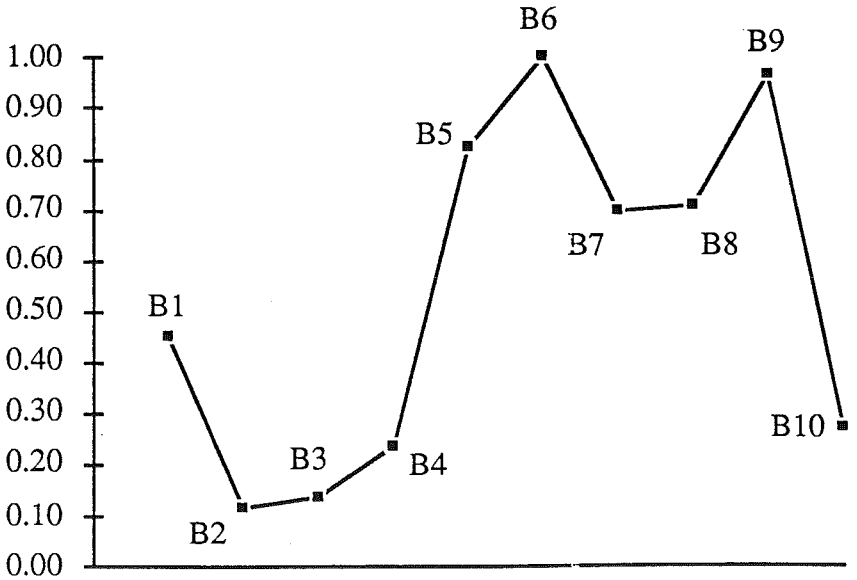

Figure 22

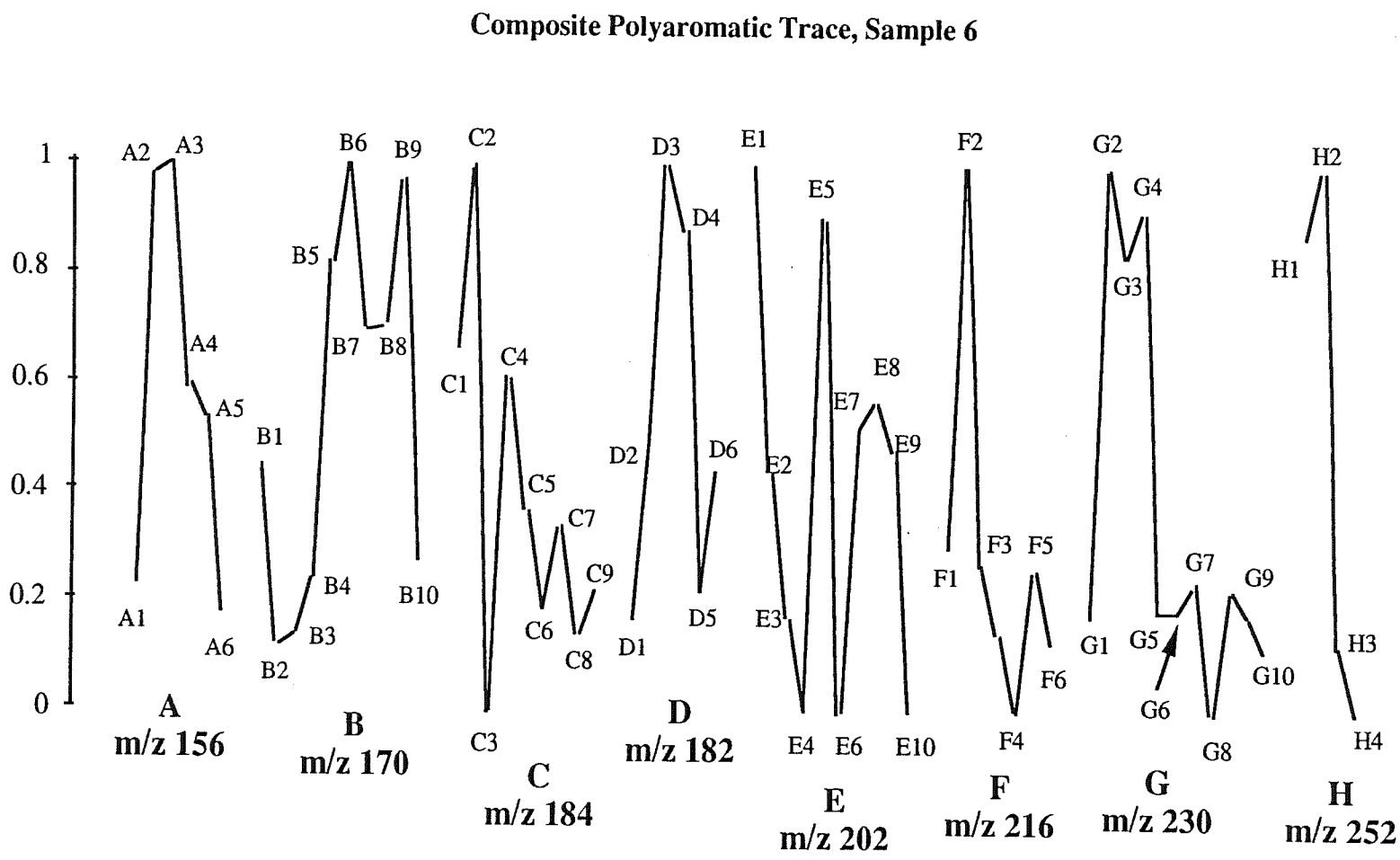

Figure 23. Example of a Composite Polyaromatic Trace (CPT) of normalized isomer clusters. Each cluster is normalized to a maximum of 1, as shown in figure 4. See figure 1 for key to peaks in traces A-C, figure 2 for traces E-G and figure 3 for traces D and H.

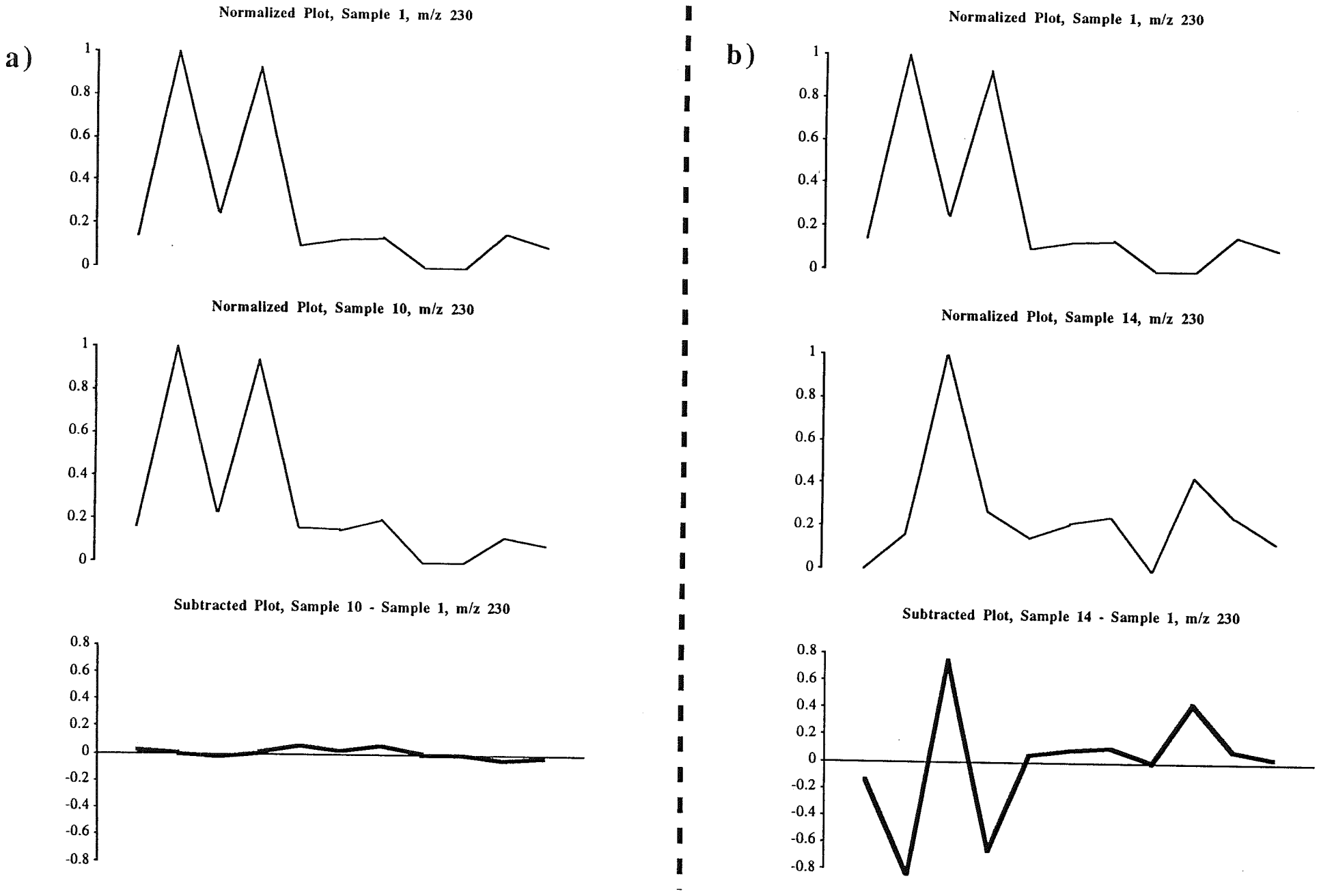

Figure 24. Example of the computation of Polyaromatic Trace remainders. a) From subtraction of traces of like samples. b) From subtraction of dissimilar samples.

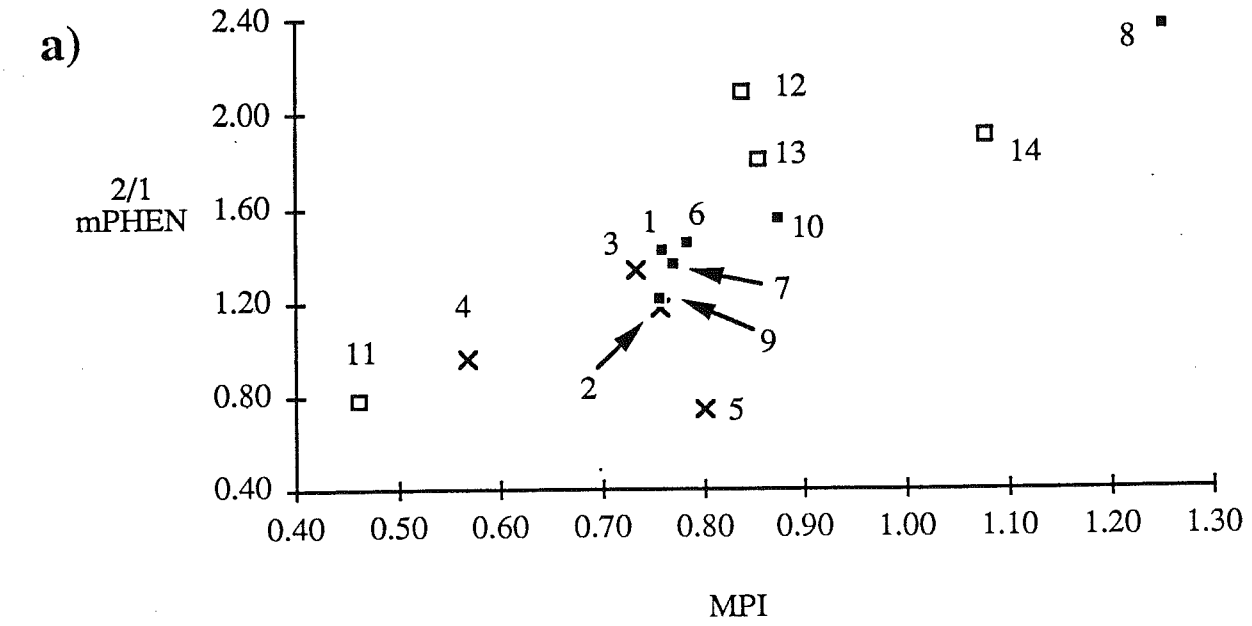

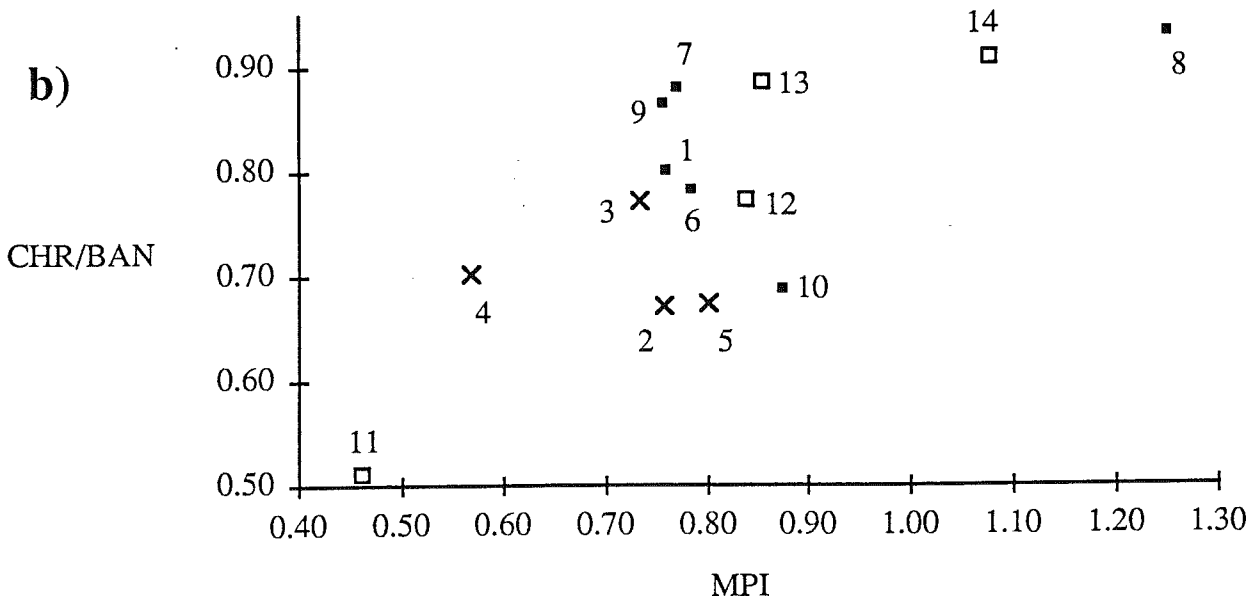

Figure 25

Maturity crossplots. a) The ratio of 2-methylphenanthrene to 1-methylphenanthrene and the Methylphenanthrene Index. b) The chrysene/benzo[*a*]anthracene ratio and the Methylphenanthrene Index. Symbol key: ▪ Group 1 petroleums. ✕ Group 2 petroleums. □ Rock extracts. Sample numbers are indicated next to the symbols.

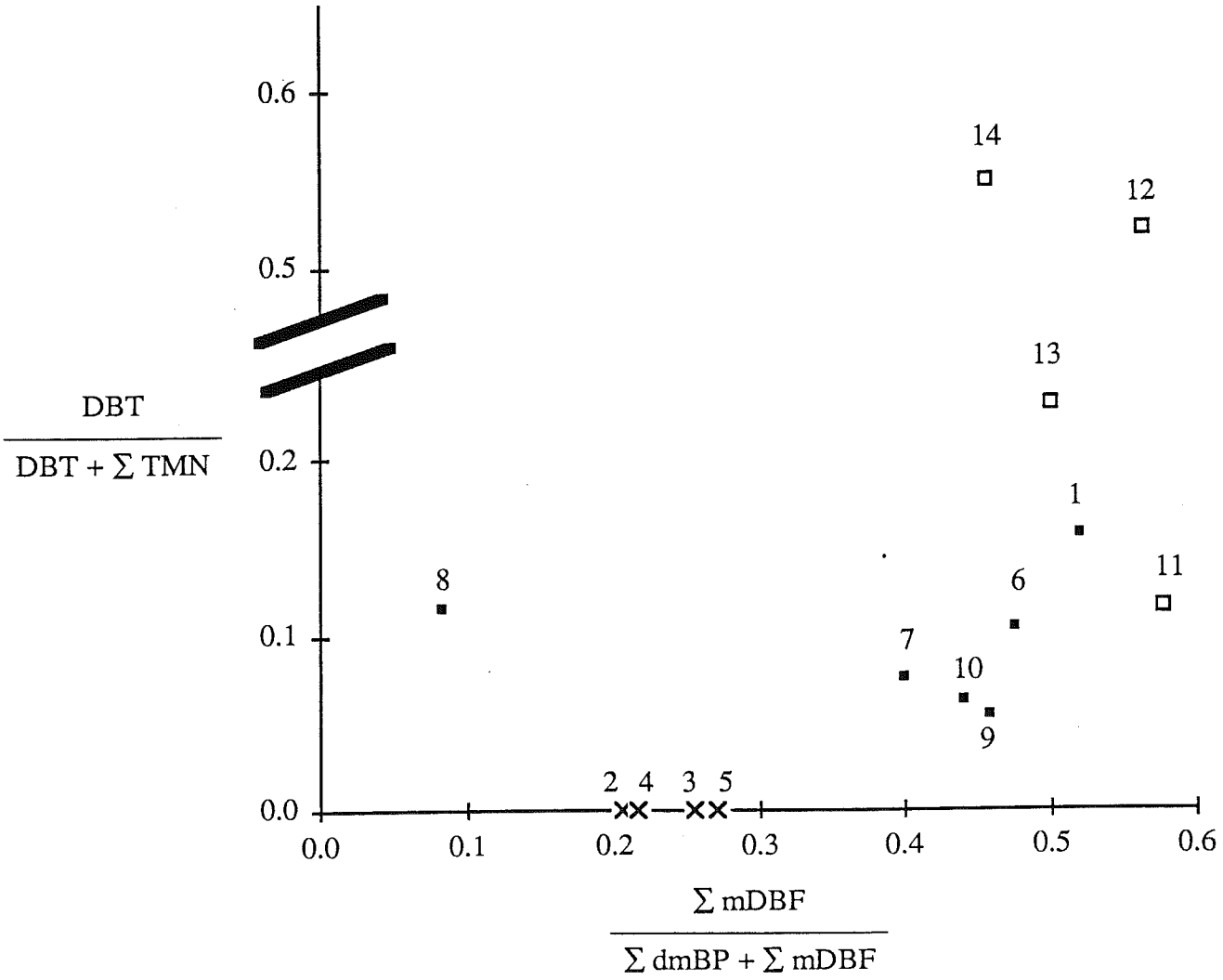

Figure 26

Crossplots of the ratio of the sum of methyldibenzofuran isomers to the sum of dimethylbiphenyl and methyldibenzofuran isomers (quantitated on m/z 182 chromatograms) and the ratio of dibenzothiophene to the sum of tetramethylnaphthalenes plus dibenzothiophene (m/z 184).
Symbol key: ▪ Group 1 petroleums. ✕ Group 2 petroleums. □ Rock extracts.
Sample numbers are indicated next to the symbols.

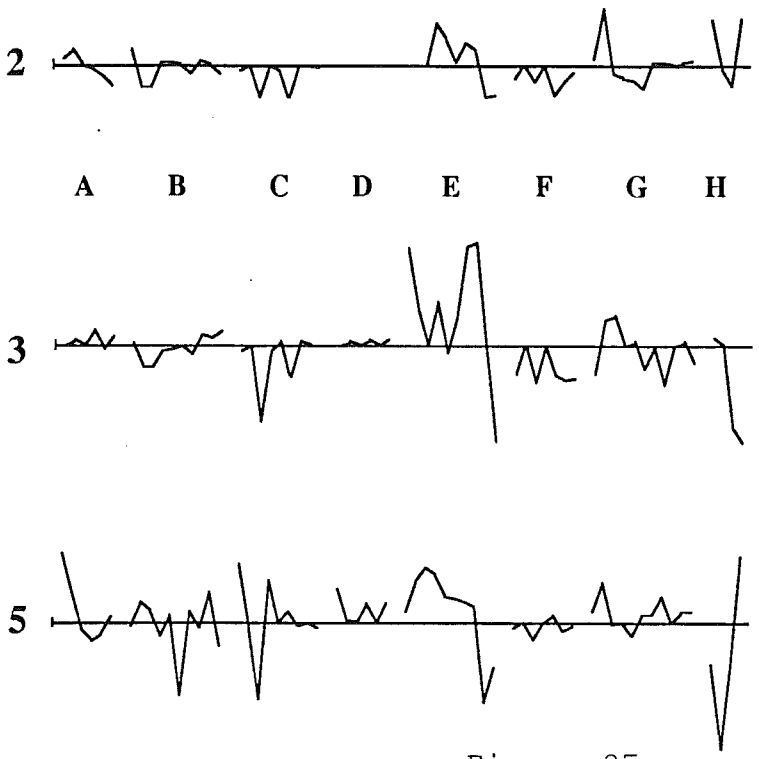

Figure 27

Composite Polyaromatic Trace remainders of "Group 2" oil samples after the subtraction of the trace of Sample 4. Sample numbers are shown to the left of each trace. See figure 5 for key to curves A through G. Scales are the same for each trace. Horizontal axis is the zero line.

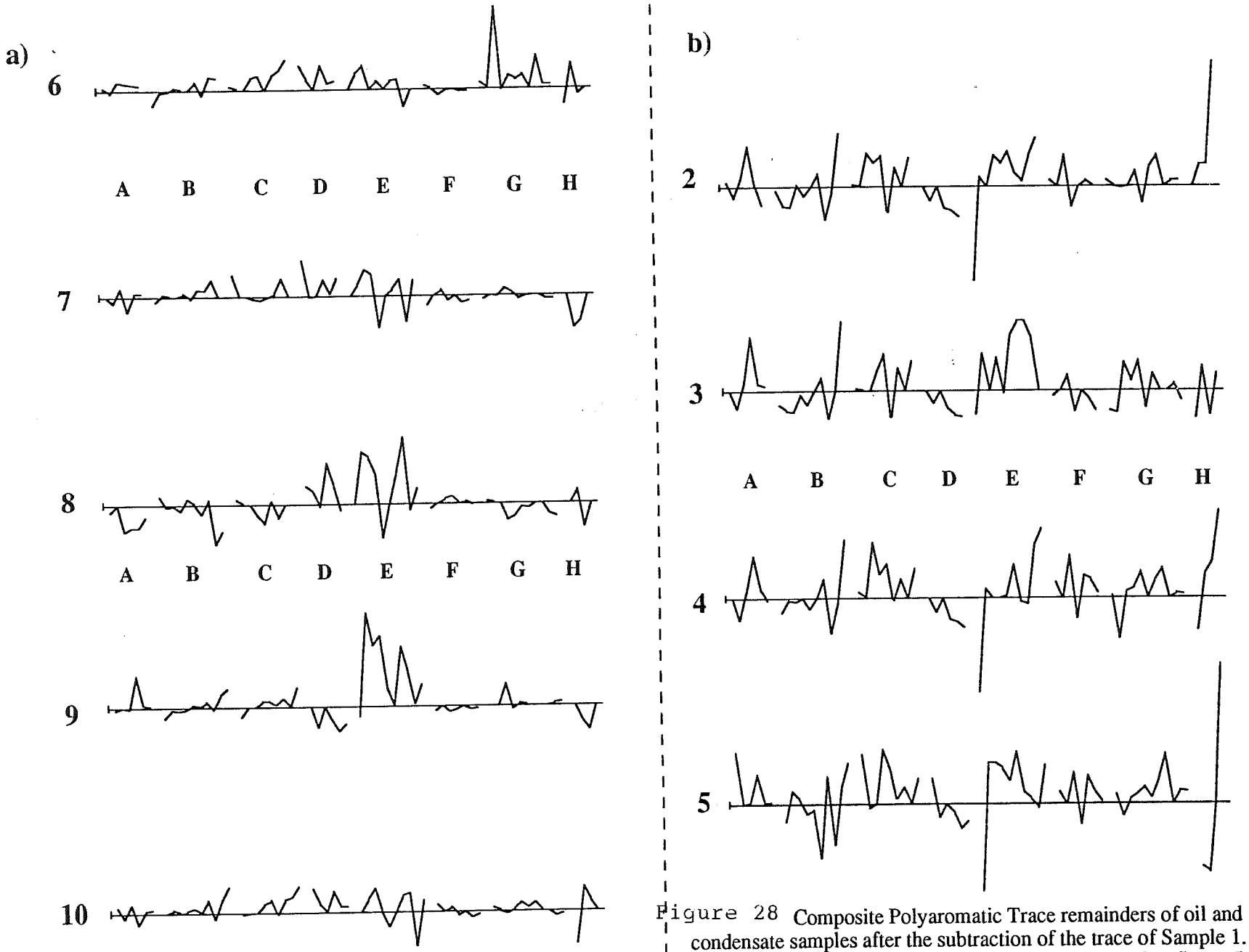

Figure 28 Composite Polyaromatic Trace remainders of oil and condensate samples after the subtraction of the trace of Sample 1. Sample numbers are shown to the left of each trace. See figure 5 for key to curves A through G. Scales are the same for each trace. Horizontal axis is the zero line. a) Group 1 petroleums. b) Group 2.

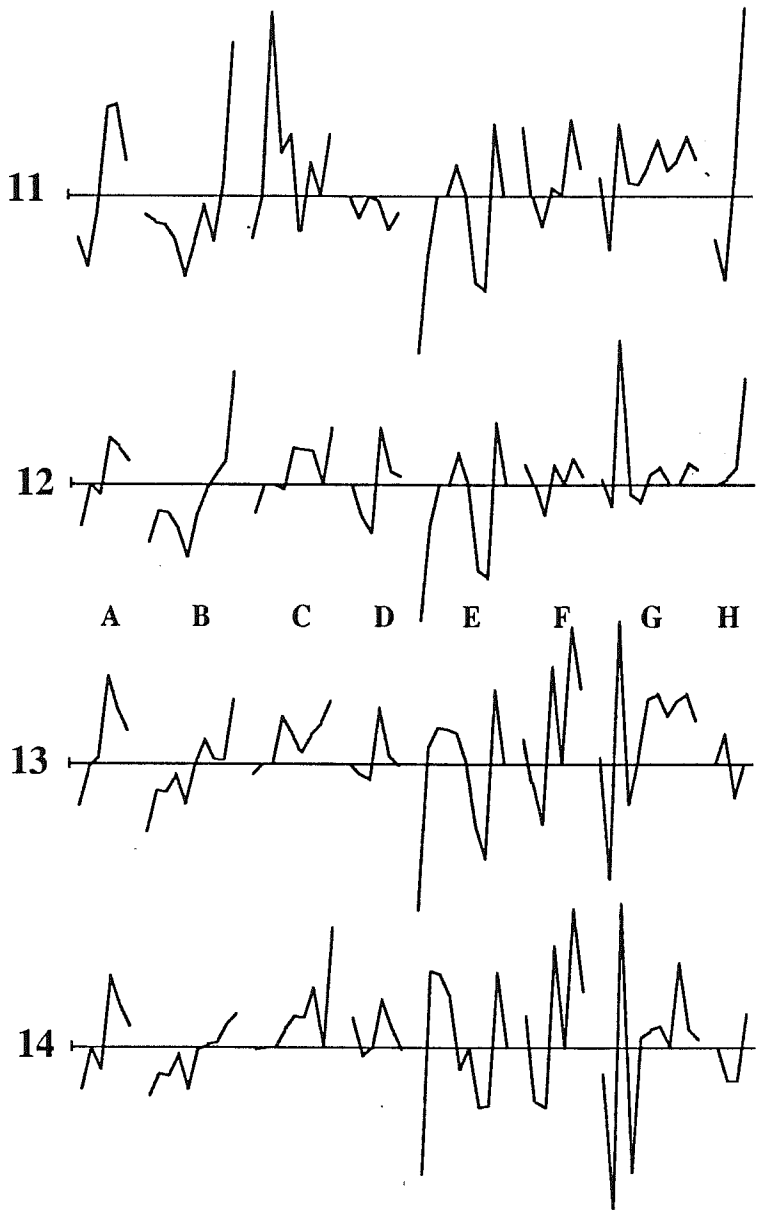

Composite Polyaromatic Trace remainders of rock extract samples after the subtraction of the trace of oil Sample 1. Sample numbers are shown to the left of each trace. See figure 5 for key to curves A through G. Scales are the same for each trace. Horizontal axis is the zero line.

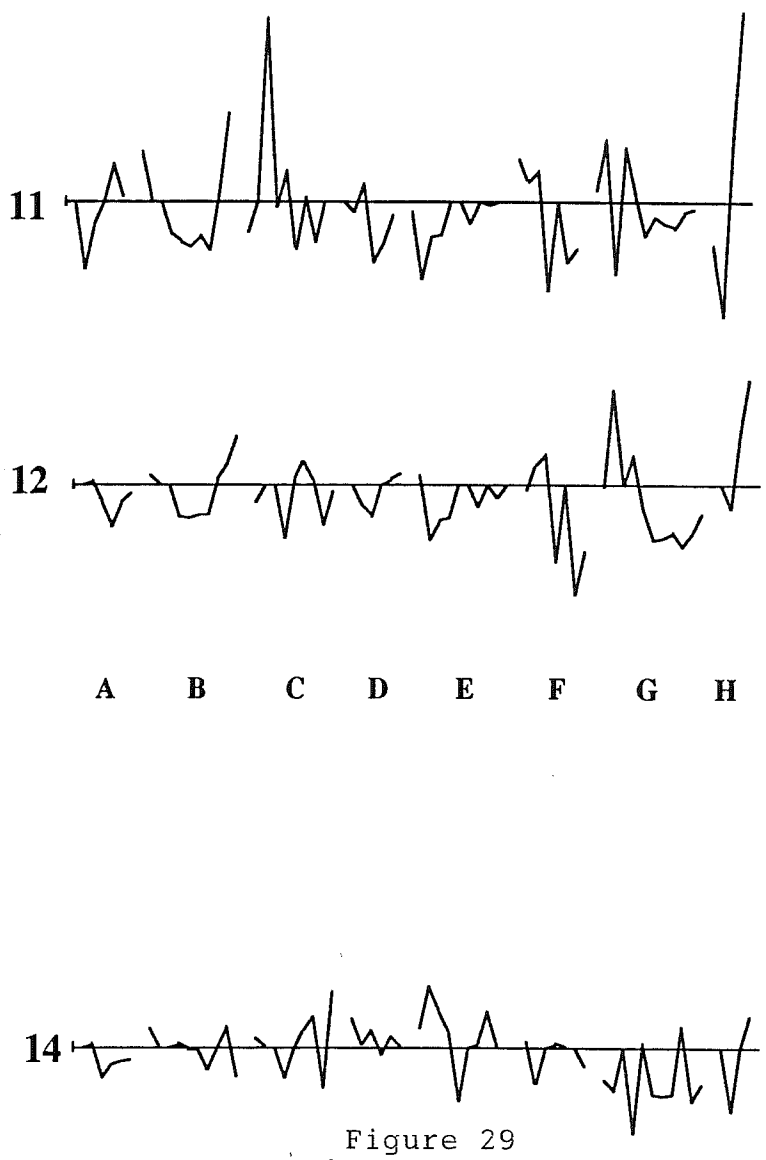

Figure 29

Composite Polyaromatic Trace remainders of rock extract samples after the subtraction of the trace of extract Sample 13.

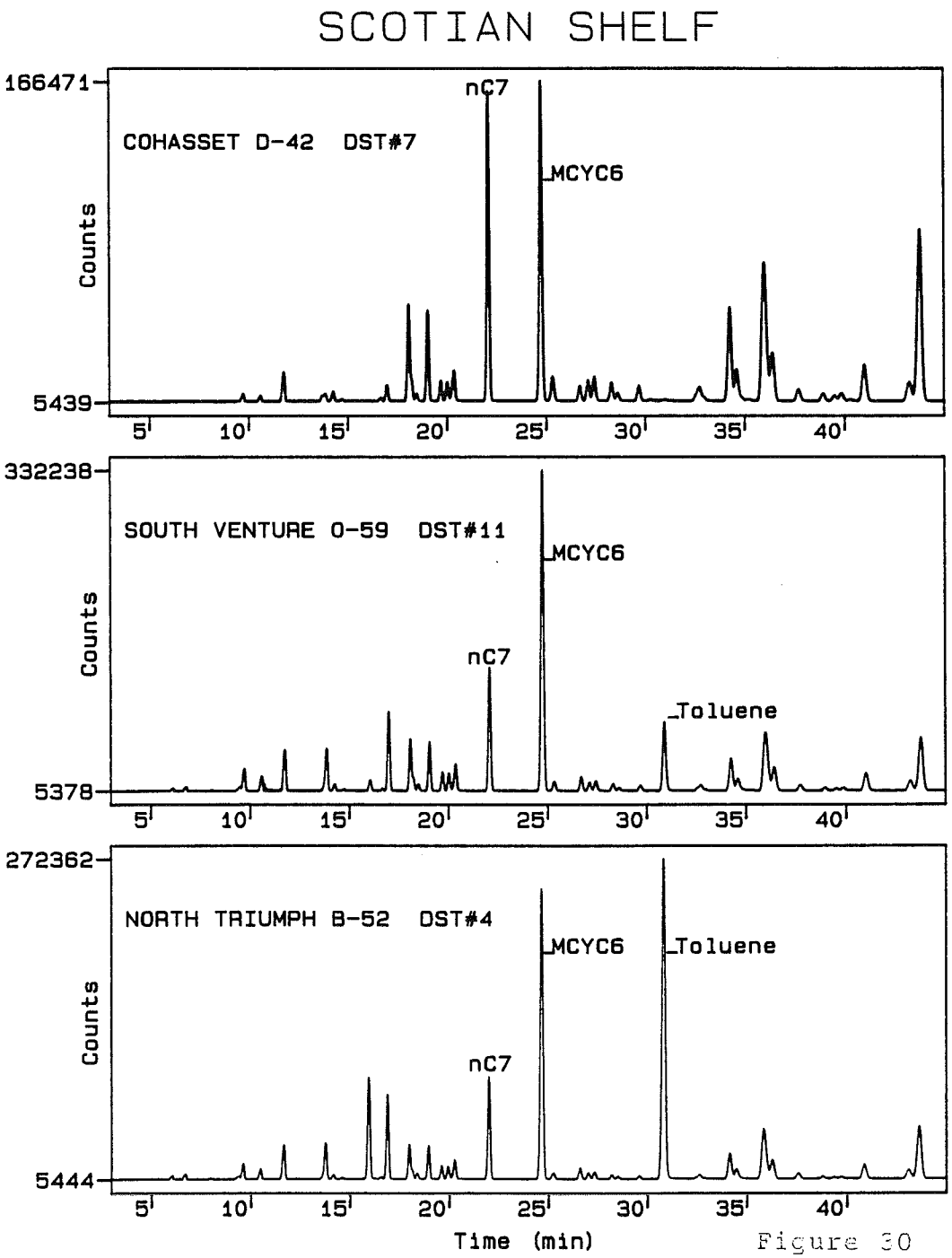
SCOTIAN SHELF
166471
nC7
COHASSET D-42 DST#7
MCYC6
Counts
5439
5 10 15 20 25 30 35 40
332238
SOUTH VENTURE O-59 DST#11
MCYC6
nC7
Toluene
Counts
5378
5 10 15 20 25 30 35 40
272362
NORTH TRIUMPH B-52 DST#4
MCYC6
Toluene
nC7
Counts
5444
5 10 15 20 25 30 35 40
Time (min)

Figure 30